Distribution Agreement

In presenting this thesis or dissertation as a partial fulfillment of the requirements for an advanced degree from Emory University, I hereby grant to Emory University and its agents the non-exclusive license to archive, make accessible, and display my thesis or dissertation in whole or in part in all forms of media, now or hereafter known, including display on the world wide web. I understand that I may select some access restrictions as part of the online submission of this thesis or dissertation. I retain all ownership rights to the copyright of the thesis or dissertation. I also retain the right to use in future works (such as articles or books) all or part of this thesis or dissertation.

Signature:

_____ _____

Nicole E. Brown **Date**

Integration of Heterotrimeric G Protein Signaling by the Regulator of G Protein Signaling 14 (RGS14): Independent Regulation of Gα Signaling by the RGS Domain and GPR Motif

By

Nicole E. Brown
Doctor of Philosophy

Graduate Division of Biological and Biomedical Sciences
Molecular and Systems Pharmacology

John R. Hepler, Ph.D.
Advisor

Randy A. Hall, Ph.D.
Committee Member

Thomas Kukar, Ph.D.
Committee Member

Eric A. Ortlund, Ph.D.
Committee Member

Accepted:

Lisa A. Tedesco, Ph.D.
Dean of the James T. Laney School of Graduate Studies

Date

Integration of Heterotrimeric G Protein Signaling by the Regulator of G Protein Signaling 14 (RGS14): Independent Regulation of Gα Signaling by the RGS Domain and GPR Motif

By

Nicole E. Brown
B.A., William Jewell College, 2010

Advisor: John R. Hepler, Ph.D.

An abstract of a dissertation submitted to the Faculty of the James T. Laney School of Graduate Studies of Emory University in partial fulfillment of the requirements for the degree of Doctor of Philosophy

in Graduate Division of Biological and Biomedical Sciences
Molecular and Systems Pharmacology
2016

Abstract

Integration of Heterotrimeric G Protein Signaling by the Regulator of G Protein Signaling 14 (RGS14): Independent Regulation of Gα Signaling by the RGS Domain and GPR Motif

By Nicole E. Brown

The Regulators of G protein Signaling (RGS) proteins are key modulators of G protein-coupled receptor and heterotrimeric G protein (Gαβγ) signaling events. One RGS protein, RGS14, is a key suppressor of synaptic plasticity, learning, and memory in the hippocampus. Like all RGS proteins, RGS14 contains an RGS domain that binds *active* Gα-GTP and catalyzes hydrolysis of GTP to GDP, thus acting as a GTPase activating protein (GAP). RGS14-mediated GAP activity accelerates the deactivation of Gαi/o proteins to terminate signaling by Gα and Gβγ subunits. RGS14 also contains a second Gα interaction site, a G Protein Regulatory (GPR) motif, which selectively binds *inactive* Gαi1/3-GDP. The GPR motif and Gβγ bind to the same site on Gα, thus RGS14 and Gβγ binding are mutually exclusive. Gαi1/3-GDP recruits RGS14 to the plasma membrane via the GPR motif to form a stable GPR:Gα-GDP complex devoid of Gβγ. Here I investigated the roles of the RGS14 RGS domain and GPR motif in regulating heterotrimeric G protein signaling. My studies highlight RGS14 as a structurally dynamic protein that is stabilized upon binding Gα at either the RGS domain or the GPR motif. Upon binding Gα through the GPR motif, RGS14 is allosterically stabilized at the RGS domain. Additionally, my studies demonstrate that despite sharing an overlapping binding site with Gβγ on Gα, RGS14 does not interfere with heterotrimer formation. Moreover, while RGS14 is capable of binding two distinct forms of Gα, my findings suggest RGS14 can functionally engage two Gα proteins simultaneously. I show that a preformed RGS14:Gαi1-GDP complex exhibits full capacity to stimulate the GTPase activity of a second Gαo-GTP protein *in vitro* and in a cellular context. Together, these studies demonstrate that despite engaging two G proteins simultaneously, the RGS domain and GPR motif function independently. Mechanistically, I propose RGS14 forms a stable complex at the plasma membrane with Gαi1-GDP through its GPR motif where the RGS domain is free to regulate a second G protein signaling event. My findings suggest that, in hippocampal neurons, native RGS14 serves as a dynamic multifunctional scaffolding protein that mediates unconventional G protein signaling events underlying synaptic plasticity.

Integration of Heterotrimeric G Protein Signaling by the Regulator of G Protein Signaling 14 (RGS14): Independent Regulation of Gα Signaling by the RGS Domain and GPR Motif

By

Nicole E. Brown
B.A., William Jewell College, 2010

Advisor: John R. Hepler, Ph.D.

A dissertation submitted to the Faculty of the James T. Laney School of Graduate Studies of Emory University in partial fulfillment of the requirements for the degree of Doctor of Philosophy

in Graduate Division of Biological and Biomedical Sciences
Molecular and Systems Pharmacology
2016

Table of Contents

List of Figures

List of Abbreviations

α2-AR	alpha 2-adrenergic receptor
ACD	asymmetric cell division
AGS	activator of G protein signaling
AMPA	α-amino-3-hydroxy-5-methyl-4-isoxazolepropionic acid
BRET	bioluminescence resonance energy transfer
CA	*Cornu Ammonis*
cAMP	cyclic adenosine monophosphate
CTZ	coelenterazine
CV	column volume
DAG	diacylglycerol
DEP	Disheveled, EGL-10, Pleckstrin
EGF	epidermal growth factor
EPSP	excitatory postsynaptic potential
ERK	extracellular signal-regulated kinase
FRET	fluorescence resonance energy transfer
GABA	gamma-aminobutyric acid
GAP	GTPase activating protein
GDI	guanine nucleotide dissociation inhibitor
GDP	guanosine diphosphate
GGL	G protein gamma-like
GIRK	G protein-coupled inwardly rectifying potassium channel
GPCR	G protein-coupled receptor
GPR	G protein regulatory motif

GST	glutathione S-transferase
GTP	guanosine triphosphate
H_6	hexahistadine
HDX	hydrogen deuterium exchange
HEK	human embryonic kidney
His_6	hexahistadine
ICL	intracellular loop
IMAC	immobilized metal ion affinity chromatography
JNK	c-Jun N-terminal kinase
LTP	long term potentiation
Luc	luciferase
MBP	maltose binding protein
NMDA	N-methyl-D-aspartate
NPC	neural progenitor cell
PDGF	platelet derived growth factor
PDZ	PSD-95/Dlg/ZO-1
PI3K	phosphoinositide 3-kinase
PIP_2	phosphatidylinositol 4,5-bisphosphate
PKA	protein kinase A
PKC	protein kinase C
PLCβ	phospholipase C beta
PSD	postsynaptic density
PTB	phosphotyrosine binding domain
RBD	Ras binding domain

RLuc	*Renilla* luciferase
RTK	receptor tyrosine kinase
RGS	regulator of G protein signaling
SE	standard error
SEC	size-exclusion chromatography
SEM	standard error mean
SNX	sorting nexin
SPC	sphingosylphosphorylcholine
TEV	tobacco etch virus
TGFβ	transforming growth factor beta
TPR	tetratricopeptide repeat
Ven	Venus
VEGF	vascular endothelial growth factor
YFP	yellow fluorescent protein

Chapter 1: Introduction

1.1 G Protein-Coupled Receptors

G protein-coupled receptors (GPCRs) are key transducers of extracellular signals to activate intracellular signaling pathways. GPCRs represent a diverse class of cell surface receptors that regulate cellular and organ physiological responses to various hormones, lipids, amino acids, neurotransmitters, purines, and sensory stimuli. Embedded within the plasma membrane, GPCRs are composed of a single polypeptide that contains an extracellular N-terminus, seven transmembrane domain regions (7-TMDs), and an intracellular C-terminus. The transmembrane domains are linked by three intracellular loops and three extracellular loops. Some GPCRs have a fourth intracellular loop created by lipid modification of the C-terminus. The intracellular domains mediate coupling of G proteins while extracellular loops along with the N-terminus mediate binding of ligands. Agonist binding of GPCRs induces an active receptor conformation that stimulates activation of the intracellular heterotrimeric G protein.

Over 800 GPCRs are encoded in the human genome (1). Based on phylogeny and functional similarity, GPCRs are classified in five different classes by the GRAFS (Glutamate Rhodopsin Adhesion Frizzled Secretin) system (2). Under this system, the largest class is the rhodopsin-like receptors (also called Class A) consisting of olfactory GPCRs as well as amine, purine, peptide, opsin, chemokine, and prostaglandin GPCRs (3). The secretin family of GPCRs (Class B) bind large peptide hormones and have cysteine rich N-termini capable of forming disulfide bridges (4). The metabotropic glutamate receptors (Class C) contain large N-termini that bind ligands via the venus flytrap (VFT) domain (5). The adhesion GPCRs have long N-terminal regions often with adhesion molecule repeats such as epidermal growth factor (EGF) domains. Most adhesion GPCRs contain GPCR proteolytic sites (GPSs) as well (6). The frizzled/smoothened (Class F) GPCRs bind Wnt signals

through Cys-rich N-termini (7).

GPCRs are key targets in pharmacology due to their versatility and role in physiology. Approximately 30% of prescribed pharmaceuticals target GPCRs (8) including some of the most profitable therapeutics. For instance, fexofenadine, marketed under Allegra®, antagonizes the H1 histamine receptor to alleviate symptoms from allergies. Antagonism of angiotensin II receptors by valsartan, trade name Diovan®, can be used to treat hypertension. Agonism of the $GABA_B$ receptor by GABApentin (Neurontin®) can alleviate neurological pain while antagonism of the $P2Y_{12}$ receptor by clopidrogel (Plavix®) can reduce the risk of stroke (8). The vast majority of GPCRs targeted by current drugs belong to the rhodopsin-like (Class A) family though others, like the $GABA_B$ receptor, belong to the metabatropic glutamate receptor family (Class C).

1.2 Heterotrimeric G Proteins

Though GPCRs mediate vast physiological responses, GPCRs share a common mechanism to transduce signals across the plasma membrane by coupling to heterotrimeric G proteins. Heterotrimeric G proteins consist of an α, β, and γ subunit. The Gα subunit binds guanine nucleotides (GDP or GTP) and possesses enzymatic GTPase activity. The Gβ and Gγ subunits form a dimer that acts as a guanine nucleotide dissociation inhibitor (GDI), preventing dissociation of GDP and spontaneous activation of the G protein (9,10). Activation of the GPCR leads the receptor to act as a guanine exchange factor (GEF). The activated receptor and G protein form a high affinity complex in which GDP is released from Gα. The nucleotide free Gα then binds GTP due to the high intracellular concentration of GTP. Then Gα-GTP and Gβγ may dissociate or rearrange to engage downstream effector molecules to propagate the signal within the cell.

In humans there are 21 Gα proteins, 6 Gβ proteins, and 12 Gγ proteins (4,11). G proteins have been grouped into four subfamilies based on sequence homology of the Gα subunit. These four families include Gαs, Gαi, Gαq, and Gα12/13. The Gαs family includes Gαs and Gαolf was named for its stimulatory effect on adenylyl cyclase (12,13). Upon binding adenylyl cyclase, Gαs stimulates the production of cAMP and gives rise to the activation of protein kinase A (PKA). The Gαi family includes Gαi1, Gαi2, Gαi3, Gαo, Gαz, Gαt and Gαgust. Gαi family members were named for their inhibitory effect on adenylyl cyclase (14,15). Upon binding adenylyl cyclase, Gαi proteins can exhibit a modest inhibition of cAMP production. While Gαi proteins are widely expressed throughout the body, other members of the Gαi family have more specialized roles. Gαo is expressed primarily in the heart and brain while Gαt (transducin) is expressed in rod and cone cells and Gαgust (gustducin) is expressed in taste cells. The Gαq family includes Gαq, Gα11, Gα14, Gα15, and Gα16. Gαq protein binding of phospholipase Cβ (PLCβ) initiates hydrolysis of phosphatidylinositol 4,5-bisphosphate (PIP_2) to produce inositol 1,4,5-trisphosphate (IP_3) and diacylglycerol (DAG). IP_3 stimulates release of Ca^{2+} from intracellular stores that along with DAG mediate the activation of protein kinase C (PKC). The Gα12/13 family binds RhoGEF to stimulate activation of Rho, a small GTPase important in actin and cytoskeletal organization.

Initially, signal propagation by heterotrimeric G proteins was believed to be mediated solely by the Gα subunit. Consequently, classic descriptions of G protein signaling often refer to canonical pathways mediated by Gα proteins, however, Gβγ was later identified as an important for component for heterotrimeric G protein signaling cascades. The first mammalian effector identified to be regulated by Gβγ was the G protein coupled inwardly rectifying potassium (GIRK) channel (16). Binding of Gβγ to GIRK channels stimulates

channel opening and efflux of K^+ ions out of the cell (17,18). Other Gβγ effectors were found to include adenylyl cyclases, PLCβ, Ca^{2+} channels, and MAPK signaling pathways among others (19-25).

All G proteins except for Gαt are palmitoylated at the N-terminus (26). Members of the Gαi/o family are also myristoylated at the N-terminus (26,27). Gγ subunits can be prenylated with geranylgeranyl modifications or farnesyl modifications in the case of Gγ1 (27). These post-translational modifications localize G proteins to cellular membranes (28,29). Coupling of G proteins to receptors is controlled by both the GPCR and the G protein. GPCR intracellular loops govern which G proteins couple to which GPCRs. Intracellular loop 2 (ICL2) and ICL3 predominately dictate GPCR coupling though ICL1 and ICL4 can provide some selectivity (30,31). Both the N-terminus and C-terminus of Gα proteins regulate coupling to receptors in addition to the α4 helix (32,33). Moreover, research suggests Gβγ subunits can drive specificity of receptor coupling (34,35). Pertussis toxin ADP-ribosylates a C-terminal cysteine to prevent coupling of Gαi proteins to GPCRs (36,37).

1.3 Regulators of G Protein Signaling

The lifetime of a heterotrimeric G protein signaling event is dependent on the GTPase of the Gα subunit. Initial characterization of transducin (Gαt) GTPase activity revealed GTP hydrolysis occurred faster *in vivo* than *in vitro* (38). The discrepancy between G protein kinetics observed *in vitro* and *in vivo* sparked a search for the GTPase activating proteins (GAPs) regulating heterotrimeric G protein signaling. The first Regulator of G protein Signaling (RGS) protein was discovered in 1982 with the identification of the SST2 gene (39). Loss of SST2 in *Saccharomyces cerevisiae* increased sensitivity to α factor signaling

(40). Later studies indicated SST2 binds the Gα protein Gpa1p to negatively regulate α factor receptor signaling (41,42). Other studies demonstrated the same phenomena in *Caenorhabditis elegans* and *Aspergillus nidulans* where EGL-10 and FlbA, respectively, were shown to regulate Gα signaling (43,44). Mammalian RGS proteins were then identified and shown to serve as GAPs for Gα proteins (45-49). It was later shown that RGS9-1 (potentiated by phosphodiesterase γ) mediated the fast deactivation kinetics observed *in vivo* for Gαt (50). Thus, with the discovery and characterization of RGS proteins, the final piece to describe the canonical G protein signaling cycle was identified.

The RGS protein family comprises GTPase activating proteins for Gαi/o and Gαq proteins. There are currently 20 RGS proteins and 19 proteins that contain RGS homology domains (51). Proteins with RGS homology domains may engage Gα proteins but do not exhibit GAP activity save for a few exceptions. Proteins containing RGS homology domains include G protein receptor kinases (GRKs), RhoGEFs, Axins, D-AKAP2, Nexins, and the RGS-like proteins (RGSL and RGS22). Of these RGS homology domain proteins, only GRKs and RhoGEFs can bind activated Gα proteins. Specifically, GRK2 and GRK3 bind activated Gαq and exert weak GAP activity (52). RhoGEFs engage Gα12/13, however some literature suggests the mild GAP effect observed is due to a fragment N-terminal to the RGS homology domain (53-57). Some studies have suggested Axin and sorting nexin (SNX) can bind Gαs proteins (58,59) however others have contested this association (51,60). Although D-AKAP2 possesses two RGS homology domains, binding of Gα proteins has not been observed (61). RGS22 has been shown to bind inactive Gα12/13 proteins (62), however, GAP activity has not been demonstrated (63).

The RGS protein family possesses canonical RGS domains and acts as effective GAPs on Gαi and Gαq proteins. The RGS family has been divided into four subfamilies

including A/RZ, B/R4, C/R7, and D/R12 (64). The A/RZ subfamily includes RGS17, RGS19, and RGS20. The A/RZ subfamily contains cysteine strings at the N-terminus that are regulated by palmitoylation and positions these RGS proteins at the plasma membrane. Members of the A/RZ subfamily are selective for Gαi proteins and engage the less ubiquitous Gαz in particular (65-68). The B/R4 subfamily is the largest and includes RGS1, RGS2, RGS3, RGS4, RGS5, RGS8, RGS13, RGS16, RGS18, and RGS21. The B/R4 subfamily features relatively simple RGS proteins in that they do not contain additional domains outside the RGS domain. Despite the lack of additional domains, research has shown these proteins to be highly regulated by mechanisms such as palmitoylation, phosphorylation, and ubiquitination (69). The B/R4 subfamily largely engages both Gαi and Gαq families except for RGS2 (67). RGS2 shows selectivity for Gαq over Gαi proteins (67,70,71). The C/R7 subfamily encompasses RGS6, RGS7, RGS9, and RGS11. The C/R7 family is characterized by the G-gamma-like (GGL) domain. The GGL domain forms an obligatory heterodimer with Gβ5 (72). Additionally, the C/R7 subfamily contains DEP (for Disheveled, EGL-10, Pleckstrin) domains. The DEP domain binds R7 binding protein (R7BP), which localizes/R7 subfamily members to the plasma membrane (73,74). The C/R7 subfamily shows selectivity for Gαi proteins over Gαq (67). The D/R12 subfamily includes RGS10, RGS12, and RGS14. RGS12 and RGS14 feature tandem Ras/Rap binding domains as well as C-terminal G protein regulatory (GPR) motifs. Though RGS10 lacks these additional domains/motifs, RGS10 shares high sequence homology with the RGS domains of RGS12 and RGS14. While RGS12 and RGS14 show strong selectivity for Gαi proteins over Gαq proteins (75,76) RGS10 can GAP both Gαi and Gαq proteins (49).

The canonical RGS domain encompasses approximately 130 amino acids and forms a bundle of nine helices (77). Upon binding activated Gα-GTP, the RGS domain stabilizes G

protein switch regions to facilitate GTP hydrolysis (77). Biochemically, RGS proteins show the highest affinity for aluminum tetrafluoride (AlF_4^-) activated Gα (78). Crystal structures of Gα proteins with RGS suggest RGS proteins stabilize the transition state of GTP hydrolysis as RGS proteins do not contribute any catalytic residues to the GTPase (77).

As RGS proteins negatively regulate G protein signaling, they modulate important physiological responses throughout the body. One of the early identified roles of RGS proteins was deactivation of Gαt in the outer segment of rod cells (50). Prior to the identification of RGS9-1, it was unclear what mediated the fast deactivation of Gαt and subsequent recovery from light stimuli. Later studies utilizing retinas from RGS9-KO mice confirmed the GAP effect of RGS9-1 on Gαt kinetics as loss of RGS9 slowed the recovery of the photo-response (79).

RGS proteins play important roles in regulating signaling in the cardiovascular system. In vascular smooth muscle cells, RGS2 regulation of Gαq is important for controlling contraction. Loss of RGS2 leads to heightened blood pressure due to enhanced Gαq signaling and subsequent Ca^{2+} mobilization (80,81). In the heart, RGS4 has been implicated in regulation of hypertrophy (82). Over expression of Gαq in cardiomyocytes results in hypertrophy that is ameliorated with co-expression of RGS4 (83).

Additionally, RGS proteins exert control over GIRK signaling in the heart. Both RGS4 and RGS6 have been previously shown to regulate M2 muscarinic receptor coupled GIRK channels (84,85). Loss of RGS4 expression results in enhanced bradycardia in response to carbachol treatment in RGS4-KO mice (86). Likewise, loss of RGS6 exaggerates bradycardia in response to carbachol in RGS6-KO mice (87).

RGS proteins have also been implicated in modulating GIRK channel responses in the brain. Studies of RGS proteins in the brain revealed regulation of GPCR-coupled GIRK

channels by RGS2, RGS6, and RGS7. In dopamine neurons of the ventral tegmental area (VTA), RGS2 expression reduces coupling of $GABA_B$ receptors to GIRK channels (88). In cerebellar granule neurons of the cerebellar cortex, loss of RGS6 expression slows GIRK deactivation kinetics in response to $GABA_B$ activation (89) and in cultured hippocampal neurons, loss of RGS7 slows GIRK deactivation via $GABA_B$ receptors (90,91).

Early studies of RGS protein regulation of M2 muscarinic receptor coupled GIRK channels demonstrated co-expression of RGS proteins in heterologous systems accelerated both activation and deactivation of GIRK channels (84,92). As negative regulators of G protein signaling, RGS proteins were expected to accelerate the deactivation kinetics while acceleration of activation kinetics came as more of a surprise. These changes in kinetic responses can be attributed the GAP function of RGS proteins (93). Upon activation of the GPCR and subsequently the heterotrimeric G protein, RGS proteins are recruited to Gα-GTP. RGS acceleration of Gα GTPase enhances the deactivation kinetics and recycles heterotrimers to the receptor, ready to be activated again. Thus, enhanced deactivation of heterotrimers allows faster activation of the next round of G proteins.

In addition to sharpening of acceleration and deactivation kinetics, RGS proteins prevent coupling to effector molecules. Acceleration of G protein GTPase not only limits the lifetime of G protein activation, but physical interaction with RGS proteins can occlude interactions with effectors. Experiments with Gαq activated with the non-hydrolyzable GTP analogue GTPγS demonstrated RGS4 and RGS19 could block activation of PLCβ (94). Moreover, in COS-7 cells, production of IP_3 in response to activation of Gαq with AlF_4^- was attenuated with RGS4 expression (95).

1.4 Non-Canonical G Protein Signaling

While heterotrimeric G protein signaling has classically been confined to GPCR, G protein, and effector pathways, increasing evidence suggests involvement of G proteins in non-canonical signaling pathways (96,97). Concomitant with the non-canonical functions of G proteins, accessory regulators have also been identified. Some of the earliest non-canonical G protein regulators identified were the Activators of G protein Signaling (AGS) proteins. AGS proteins were first identified in yeast screens for G protein activation in the absence of a GPCR. *Saccharomyces cerevisiae* lacking the GPCR pheromone receptor transformed with adult human liver cDNA were screened for functional output of G protein signaling (98). Similar yeast screens identified AGS2 and AGS3 from rodent brain cDNA libraries (99).

Though AGS1, AGS2, and AGS3 were identified as G protein activators, each has a different mechanism of G protein regulation. AGS proteins have subsequently been classified into three groups based on their effects on G protein signaling. Group I AGS proteins encompass non-receptor GEFs. Group II AGS proteins are defined by their shared G Protein Regulatory (GPR) motifs and act as guanine-dissociation inhibitors (GDIs). Group III AGS proteins modulate G protein signaling through binding of Gβγ. Group I and Group III AGS proteins lack a common domain/motif to define their activity and will be discussed below. Group II AGS proteins will be discussed in the next section.

The Group I AGS proteins include AGS1 (also called DexRas1 or RASD1), GIV/Girdin, Ric-8A, and Ric-8B which catalyze the release of GDP from Gα to allow GTP binding (100-102). Unlike traditional G protein GEFs (e.g., GPCRs) that are embedded within the plasma membrane, Group I AGS proteins are associated with structures throughout the cytoplasm (103-105). Moreover, the Group I AGS proteins lack a common

domain/motif that mediates GEF activity.

AGS1 was independently identified as DexRas1, a GTP-binding protein inducible by the glucocorticoid hormone dexamethasone (106,107). Protein sequence analysis revealed homology with small GTPases Ras and Rap (107) while functional analysis demonstrated a non-receptor GEF role for Gαi proteins (101). Characterizations of AGS1 activity suggest AGS1 can activate ERK signaling (101) and antagonize GIRK signaling (108). Mechanistically, the integration between the Ras-like domain and GEF activity of AGS1 remain unclear.

GIV (also called Girdin) was initially identified as a binding partner of Akt (109) and later shown to activate Gαi proteins (102). *In vitro* characterization of GIV demonstrated it can uncouple Gαβγ heterotrimers (102). GIV has been implicated in signaling pathways mediating cell survival, activating PI3K and TGFβ pathways (110). Mutation of the GEF motif causes apoptosis suggesting a key role for Gα signaling in survival pathways (111). GIV appears to operate downstream of receptor tyrosine kinases (RTKs) and activate G protein signaling in response to a variety of growth factors including VEGF, EGF, PDGF, and insulin (112). Thus, GIV provides a unique mechanism of signaling crosstalk.

Ric8-A is a non-receptor GEF for Gαi, Gαq, and Gα12/13 (113,114). Loss of Ric-8A decreases ERK activation in response to Gαq activation by the P2Y receptor (115). Ric-8B is a non-receptor GEF for Gαs proteins (116). Overexpression of Ric-8B leads to activation of adenylyl cyclase by Gαolf, a Gαs family member (117). While Ric-8A and Ric-8B were initially characterized as non-receptor GEF proteins, recent evidence has emerged implicating Ric-8 proteins as Gα chaperones (118,119). Loss of Ric-8 expression in mouse embryonic stem cells results in reduction of steady-state G protein production and prompts GPCR signaling defects (118). Recent models of Ric-8 function suggest GEF activity is due

to partial unfolding of Gα during the chaperoning process and highlight GEF function distinct from that of GPCRs (120).

AGS2 belongs to a separate class of AGS proteins that modulate G protein signaling by binding Gβγ (99,121). These Group III AGS proteins include AGS2, AGS7, AGS8, and AGS9. The most studied Group III AGS proteins is AGS2. AGS2, also called Tctex-1 or DYNLT1, is a component of cellular motor protein dynein (122). Evidence suggests AGS2 regulates neurite outgrowth as a Gβγ effector free of dynein (123). Like the Group I AGS proteins, Group III AGS proteins lack a consensus domain or motif that mediates its non-canonical effect on G protein signaling. Future research is required to determine the mechanistic function of these proteins.

1.5 G Protein Regulatory Motif Proteins

The most studied and best characterized AGS proteins belong to Group II. Group II AGS proteins are defined by the presence of G protein regulatory (GPR) or GoLoco motifs that can bind inactive Gα proteins and demonstrate selectivity for the Gαi/o class. The GPR motif was first identified upon cloning of the *Drosophila* protein Loco (124). Loco, also an RGS-containing protein and an orthologue of RGS12, was identified to bind inactive Gαi proteins through a distinct ~20 amino acid motif separate from the RGS domain (124). This motif was then shown to exist in other proteins including LGN, Pcp2, Rap1GAP1, AGS3, AGS4, RGS12, and RGS14 (99,125-127).

Group II AGS proteins are classified as guanine dissociation inhibitors (GDIs) since binding of inactive Gα subunits prevents spontaneous dissociation of GDP nucleotides in a manner analogous to Gβγ (128-131). The N-terminus of the GPR motif forms an amiphipathic helix that contacts the Ras-like lobe of Gα proteins. The C-terminus of the

GPR motif features an acidic-glutamine-arginine, (D/E)QR, triad that is important for binding Gα (132). Moreover, residues C-terminal to the (D/E)QR triad make contact with the α-helical lobe of Gα proteins and contribute to the selectivity of GPR motifs (132).

Structural analysis of GPR motifs with Gα suggest the binding sites of Gβγ and GPR motifs overlap on Gα (132) and GPR motif proteins have been identified in complex with Gα devoid of Gβγ (99). As interactions of GPR motifs and Gβγ appear to be mutually exclusive, the role of GPR proteins in heterotrimeric signaling remains an important area of research. *In vitro* analysis of heterotrimer interactions with GPR motif suggests some GPR motifs cannot dissociate Gβγ from Gα (133). Alternatively, other research suggests GPR motif proteins can prevent the formation of Gαβγ heterotrimers *in vitro* (134-136) and stimulate Gβγ effectors (137). In this way, Group II AGS proteins may activate G protein signaling through the release of free Gβγ.

Group II AGS proteins can be classified by the number of GPR motifs they contain. AGS3, AGS4, LGN, PCP2 each contain multiple GPR motifs. AGS3 and LGN each have four GPR motifs while AGS4 has three and PCP2 has two GPR motifs, respectively. RGS12, RGS14, and Rap1GAP1 all possess a single GPR motif (125). AGS3 and LGN share similar domain structures and feature seven tetratricopeptide repeat (TPR) domains at the N-terminus (138). In the brain, AGS3 is expressed as a full-length protein. In the heart, a short isoform featuring solely three GPR motifs is expressed (139).

AGS4 and PCP2 are relatively simple GPR motif proteins and do not appear to have additional domains outside of the GPR motifs. RGS12, RGS14, and Rap1GAP1 all have additional GAP domains outside the GPR motif. RGS12 and RGS14 possess RGS domains that GAP heterotrimeric G proteins (140) while Rap1GAP1 is a GAP for the small GTPase Rap proteins (141). Both RGS12 and RGS14 also feature tandem two Ras/Rap binding

domains (RBDs) (126). RGS12 features two additional domains with N-terminal PDZ and PTB domains (76).

Group II AGS proteins containing multiple GPR motifs can bind multiple G proteins simultaneously (134,142,143). It has been postulated that these multiple G protein binding sites may allow GPR proteins to form scaffolds and organize Gα proteins within cellular membranes (143,144). Potentially multiple GPR motif containing proteins tether Gα proteins in microdomains to regulate GPCR or other non-canonical signaling.

Group II AGS proteins have been implicated in non-canonical G protein signaling in the Golgi. G proteins are known to exist within the Golgi where they are modified and trafficked to the plasma membrane (28,145,146). Additionally, after receptor stimulation, AGS3 has been reported to translocate to the Golgi, where it may regulate the function of Gα (147). AGS4 has also been implicated in regulation of Gα signaling within the Golgi where it was also shown to bind Gβ (148). Nevertheless, while GPR motif proteins have been observed in the Golgi, the functional role of these proteins in the Golgi remains to be fully elucidated.

A large focus of non-canonical G protein signaling has focused on the role of Gα and accessory proteins in cell division. Group II AGS proteins have been heavily implicated in asymmetric cell division (ACD). The role of GPR proteins in ACD was first identified in partner of inscuteable (Pins) (138,149,150). Pins, the *Drosophila* homologue of LGN and AGS3, forms a ternary complex with inscuteable (Insc) and inactive Gαi1-GDP that localizes to the apical cell cortex to direct spindle orientation in *Drosophila* neuroblasts (149,151,152). The ternary complex then interacts with Mud, the *Drosophila* homologue of NuMA and a microtubule binding protein, to recruit dynein and position the mitotic spindle on the apicobasal axis (153-156).

As homologues of Pins, AGS3 and LGN have been intensely studied for their roles in mammalian cell division. AGS3 and LGN exhibit 59% sequence identity, with most sequence variations found in linker regions between the seven TPR domains and four GPR motifs. AGS3 is expressed in the brain, testes, and heart (139) while LGN is ubiquitous throughout the body (157). In the brain, AGS3 expression is restricted to neurons while LGN is expressed in neurons, astrocytes, and glia (157). In primary human neural progenitor cells (NPCs), LGN was shown to localize asymmetrically during mitosis while AGS3 remains symmetrically distributed suggesting LGN has a similar role to Pins in mammalian ACD (158).

While a majority of research has focused on the role of Pins/LGN in mitotic spindle formation, other GPR motif proteins have been implicated in cell division dynamics as well, including RGS12 (159) and RGS14 (160). Moreover, Group I AGS proteins, specifically Ric-8, have been implicated in regulating mitotic spindle formation (161). These studies highlight the non-canonical role G proteins play in cell division dynamics and also the roles of non-canonical G protein accessory proteins.

1.6 Regulator of G Protein Signaling 14 (RGS14)

The Regulator of G protein Signaling 14 (RGS14) is a multifunctional scaffolding protein providing unique regulation of heterotrimeric and small G protein signaling. RGS14, a member of the D/R12 family of RGS proteins, features an N-terminal RGS domain, two tandem Ras/Rap binding domains (RBDs), and a C-terminal GPR motif. RGS14, along with RGS12, are the only two known proteins to possess an RGS domain and GPR motif. This unique domain structure provides an intriguing link between canonical G protein signaling (RGS domain) and non-canonical G protein signaling (GPR motif) (Figure 1.1).

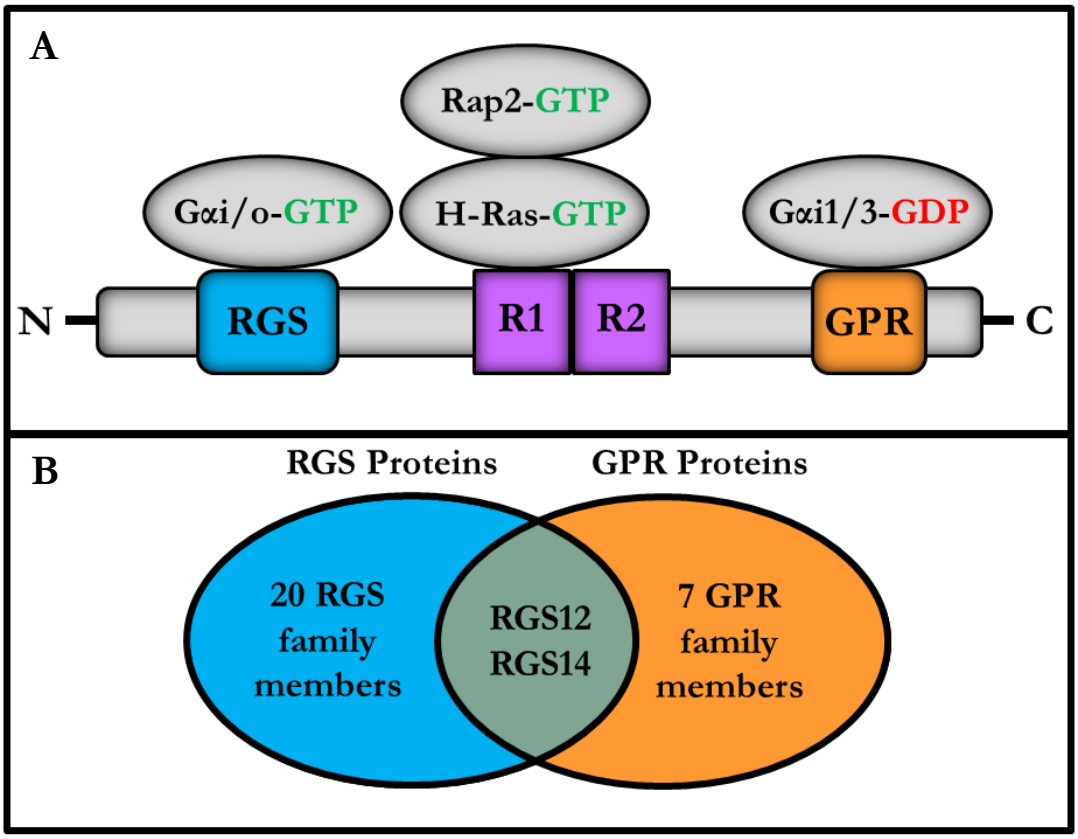

Figure 1.1. RGS14 Domain Structure, Binding Partners, and Placement in RGS and GPR Families. (A) RGS14 possesses an RGS domain, two tandem Ras binding domains (R1, R2), and a GPR motif. The RGS domain selectively binds activated Gαi/o proteins. Activated Rap2 and H-Ras proteins bind the first (R1) of the two Ras binding domains. The GPR motif specifically binds inactive Gαi1/3 proteins. **(B)** RGS14 is one of two proteins that contain both an RGS domain and a GPR motif. With an RGS domain and a GPR motif, RGS14 sits at the intersection of canonical and non-canonical G protein signaling pathways.

RGS14 was first deposited in GenBank as a novel Rap binding partner (GenBank U85055) and later identified as a Rap2 effector in a yeast two-hybrid screen (162). An independent PCR screen for RGS proteins first cloned the full length RGS14 cDNA from rat (140). Early *in vitro* characterization studies demonstrated the RGS domain serves as a GAP for Gαi/o proteins (75,162,163) while the GPR motif specifically binds Gαi1/3 proteins (130,163,164). Later, RGS14 was also shown to bind activated H-Ras (165-167). Binding of both H-Ras and Rap2 was shown to be mediated by the first RBD as mutation of a key arginine residue (R333 in rat) resulted in loss of binding by these small GTPases (133,165,166,168).

RGS14 is expressed in the thymus, lymphocytes, and spleen suggesting a role for RGS14 within the immune system (140,162,163). RGS14 expression increased after anti-CD40/anti-IgM challenge to primary B cells (75). Additionally, RGS14 expression also increased after anti-CD3/IL-2 challenge to primary T cells (75). Though the role of RGS14 in the immune system has not been fully characterized, some evidence suggests RGS14 regulates chemokine signaling downstream of the IL-8 receptor (75).

RGS14 is also highly expressed in the brain (140,162,163), specifically within pyramidal neurons of area CA2 of the hippocampus (169,170). Examination of hippocampal RGS14 expression in C57BL/6J mice demonstrated both mRNA and protein became detectable at postnatal day 7 (P7) and increased into adulthood (170). The functional role of RGS14 in the brain began to be elucidated in an RGS14-KO mouse model. RGS14-WT mice are naturally resistant to long-term potentiation (LTP) at CA3 Schaffer collateral synapses onto CA2 neurons (169,171). LTP is believed to be the molecular correlate of learning and memory. In addition to excitatory postsynaptic potentials (EPSPs) of the postsynaptic neuron, cytoskeletal, transcriptional, and translational changes occur to

strengthen the synapse. Loss of RGS14 expression in RGS14-KO mice resulted in robust induction of LTP in response to high frequency stimulation (169). Moreover, RGS14-KO mice demonstrated enhanced spatial learning and object recognition memory compared to their wild-type littermates (169). These results highlight the role of RGS14 as a natural suppressor of hippocampal-dependent learning and memory.

While RGS14 has been implicated in regulation of LTP, learning, and memory, how RGS14 regulates and integrates synaptic signaling is not well understood. Electron microscopy revealed RGS14 is expressed within dendritic spines, necks and at the postsynaptic density (PSD) of CA2 pyramidal neurons (169), suggesting RGS14 regulates synaptic signaling. As RGS14 possesses two G protein interaction sites, RGS14 may suppress LTP through regulation of heterotrimeric G proteins.

Previous studies demonstrate RGS14 regulates G protein signaling in heterologous expression systems. In HeLa cells expressing RGS14, co-expression with inactive Gαi1/3 protein localizes RGS14 to the plasma membrane (172). Furthermore, recent evidence suggests GPR proteins form Gα-dependent complexes with GPCRs at the plasma membrane (173-175). In particular, RGS14 has been shown to associate with the α2A-adrenergic receptor via inactive Gα proteins in HEK 293 cells (173). Activation of the receptor causes this association to decrease, suggesting RGS14 binds inactive Gα proteins through its GPR motif to associate with the receptor (173).

It remains unclear whether RGS14 regulates G protein signaling downstream of a GPCR *in vivo*. Moreover, the role of postsynaptic Gαi/o signaling in CA2 hippocampal neurons is still being explored. The Gαi/o coupled A1 adenosine receptor is highly expressed in CA2 neurons. Antagonism of A1 receptors in CA2 with caffeine resulted in robust induction of LTP (176), though whether or not RGS14 plays a role in this mechanism

remains unknown.

RGS7, another Gαi/o selective GAP, has been shown to regulate synaptic plasticity in the CA1 subregion of the hippocampus. In an RGS7 knockout mouse model, loss of RGS7 results in hippocampal learning and memory deficits (91). The effects observed upon knockout of RGS7 appear to be mediated through $GABA_B$-GIRK channels (91). Loss of RGS7 potentiates $GABA_B$-GIRK signaling to hyperpolarize neurons and prevent LTP induction (91).

In contrast to RGS7, loss of RGS14 results in enhanced hippocampal learning and memory (169). This fundamental difference suggests RGS14 functions in a different manner than RGS7. Moreover, the presence of a secondary G protein interaction site in RGS14, namely the GPR motif, may introduce additional complexity to RGS14 function in regulating synaptic signaling.

1.7 Overall Hypothesis and Objective of this Research

One key question in dissecting RGS14 function is: how does RGS14 integrate Gα signaling? With an RGS domain and a GPR motif, RGS14 has the potential to engage Gαi proteins in a complementary manner in which the RGS domain could accelerate G protein inactivation and the GPR motif could then bind the newly inactivated G protein. Alternatively, one domain/motif may predominately dictate the overall function of RGS14 or each domain/motif may function independently from one another, regulating different areas of G protein signaling separately (Figure 1.2A).

A second key question is: does the GPR motif interfere with Gαβγ heterotrimer formation and impact Gβγ signaling? The binding of Gβγ and GPR motif proteins to Gα is mutually exclusive and other GPR motif containing proteins have been shown to interrupt

formation of Gαβγ heterotrimers (134-136). Additionally, GPR proteins, including RGS14, have been shown to associate with GPCRs through the GPR motif (173-175). Accordingly, RGS14 may function to displace Gβγ to limit Gα signaling and promote Gβγ signals (Figure 1.2B).

The primary goal of my dissertation project has been to understand the structure and function of RGS14. Crucial for understanding of RGS14 function is to understand how each domain/motif engages binding partners to integrate signals. Previous research in the Hepler Lab focused on each domain/motif in isolation, however the mechanism by which RGS14 integrates G protein signaling remains unknown.

Aim 1 of this project was to purify high quality RGS14 for biochemical characterization. Previously, RGS14 had been purified with the addition of tags which could alter the function of RGS14. I wanted to generate an untagged RGS14 in order to perform hydrogen-deuterium exchange coupled to mass spectrometry (HDX-MS) and single-turnover GTPase assays.

Aim 2 of this project was to study cell dynamics with bioluminescence resonance energy transfer (BRET). Utilizing different combinations of BRET tags on RGS14 and Gα binding partners, I wanted to examine RGS14 dynamics in live cells. Moreover, I wanted to study the effect of RGS14 on heterotrimeric signaling utilizing kinetic BRET. The methods for purifying high quality RGS14 and performing BRET assays in live cells are discussed in Chapters 2 and 3.

Aim 3 of this project was to understand the integration of two G protein binding sites by RGS14. As RGS14 contains an RGS domain to limit Gαi/o signaling and a GPR motif to bind inactive Gαi1/3 proteins, RGS14 is positioned to regulate G protein signaling in a unique way. I wanted to understand the structural dynamics regulating these interactions

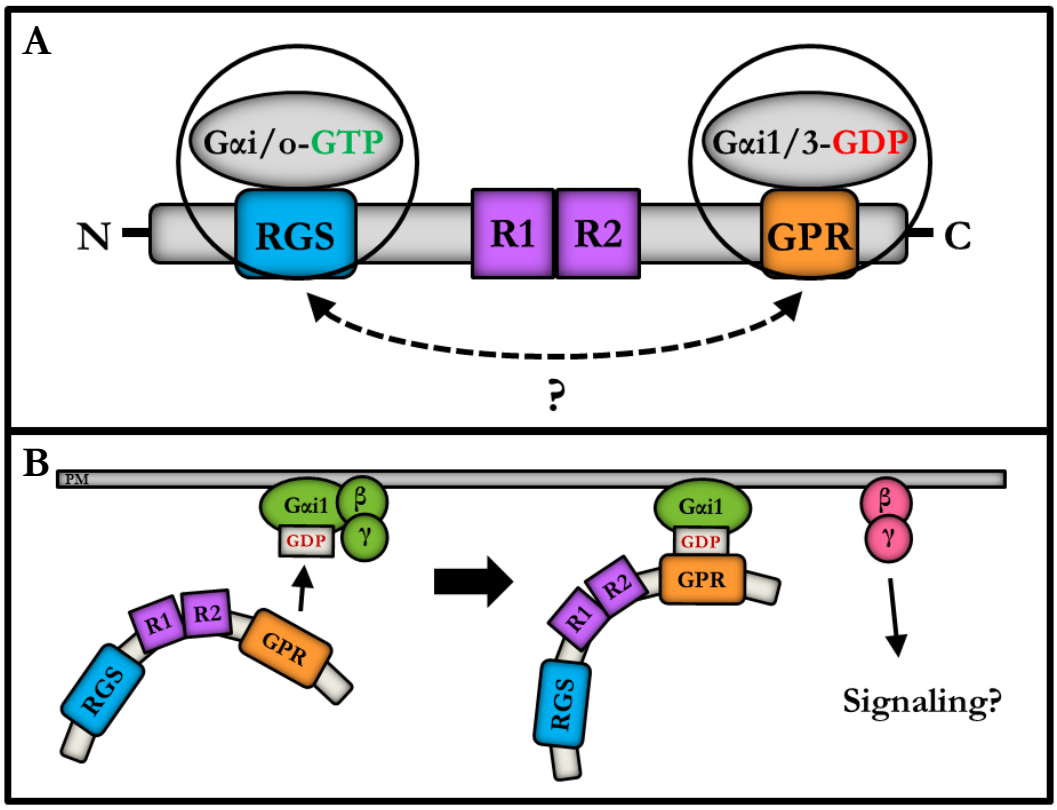

Figure 1.2. Potential Mechanisms of G Protein Regulation by RGS14. (A) With an RGS domain and a GPR motif, RGS14 has two distinct G protein interaction sites. These two sites may function independently or coordinate with one another to regulate G protein signaling output. **(B)** RGS14 selectively binds inactive Gαi1/3 proteins through its GPR motif to form a complex free of Gβγ. The GPR motif may be able to displace Gβγ prior to or after receptor stimulation. Competitive binding of the GPR motif could prevent Gβγ binding to Gα and promote Gβγ signaling cascades.

using purified proteins in conjunction with HDX-MS and single-turnover GTPase assays as well as cellular dynamics utilizing confocal microscopy and BRET. The results of these studies are discussed in Chapter 4.

Aim 4 of this project was to understand the role of RGS14 in Gβγ signaling. As RGS14 binds Gα subunits devoid of Gβγ, I wanted to understand the consequent effects of RGS14:Gαi complex formation on Gβγ signaling. Utilizing a biosensor for Gβγ activation, I monitored the effect of RGS14 on heterotrimeric signaling in response to GPCR activation. The results of these studies are discussed in Chapter 5.

The overall goal of these studies was to understand how RGS14 utilizes its two G protein binding sites to regulate heterotrimeric G protein signaling. The primary findings of these studies indicate: [1] RGS14 is a dynamic protein that adopts different conformations upon binding different partners; [2] RGS14 engages two G proteins simultaneously; [3] binding of a G protein at the GPR motif does not alter GAP activity at the RGS domain; and [4] RGS14 does not alter the assembly of G protein heterotrimers before or after receptor stimulation.

Chapter 2: Protein Purification Methods to Purify RGS14 and RGS14:Gα Complexes

2.1 Introduction

RGS14 is a multifunctional scaffolding protein that integrates different G protein signaling pathways. With an N-terminal RGS domain, two tandem Ras binding domains (RBDs), and a C-terminal GPR motif, RGS14 sits at the intersection of multiple signaling pathways. The RGS domain selectively binds activated Gαi/o proteins and stimulates their intrinsic GTPase activity to terminate G protein signaling (75,162,163). The GPR motif specifically binds inactive Gαi1/3 proteins to prevent GDP dissociation (130,163,164). The first RBD has been shown to bind activated H-Ras and Rap2 proteins while the second RBD has still yet to be characterized with biochemical function (165-167).

Earlier work in the Hepler lab had determined that RGS14 is an intrinsically unstable protein that readily degrades when over-expressed as a recombinant protein. Therefore, in order to better understand the biochemistry of RGS14, I embarked on developing a strategy for the purification of full length RGS14 as well as several truncation mutants. Purified RGS14 is crucial for biochemical study of RGS14 function. RGS14 can be co-purified with protein binding partners to examine the functional consequences of RGS14 in complex. Dynamics can be studied utilizing hydrogen-deuterium exchange mass spectrometry (HDX-MS) (177). Purified RGS14 can be utilized in GTPase assays to examine the effect of the RGS domain on the intrinsic GTP activity of Gαi/o proteins (163,177). Phosphorylation can be assessed utilizing *in vitro* phosphorylation assays (178). The function of the GPR motif can be assessed by monitoring the dissociation of guanine nucleotides from G protein binding partners (163). Moreover, if purified to homogeneity, proteins can be utilized in crystallization screens as a precursor to x-ray crystallography or single particle analysis as a precursor to cryo-electron microscopy for structural determination (179).

Purification of recombinant proteins is most easily accomplished in *Escherichia coli*, a

Gram negative bacterium. Other commonly used methods rely on *Spodoptera frugiperda* 9 (SF9) insect cells or human embryonic kidney (HEK) 293 cells, though these methods are more laborious and costly. SF9 cells require the use of baculovirus for delivery of the recombinant DNA which is more time consuming and expensive to develop (180). HEK 293 cells are more costly to maintain than both *E. coli* and SF9 cells (180). Despite these drawbacks, SF9 cells and HEK 293 cells are particularly useful for purifications in which *E. coli* codon bias alters expression or folding of the protein from the original host (181). Moreover, *E. coli* lack the modifying enzymes and molecular machinery to recognize eukaryotic sites for post-translational modifications. Accordingly, important functional modifications may not be present in proteins purified from bacterial hosts (182). Due to the ease and lower cost of production in *E. coli*, researchers often attempt to purify recombinant proteins in *E. coli* first and then attempt SF9 or HEK 293 cells if the resulting protein is insufficient. As such, approximately 90% of proteins deposited within the Protein Data Bank have been produced in *E. coli* (180).

Common purification strategies utilize affinity tags to aid the purification. Often, affinity chromatography is the first step in a purification scheme as it provides easy capture of the target protein. Small affinity tags such as hexahistadine (His_6) allow for easy purification and the small size of the tag may not disrupt the function of the recombinant protein. Hexahistidine tags are utilized in immobilized metal ion affinity chromatography (IMAC) (183). IMAC columns are commonly composed of transition metals, such as Ni^{2+} or Co^{2+}, covalently bound to agarose. Hexahistidine tags bind specifically and with high affinity to the metal while other untagged proteins do not bind and remain in the flow through. Bound proteins can be eluted with imidazole, which competes with the histidine moieties within the protein tag for metal binding sites (183).

Other common affinity tags include maltose binding protein (MBP) or glutathione S-transferase (GST). MBP fusion proteins can be purified with immobilized amylose resins while GST fusion proteins can be purified with glutathione conjugated resins (184,185). While these tags add bulk to the purified protein, they also can increase the solubility of the protein (186). In comparison to hexahistidine tags, MBP and GST affinity tags often result in cleaner purifications that may not require additional polishing steps. However, amylose resins can be cumbersome and reduced glutathione can become expensive if utilized constantly. This has prompted many researchers to adopt a dual tag technique in which the recombinant protein is fused to both hexahistidine and MBP or GST tags (185). While MBP and GST aid in soluble expression of the recombinant protein, the protein can be recovered easily and in a cost effective manner through the hexahistidine tag (185).

Depending on purity after the initial capture, additional polishing steps may be required. Polishing steps often include techniques such as size-exclusion and/or ion exchange chromatography. In size-exclusion chromatography, proteins are applied to a column made from Superdex, Sephadex, or Sephacryl resins. These resins are composed of cross-linked sugar moieties that form small pores (187). Upon adding a protein sample to the resin, larger proteins are excluded from the pores, while smaller proteins become entrenched and take longer to move through the column (187). In this way, size-exclusion chromatography separates proteins by size.

Ion exchange chromatography separates proteins by charge. Ion exchange columns can be positively charged or negatively charged. Protein samples are loaded with a low salt buffer, or low ionic strength. The low salt buffer allows the proteins to interact with the column. After binding, proteins can be eluted with increasing ionic strength by increasing the salt concentration of the buffer (187). As the ionic strength increases, the ions displace the

protein from the column. Alternatively, proteins can be eluted off by a change in pH. Depending on the isoelectric point of the protein of interest, changing the pH alters the affinity of the protein for the ion exchange matrix (187). Of note, care must be taken to ensure the protein of interest is stable within the pH range used.

With every purification strategy, addition of a fusion tag may alter the function of the protein (188). Therefore it is often advantageous to remove the purification tag before using the protein in functional assays. One strategy to remove fusion tags has been to encode consensus protease cleavage sites between the tag and the recombinant protein of interest. Purification tags have successfully been removed with proteases such as enteropeptidase and thrombin, though these proteases can cleave elsewhere besides their target cleavage sites. Tobacco Etch Virus (TEV) protease has greater specificity for its target sequence and has been utilized for removal of recombinant fusion protein tags (189).

Using a simple affinity tag approach, such as hexahistidine, does not allow for optimal production of recombinant RGS14 in *E. coli*. Recombinant His_6-RGS14 is not well expressed in *E. coli* and leads to small recovery of the full length protein. Thus, I embarked on creating a dual-tagged RGS14 utilizing the pLIC-His_6-MBP-TEV vector. The pLIC-His_6-MBP-TEV vector contains a hexahistidine tag for affinity purification followed by an MBP tag to increase expression of soluble protein in the *E. coli* host. Moreover, a TEV protease cleavage site placed between the His_6-MPB tag and the RGS14 cDNA allows removal of His_6-MBP after the initial affinity purification step. The His_6-MBP tag and TEV protease can then be separated from RGS14 using size-exclusion chromatography with tandem Superdex S75/S200 columns to provide optimal separation. Thus, my strategy for purification of RGS14 requires three steps: immobilized metal affinity chromatography utilizing Ni^{2+}, cleavage of the His_6 affinity and MBP expression tags, and size-exclusion chromatography.

I have successfully applied this approach to the purification of full length RGS14 as well as RGS14 truncation mutants. The full length RGS14 protein encompasses amino acids 1-544 of rat RGS14 while the truncations encompass amino acids 300-525 and 300-444 (Figure 2.1). The 300-525 truncation mutant includes both Ras binding domains (RBDs) and the GPR motif while the 300-444 truncation is limited to just the RBDs. While the purification of Gα proteins is described elsewhere (190), I detail the purification of RGS14:Gα complexes for use in biochemical assays.

2.2 Materials

2.2.1 Bacterial Strain and Plasmid

1. BL21 (DE3) *Escherichia coli* (*see* **Note 1**)
2. pLic-His_6-MBP-TEV vector containing RGS14 (*see* **Note 2**)

2.2.2 Bacterial Culture Media

1. Luria-Bertani (LB) media
    a. 1% (w/v) tryptone, 1% (w/v) NaCl, and 0.5% (w/v) yeast extract prepared in dH_2O
    b. Prepare 200 mL LB media in 500 mL Erlenmeyer flasks and 1 L LB media in 2 L Erlenmeyer flasks.
    c. Sterilize LB media by autoclaving and store at room temperature.
2. Isopropyl β-D-1-thiogalactopyranoside (IPTG)
    a. Stock concentration: 1 M
    b. Store at -20°C
3. Carbenicillin (*see* **Note 3**)
    a. Stock concentration: 50 mg/mL

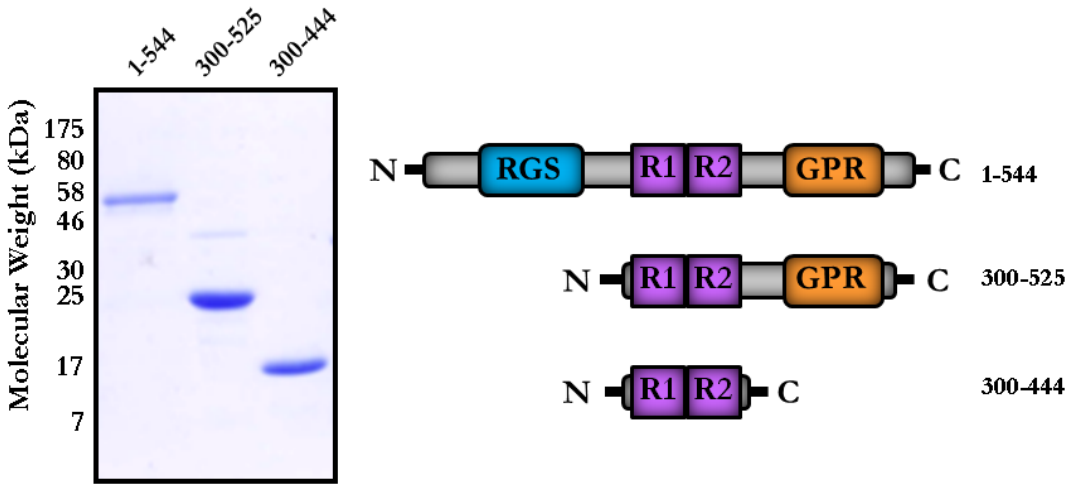

Figure 2.1. Coomassie Stained Gel of Full Length RGS14 and RGS14 Truncations. Full length RGS14 (amino acids 1-544) was purified using a combination of Ni^{2+} affinity chromatography and tandem S75/S200 size-exclusion chromatography. The same method was applied to purification of two RGS14 truncation mutants. The first truncation mutant features amino acids 300-525 and contains both Ras binding domains and the GPR motif. The second truncation mutant features amino acids 300-444 and contains only the Ras binding domains.

b. Store at -20°C

2.2.3 Reagents

1. Purified TEV-protease (*see* **Note 4**)
2. Purified Gαi/o proteins as described previously (190)
3. Slide-A-Lyzer™ Dialysis Cassettes (Thermo) with 3500 Da molecular weight cut off
4. Amicon® Ultra Centrifugal Concentrators with 10,000 Da molecular weight cut off
5. 0.22 μm vacuum filters (Nalgene Rapid Flow)
6. SDS-PAGE apparatus and polyacrylamide gels
7. Coomassie Brilliant Blue Stain
8. Bovine pancreas DNase I (Sigma)
9. cOmplete EDTA-free protease inhibitor tablets (Roche)

2.2.4 Buffer Compositions

1. Resuspension Buffer
    a. 50mM HEPES pH 7.4, 150 mM NaCl, 2mM β-mercaptoethanol (BME), 0.1 mM phenylmethylsulfonyl fluoride (PMSF), 10% glycerol, 20mM imidazole
2. Loading Buffer
    a. 50mM HEPES pH 7.4, 150 mM NaCl, 2mM β-mercaptoethanol (BME), 0.1 mM phenylmethylsulfonyl fluoride (PMSF), 10% glycerol, 20mM imidazole
    b. Filtered and degassed utilizing 0.22 μm vacuum filters and cooled to 4°C prior to use
3. Elution Buffer
    a. 50mM HEPES pH 7.4, 150 mM NaCl, 2mM β-mercaptoethanol (BME), 0.1 mM phenylmethylsulfonyl fluoride (PMSF), 150mM imidazole
    b. Filtered and degassed utilizing 0.22 μm vacuum filters and cooled to 4°C

prior to use

4. Dialysis Buffer
    a. 50mM HEPES pH 7.4, 150 mM NaCl, 2mM DTT
    b. Cooled to 4°C prior to use
5. Size-Exclusion Chromatography Buffer
    a. 50mM HEPES pH 7.4, 150 mM NaCl, 2mM DTT
    b. Filtered and degassed utilizing 0.22 μm vacuum filters and cooled to 4°C prior to use
6. Size-Exclusion Buffer Chromatography for Purification of RGS14:Gα Protein Complexes
    a. For RGS14 GPR:Gα complexes, utilize 50mM HEPES pH 7.4, 150 mM NaCl, 2mM DTT, 2 mM $MgCl_2$, 10 μM GDP
    b. For RGS14 RGS:Gα complexes, utilize 50mM HEPES pH 7.4, 150 mM NaCl, 2mM DTT, 10 μM GDP, 10 mM NaF, 10 $MgCl_2$, 30 μM $AlCl_3$ (*see* **Note 5**)
    c. All buffers must be filtered and degassed utilizing 0.22 μm vacuum filters and cooled to 4°C prior to use.

2.2.5 Nickel Affinity Chromatography

1. His-Trap FF crude 1 mL column (GE) (*see* **Note 6**)

2.2.6 Size-Exclusion Chromatography

1. Superdex 75 G10/300 24 mL column (separation 3,000-70,000 Da) (GE)
2. Superdex 200 G10/300 24 mL column (separation 10,000 – 600,000 Da) (GE)

2.2.7 Instrumentation

1. French Press (*see* **Note 7**)

2. Äkta Purifier (GE) stored in 4°C cold box (*see* **Note 8**)

2.3 Methods

2.3.1 Large-Scale Bacterial Culture

a. Begin a starter culture early in the day by inoculating 5 mL of LB media containing 50 μg/mL carbenicillin with a single colony picked from a freshly streaked plate of transformed *E. coli*.

b. Place the starter culture in a shaking incubator at 37°C at 200 rpm.

c. At the end of the day, add the 5 mL starter culture to 200 mL of LB containing 50 μg/mL carbenicillin and grow in a shaking incubator at 37°C overnight at 200 rpm.

d. The following day, add 20 mL of the overnight culture to 1liter of LB containing 50 μg/mL carbenicillin (s*ee* **Note 9**).

e. Place the flasks in a shaking incubator at 37°C and grow until the optical density 600 (OD600) reaches 0.6.

f. Add 1 mM IPTG to induce recombinant protein expression for 4 hours at 37°C in a shaking incubator at 200 rpm (s*ee* **Note 10**).

g. Transfer cultures to 1 L bottles and centrifuge at 3,000 rpm for 20 minutes to pellet bacteria.

h. After centrifugation, remove the LB media supernatant and treat with Bacdown Detergent Disinfectant or other bacterial disinfectant for 20 minutes prior to disposal.

i. Resuspend the bacterial pellet in the Resuspension Buffer using approximately 30 mL Resuspension Buffer for each liter of bacteria.

j. Place the resuspended bacteria into 50 mL conical tubes and snap freeze in liquid

nitrogen.

k. Store frozen cell pellets at -80°C until needed.

2.3.2 Cell Lysis

a. Thaw frozen cell pellet in a 37°C water bath until just thawed, then place on ice.

b. While thawing, add 5 mM $MgCl_2$, 1X cOmplete protease inhibitor tablet, and 10 mg of DNase I to each conical tube.

c. Use French Press apparatus to lyse bacteria (*see* **Note 7**).

d. Remove lysed membranes and any unlysed bacteria by centrifugation in a Ti45 rotor at 36,000 rpm at 4°C for 1 hour.

e. Collect the supernatant for nickel affinity chromatography.

2.3.3 Nickel Affinity Chromatography

a. Perform all steps at 4°C.

b. Connect 1 mL prepacked (HisTrap FF crude) column to Äkta Purifier.

c. Prepare the column by washing the resin with 5 column volumes (CV) of cold, filtered, and degassed dH_2O (*see* **Note 11**).

d. Equilibrate the column with 5 CV of Loading Buffer.

e. Apply the cleared lysate to the column and collect the flow through.

f. Apply the flow through to the column two additional times to ensure adequate binding of protein to the resin.

g. Wash the column with 20 CV Loading Buffer to remove any contaminating proteins.

h. Elute with 10 CV Elution buffer and collect fractions.

i. Assay fractions with SDS-PAGE and coomassie staining as shown in Figure 2.2A.

j. Pool fractions containing RGS14.

k. Determine protein concentration using Bradford Assay.

l. Add TEV protease (1:200) and dialyze overnight into Dialysis Buffer using Slide-A-Lyzer™ dialysis cassettes at 4°C.

2.3.4 Size-Exclusion Chromatography

a. Perform all steps at 4°C.

b. Connect 24 mL S75 and S200 columns in tandem to Äkta Purifier.

c. Equilibrate columns with 100 mL of Size-Exclusion Chromatography Buffer (*see* **Note 12**).

d. Remove protein sample from Slide-A-Lyzer™ dialysis cassette and concentrate to less than 2 mL using Amicon® Ultra Centrifugal Concentrators.

e. Load the concentrated protein sample to the Äkta Purifier utilizing an appropriately sized attached loop.

f. Apply the protein to the tandem S75/S200 columns and collect fractions.

g. Assay fractions with SDS-PAGE and coomassie staining as shown in Figure 2.2B.

h. Pool fractions containing RGS14.

i. Determine protein concentration using Bradford Assay.

j. Aliquot RGS14 protein, snap freeze in liquid nitrogen, and store at -80°C.

2.3.5 Size-Exclusion Chromatography Purification of RGS14:Gα Protein Complexes

a. Perform all steps at 4°C.

b. Connect 24 mL S75 and S200 columns in tandem to Äkta Purifier.

c. Equilibrate columns with 100 mL of Size-Exclusion Chromatography Buffer for either GPR:Gα complexes or RGS:Gα complexes.

d. Thaw RGS14 and Gα aliquots in 37°C water bath and transfer to ice immediately once thawed.

e. Combine RGS14 and Gα proteins 1:2 (RGS14:Gα) and incubate for 1 hour at 4°C

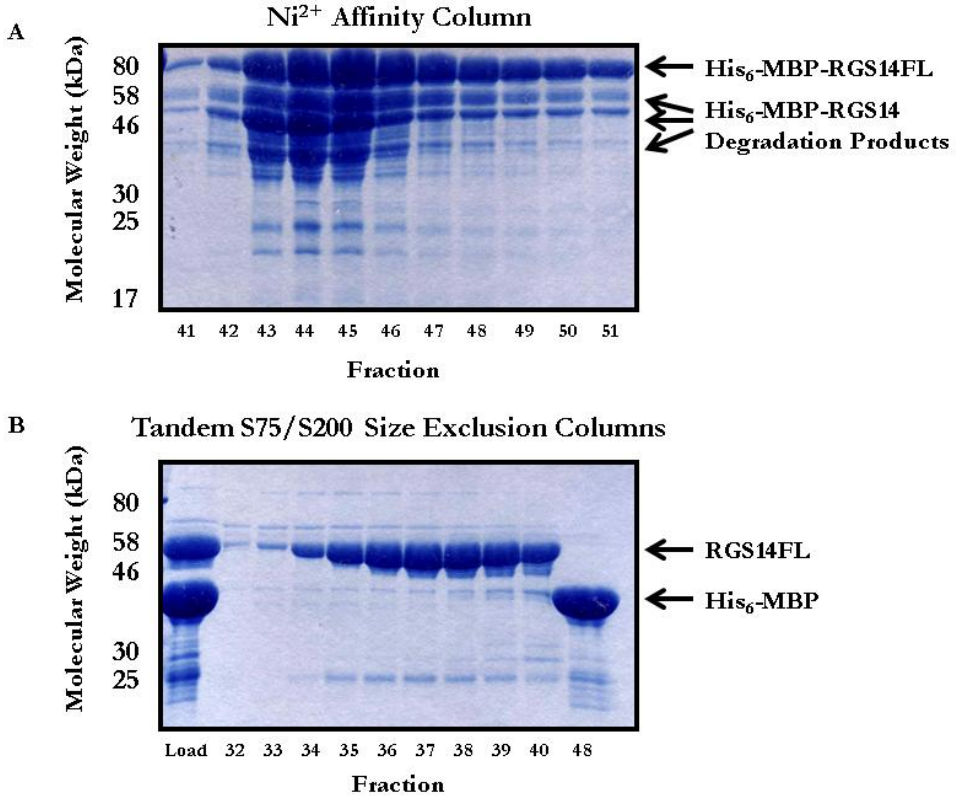

Figure 2.2. Purification of Full Length RGS14. **(A)** Heterologously expressed His_6-MBP-TEV-RGS14 was purified from *E.coli* lysate by Ni^{2+} affinity chromatography. After binding of His_6-MBP-TEV-RGS14 to the Ni^{2+} column, the column was washed with Loading Buffer and eluted with Elution Buffer. The collected elution fractions are show above. His_6-MBP-TEV-RGS14 is partially degraded when expressed in *E. coli* and three main degradation products were recovered along with the full length protein (His_6-MBP-RGS14FL). Fractions containing RGS14 were pooled and TEV protease was added prior to dialysis. **(B)** Dialyzed, TEV protease treated RGS14 was loaded to tandem S75/S200 size-exclusion columns. As shown in the Load, TEV protease treatment resulted in two main constituents: full length RGS14 and His_6-MBP. Separation over size-exclusion columns resulted in the fractions above. His_6-MBP (Fraction 48) eluted later than RGS14.

prior to beginning size-exclusion chromatography.

f. If necessary, concentrate to less than 2 mL using Amicon® Ultra Centrifugal Concentrators.

g. Load the protein sample to the Äkta Purifier utilizing an appropriately sized attached loop.

h. Apply the protein to the tandem S75/S200 columns and collect fractions.

i. Assay fractions with SDS-PAGE and coomassie staining as shown in Figure 2.3 and Figure 2.4.

j. Pool fractions containing RGS14:Gα complex.

k. Determine protein concentration using Bradford Assay.

l. Utilize RGS14:Gα complex in biochemistry assays or aliquot RGS14:Gα protein, snap freeze in liquid nitrogen, and store at -80°C.

2.4 Notes

1. BL21 (DE3) *E. coli* contain T7 polymerase incorporated into the bacterial genome under control of the lac operon (191,192). Addition of IPTG (a non-hydrolyzable lactose analogue) releases repression of T7 polymerase expression. *E. coli* transformed with a bacterial expression vector under a T7 promoter can then express the protein of interest. As *E. coli* lack endogenous T7 promoter sites, T7 polymerase only transcribes the transformed recombinant gene. BL21 (DE3) *E. coli* are advantageous heterologous protein expression hosts as they are a protease-deficient strain that allow high accumulation of recombinant proteins (182). Other strains have been optimized for expression of other recombinant

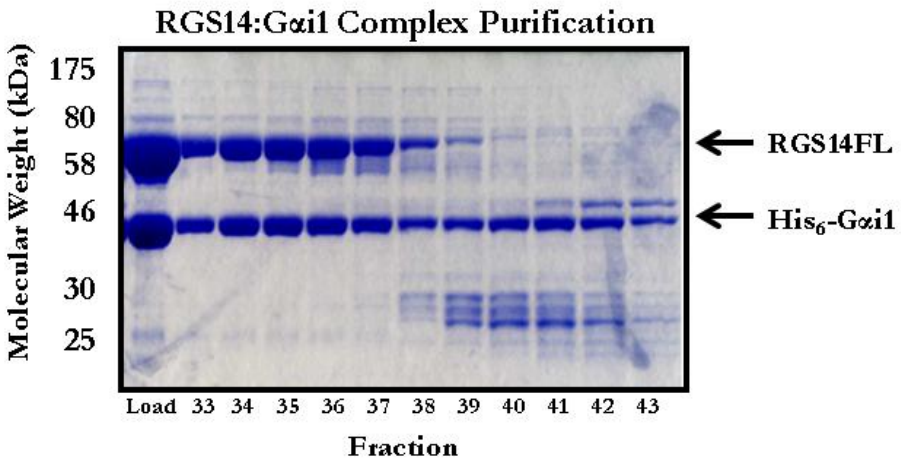

Figure 2.3. Purification of RGS14:Gαi1 Complex. RGS14 binds inactive Gαi1/3 proteins through the GPR motif. In order to make an RGS14:Gαi1 complex for biochemical characterization, full length RGS14 was incubated with inactive Gαi1-GDP for one hour prior to size-exclusion chromatography over tandem S75/S200 columns. Gαi1-GDP co-eluted with RGS14 in Fractions 33-37 while excess Gα eluted later in Fractions 40-43.

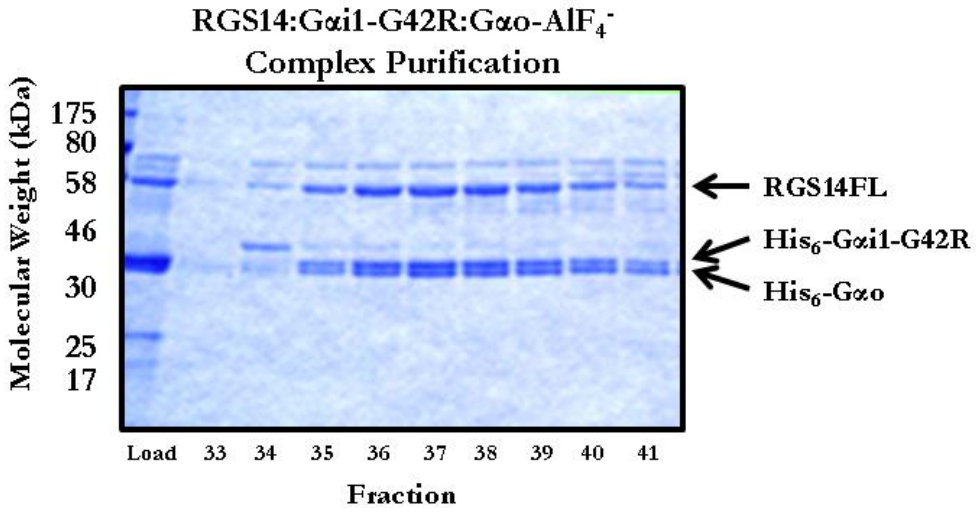

Figure 2.4. Purification of RGS14:Gαi1-G42R:Gαo-AlF_4^- Complex. RGS14 binds activated Gαi/o-GTP proteins through the RGS domain and inactive Gαi1/3-GDP proteins through the GPR motif. In order to form a high affinity complex between RGS14 and G proteins at the RGS domain, AlF_4^- must be added to mimic an activated G protein. In order to examine whether RGS14 can bind two G proteins simultaneously, with one G protein at the RGS domain and one G protein at the GPR motif, a mutant of Gαi1 that can bind the GPR motif in the presence of AlF_4^- was employed (Gαi1-G42R). Full length RGS14 was incubated with inactive Gαi1-G42R and Gαo in the presence of AlF_4^- for one hour prior to size-exclusion chromatography over tandem S75/S200 columns. Both Gαi1-G42R and Gαo co-eluted with RGS14 in Fractions 35-40, indicative of a trimeric complex.

proteins. For instance, C41 (DE3) and C43 (DE3) *E. coli* are useful for expression of membrane and toxic proteins (193). The choice of heterologous expression host for must be determined empirically. Bacterial hosts should be examined for expression of the full length recombinant protein upon induction. Moreover, purified protein should be assayed for function to ensure proper production in bacterial hosts.

2. Other bacterial expression vectors may be used with similar success. Traditional bacterial expression vectors such as pQE are commonly utilized protein expression vectors. Like pLIC vectors, pQE vectors utilize the T7 promoter which can be transcribed upon induction of T7 polymerase with IPTG. Other vectors, such as pBAD vectors, allow for titratable protein expression under the arabinose promoter.
3. We use carbenicillin for selection of ampicillin-resistant bacteria as carbenicillin is broken down more slowly by β-lactamase than ampicillin.
4. We utilize His_6-TEV protease that is purified in house though it can be purchased from commercial sources.
5. In order to prevent precipitation of aluminum, NaF, $MgCl_2$, and $AlCl_3$ must be added to the Size-Exclusion Chromatography Buffer in a specific order. NaF is added first, followed by $MgCl_2$, and finally $AlCl_3$.
6. For purification of full length RGS14 we typically employ a 1 mL HisTrap FF crude column (GE). The binding capacity of HisTrap columns is 40 mg His_6-tagged protein/1 mL resin bed. Truncated RGS14 constructs express better in BL21 (DE3) *E. coli* than the full length RGS14. Accordingly, we occasionally use a 5 mL HisTrap column with a total binding capacity of 200 mg for initial capture of RGS14 truncation proteins.
7. If a French Press is not available, *E. coli* can be lysed utilizing lysozyme and/or sonication. Lysozyme is a glycoside hydrolyase that breaks down the cell walls of bacteria

while sonication uses sound waves to disrupt cell membranes. When used in combination, lysozyme can reduce the amount of sonication required while sonication can enhance the efficiency of lysozyme by disrupting the outer cell membranes of Gram negative bacteria (194).

8. Other liquid chromatography systems can be utilized for protein purification with similar results. Ensure compatibility of all purification columns before embarking on purification with alternative equipment.
9. Typically we grow up 4-6 liters of bacterial culture at a time. More or less can be grown up depending on need and availability of shaking incubator space.
10. Induction of protein expression too quickly can result in misfolded, aggregated protein that can form insoluble inclusion bodies (195). Lowering the temperature to 15-23°C during induction can slow expression so that induced proteins have enough time to fold properly (182). The appropriate temperature for induction varies for different proteins and must be determined empirically.
11. Typically HisTrap FF crude columns can be run at a flow rate of 1 mL/min. For tandem S75/S200 columns the flow rate is typically 0.3 mL/min. These flow rates are chosen to prevent excess backpressure on the column beds that may ruin the column. For any column, ensure the backpressure does not exceed the limit specified by the column manufacturer.
12. Tandem S75/S200 column equilibration may be done overnight.

Chapter 3: Bioluminescence Resonance Energy Transfer to Detect Protein-Protein Interactions in Live Cells[1]

[1]This chapter has been slightly modified from the published manuscript. Brown NE, Blumer JB, and Hepler JR (2015) Bioluminescence Resonance Energy Transfer to Detect Protein-Protein Interactions in Live Cells. In: Protein-Protein Interactions: Methods and Applications, *Methods in Molecular Biology*, Second Edition (CL Meyerkord and H Fu, Editors), 1278, 457-65.

3.1 Introduction

Bioluminescence Resonance Energy Transfer (BRET) is a method of studying protein-protein interactions in live cells (196). BRET utilizes non-radiative energy transfer between energy donor and energy acceptor protein tags. The energy transfer occurs when the protein tags are in close proximity, as described by the Förster distance (197). As shown in Figure 3.1, BRET serves as a molecular ruler, detecting protein-protein interactions under 10 nm (*see* **Note 1**). For a comprehensive review, *see* refs. (198,199).

BRET makes use of a bioluminescent energy donor while the energy acceptor is a fluorophore. The choice of BRET pair is based on the overlap of the bioluminescent protein (donor) emission spectrum with the excitation spectrum of the fluorescent protein (acceptor). For BRET experiments, the most commonly chosen bioluminescent donor is luciferase from the sea pansy *Renilla reniformis*. *Renilla* luciferase (RLuc) catalyzes the oxidation of its substrate, coelenterazine, to produce blue light at 482 nm. The emission spectrum of RLuc overlaps well with the excitation spectra of the yellow fluorescent protein (YFP) family of proteins including the mutant YFP variants enhanced YFP (EYFP) and Venus (200) which emit light at ~527 nm (Figure 3.2). For more information on BRET pairs, *see* **Note 2**.

BRET has distinct advantages over other techniques to detect protein-protein interactions. First, BRET is amenable to detecting interactions in live cells, thus proteins retain posttranslational modifications and cellular trafficking regulations that may be important for protein-protein interactions. BRET is readily adaptable to almost any cell type that allows expression of the donor and acceptor proteins. In live cells, protein-protein interactions can be monitored in real time over a time-course or for a fixed time interval in

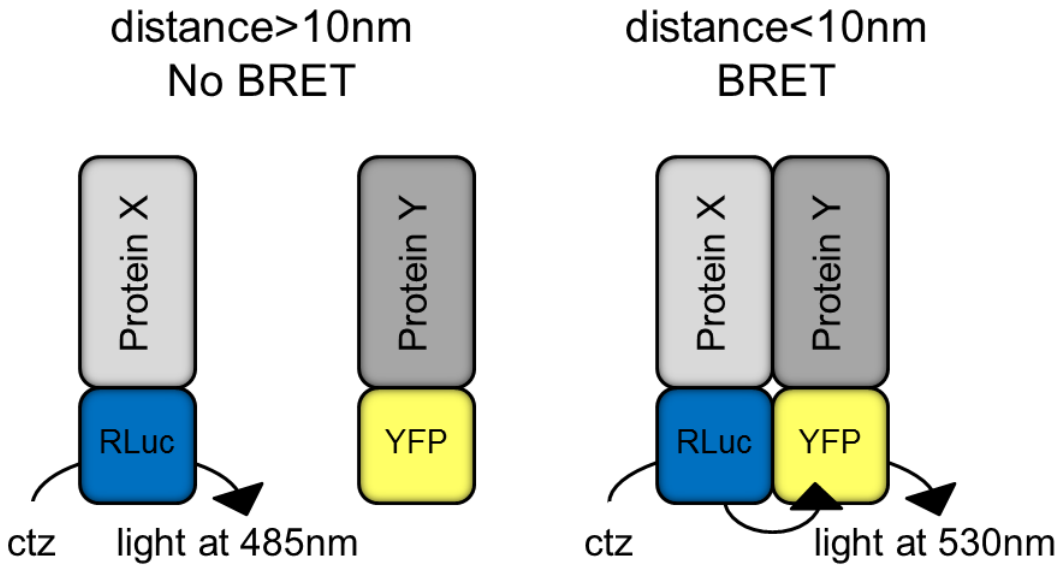

Figure 3.1. BRET is Dependent on the Distance between the Donor Luciferase and the Acceptor Fluorophore. Addition of the cell permeant Renilla luciferase substrate coelenterazine (ctz) results in oxidation of the substrate to coelenteramide, which produces blue light at 482 nm. When protein-protein interactions between Protein X and Protein Y bring the donor luciferase (RLuc) and acceptor fluorophore (YFP) in close proximity (<10 nm), the energy from the donor can be transferred to the acceptor and light is produced at 527 nm. When the BRET tags are not in close enough proximity, light is only emitted at 482 nm.

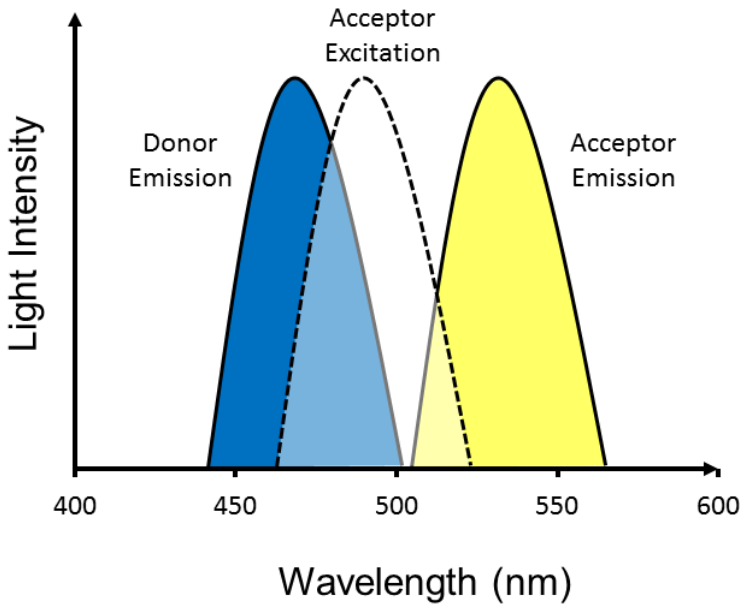

Figure 3.2. The Energy Transfer between BRET Pairs Depends on the Overlap of the Donor Emission Spectrum with the Excitation Spectrum of the Acceptor. For *Renilla* luciferase, oxidation of coelenterazine results in an emission peak at 482 nm. This emission overlaps well with the excitation spectrum of yellow fluorescent protein (excitation peak: 514 nm). The resulting energy transfer yields yellow light with an emission peak of 527 nm.

response to cellular treatments such as exposure to GPCR agonists, growth factors, or other drugs as an approach to define the regulation of protein complexes (173,175,201-205). Additionally, fusion of BRET pairs to the same recombinant protein can be used to develop small molecule biosensors (206). Methods have also been developed using BRET as a reporter for movement and subcellular location of target proteins (207). Moreover, unlike the similar technique fluorescence resonance energy transfer (FRET), BRET does not require external excitation but instead relies on the addition of the cell permeant substrate coelenterazine to initiate the assay, thereby endowing the experimenter with temporal control over the assay and preventing unintentional activation of the acceptor fluorophore. Given these many advantages, BRET can be readily adapted for high throughput screening for small molecule modulators of protein-protein interactions. For review, *see* refs. (204,208).

Below we describe a BRET experiment to explore the interactions between Regulator of G protein Signaling 14 (RGS14) and its binding partner Gαi1. RGS14 has previously been shown to interact with Gαi1 through its G protein regulatory (GPR) motif by traditional biochemical methods (130,163). We detail transfection of a C-terminal luciferase tagged RGS14 (RGS14-Luc) donor and internal YFP tagged Gαi1 (Gαi1-YFP) acceptor. We demonstrate a robust BRET signal between wild type RGS14 and Gαi1 that is disrupted with a mutant RGS14 (Q515A/R516A) that can no longer bind Gαi1. In our example, we show how to vary the acceptor protein expression level to achieve optimal net BRET signal. We describe how to calculate net BRET, acceptor/donor ratio, and fit the data using graphing software.

3.2 Materials

3.2.1 Cell Lines

1. Maintain HEK 293 cells in 1× Dulbecco's Modified Eagle Medium (DMEM) without phenol red indicator, supplemented with 2 mM L-glutamine, 100 U/mL penicillin, 100 mg/mL streptomycin, and 10 % fetal bovine serum (5 % for transfection). Grow cells in a humidified incubator with 5 % CO_2 at 37 °C.

3.2.2 Buffer Compositions/Stock Solutions

1. BRET buffer (Tyrode's solution): 140 mM NaCl, 5 mM KCl, 1 mM $MgCl_2$, 1 mM $CaCl_2$, 0.37 mM NaH_2PO_4, 24 mM $NaHCO_3$, 10 mM HEPES, pH 7.4, 0.1 % glucose.
2. Polyethylenimine (PEI) transfection reagent stock solution: Dissolve PEI (1 mg/mL) in dH_2O at 80 °C while stirring, cool and adjust to pH 7.2 using 0.1 N HCl and filter-sterilize. Aliquot and store at −80 °C. Use each aliquot only once.
3. Luciferase substrate stock solution: 2 mM benzyl coelenterazine H in 100 % ethanol containing 60 mM HCl, aliquot and store at −80 °C.

3.2.3 Instrumentation

1. Microplate reader with 485 nm emission and excitation filters, 530 nm emission filters, and compatible white-bottomed 96-well plates (*see* **Note 3**).
2. Compatible microplate reader, spreadsheet, and graphing software (*see* **Note 3**).

3.2.4 Plasmids

1. Donor plasmids can be constructed by inserting your gene of interest into a vector containing the humanized RLuc gene. For construction of RGS14-Luc constructs presented below, rat RGS14 cDNA was inserted into the phRLuc-N2 vector, which places the RLuc tag at the C-terminus of RGS14. Determining the optimal location of the Rluc tag relative to the protein of interest is an important parameter and must be determined empirically (*see* **Note 1**).

2. For many BRET experiments, acceptor plasmids can be constructed by inserting your gene of interest into a commercially available vector encoding YFP, EYFP or Venus. For construction of Gαi1-YFP used below, insertion of the YFP tag at either terminus compromised the function of Gαi1. Thus, the Gαi1-YFP construct was engineered by inserting the YFP coding sequence between the b and c helices of the helical domain of Gαi1 which was then expressed in a pcDNA3.1 vector (34).

3.3 Methods

3.3.1 Experimental Setup

1. Below we describe an experiment where the donor expression level is set and the acceptor expression level is varied. This experimental setup will allow the acceptor to saturate the donor and provide a maximal BRET signal. The expression level should be empirically determined; however, we typically use donor plasmid amounts that yield relative luminescence units (RLU) of 100,000–350,000 in our microplate reader (TriStar LB 941). In our example, 5 ng of phRLuc-N2:: RGS14 yields an RLU of ~100,000–300,000 but this will vary for other donor constructs depending on transfection efficiency, the ability of the transfected cells to express the donor protein and the type of instrument used for detection. Additionally, on our microplate platform, we typically use acceptor plasmid amounts that yield relative fluorescence units (RFUs) of 30,000–200,000. In our example experiment, pcDNA3.1::Gαi1-YFP typically yields ~30,000–60,000 RFUs.
2. For the present experiment, 5 ng of the donor plasmid (RGS14-WT-Luc or RGS14-Q515A/R516A-Luc) was transfected with increasing amounts of acceptor (0, 10, 50, 100, 250, and 500 ng pcDNA3.1::Gαi1-YFP) (*see* **Note 4**).

3.3.2 Transient Transfection with Polyethylenimine (PEI) (See Note 5)

1. Seed 8×10^5 cells per well in six-well plates in 2 mL medium per well, grow in a humidified incubator at 37 °C overnight with 5 % CO_2.
2. Prior to transfection, change medium to 1× DMEM containing 2 mM L-glutamine, 100 U/mL penicillin, 100 mg/mL streptomycin, and 5 % fetal bovine serum, 2 mL per well.
3. Generate *solution A* by adding 8 µL of 1 mg/mL PEI from stock to 92 µL of serum-free medium for each well, allow this solution to incubate for 3 min.
4. Generate *solution B* by adding up to 1.5 µg of DNA to 100 µL of serum-free medium for each condition in 1.5 mL microcentrifuge tubes. DNA amount is adjusted to a final concentration of 1.5 µg by adding empty pcDNA3.1 plasmid.
5. Add 100 µL of solution A to microcentrifuge tubes containing solution B to create *solution C*.
6. Cap the 1.5 mL microcentrifuge tube and immediately vortex for 3 s.
7. Incubate solution C at room temperature for 15 min.
8. Add solution C (~200 µL) dropwise to the appropriate well of cells in the six-well plates.
9. Allow cells to grow for 1–2 days (the medium does not need to be changed for PEI transfection).

3.3.3 BRET

1. Immediately prior to beginning the BRET experiment, prepare coelenterazine by diluting the stock solution to 50 µM in room temperature BRET buffer (*see* **Note 6**).
2. Aspirate the transfection medium from the six-well plates.

3. To each well, add 750 µL of room temperature BRET buffer, using a pipette to gently remove the cells from the plate.
4. Plate 90 µL of the cells in triplicate into white-bottomed 96-well plates.
5. Load plate into plate reader and detect fluorescence levels (excitation: 485 nm, emission: 530 nm) using microplate reader software (*see* **Note 7**).
6. Add 10 µL of coelenterazine solution to each well (5 µM final concentration of coelenterazine per well).
7. Incubate the cells with coelenterazine for 2 min at room temperature.
8. Take BRET readings by measuring luminescence at 485 ± 20 nm and fluorescence at 530 ± 20 nm (*see* **Note 8**).

3.3.4 Analysis

1. Export fluorescence and BRET data into spreadsheet software.
2. The BRET ratio can be determined by dividing fluorescence by luminescence (BRET readings at 530/485 nm).
3. Calculate net BRET by subtracting out background luminescence (BRET readings in cells expressing the donor without any acceptor).
4. Calculate the acceptor/donor ratio by dividing the initial fluorescence measurements (530 nm) by the luminescence measurements (485 nm).
5. Using graphing software, plot the acceptor/donor ratio against the net BRET as in Figure 3.3. The data can then be fit using a nonlinear regression, (typically a one-site binding [hyperbola] is the most appropriate) to observe BRET saturation as a key indicator of signal specificity.

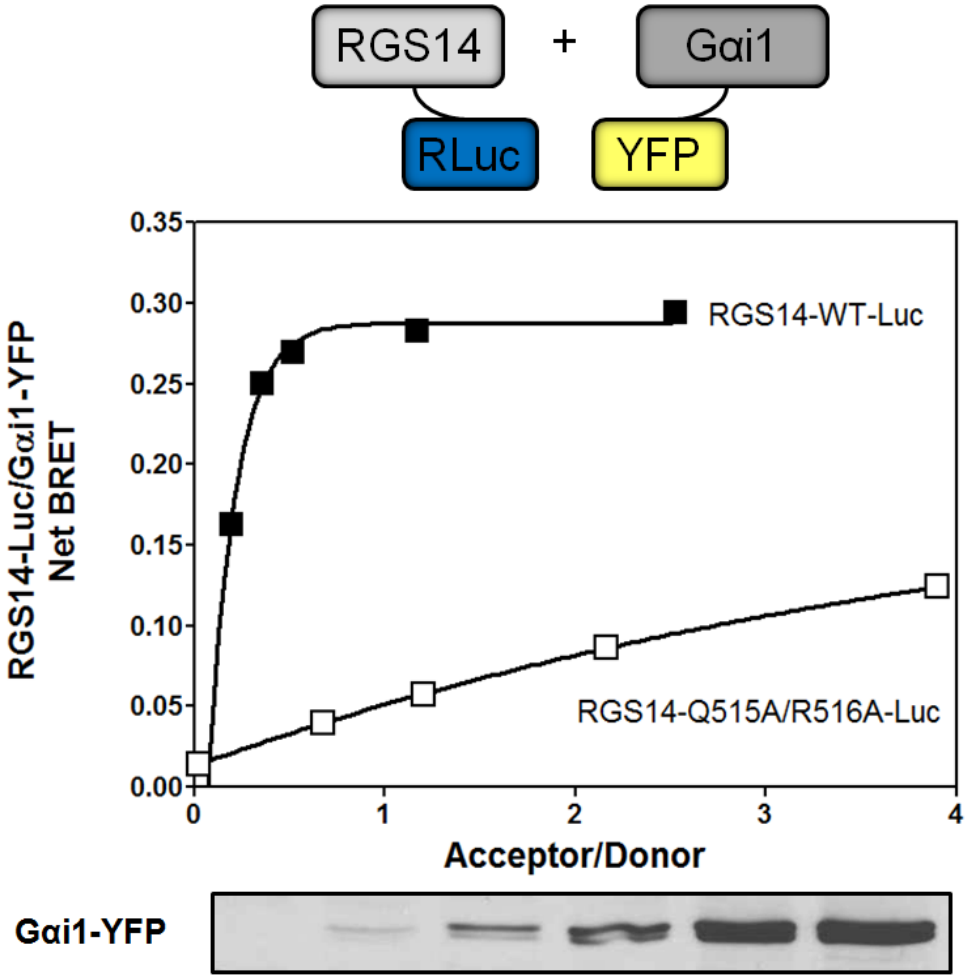

Figure 3.3. RGS14-Luc Exhibits Robust Net BRET with Gαi1-YFP. HEK 293 cells were transfected with increasing amounts of Gαi1-YFP (0, 10, 50, 100, 250, and 500 ng) and either 5 ng RGS14-WT-Luc or RGS14-Q515A/R516A-Luc. Wild type RGS14 shows a robust BRET signal with Gαi1. Conversely, the RGS14 mutant (Q515A/R516A) that can no longer bind Gαi1 shows a drastically reduced maximal BRET signal indicating a disruption in the protein-protein interaction. The above data is representative of three independent experiments. Curves were generated with GraphPad Prism 5 using the one-site binding curve fitting function. Additionally, Gαi1-YFP expression levels were verified by immunoblot analysis.

3.4 Notes

1. BRET efficiency (donor energy transfer to acceptor) is sensitive to the donor-acceptor proximity and is inversely proportional to the sixth power of distance between them. Thus, BRET signals generally reflect direct protein association; however, non-robust BRET signals can be detected due to close proximity without the occurrence of direct binding. For example, when a third intermediate protein brings the donor and acceptor into close proximity (173,175,205). In addition to proximity, BRET also depends on the orientation of the protein tag dipoles. Inefficient dipole coupling can prevent energy transfer, despite protein-protein interactions. Thus, it is advantageous to use linkers (typically four or more Gly residues) inserted between the proteins of interest and the BRET tags to allow sufficient movement of the tags. Moreover, placement of tags must be considered when engineering recombinant proteins with BRET tags. Placement of the BRET tag at the N-terminus, internally, or at the C-terminus of the protein can have a profound impact on the observed BRET signal and whether protein function is compromised. For example, placement of the luciferase tag at the N-terminus of RGS14 rather than the C-terminus results in a dramatic reduction in BRET signal with Gαi1-YFP. As another example, the acceptor YFP tag in Gαi1 cannot be placed at either termini without affecting protein function, and was placed internally between the b and c helices of the alpha helical domain with minimal consequences to Gαi1 function (34). Due to these considerations, two interacting proteins may not always be detected by BRET due to the distance between the tags or abnormal protein function or localization through improper tag placement.
2. Additional BRET pairs and BRET substrates have been developed. Many of these BRET pairs can be used with the method described above. For a comprehensive review

of other BRET pairs and substrates, *see* ref. (209).

3. We use the TriStar LB 941 Multimode Microplate Reader (Berthold Technologies) for our BRET experiments; however, other plate readers can be used with similar results. The plate reader must detect light signals at two distinct wavelengths either simultaneously or sequentially. In our assay, we use Berthold Technologies filters at 485 nm to measure luminescence and at 530 nm to measure fluorescence though similar filters can be purchased from other vendors. To collect BRET data, we use the MikroWin 2000 software (Mikrotek). MikroWin is specialized for microplate experiments and optimized to run with a variety of instruments from various manufacturers. Additionally, data collected in MikroWin can be exported and further analyzed in spreadsheet software such as Microsoft Excel. Data can then be graphed in graphing software such as GraphPad Prism.
4. In order to calculate net BRET, it is necessary to include a donor-only control (donor transfected without any acceptor). The donor-only control is used to assess any background BRET observed in the absence of acceptor. BRET from donor-only controls are subtracted from observed BRET values to calculate the net BRET.
5. Other transfection reagents can be used with similar results. We choose to use PEI as it yields high transfection efficiency and reproducibility at very affordable cost.
6. Coelenterazine is light sensitive and should be kept away from light exposure until ready to use. Dilute coelenterazine stock immediately before performing BRET to prevent breakdown of the substrate.
7. Initial fluorescence levels are taken to determine the acceptor/donor ratio as well as an internal control to verify expression of the fluorescently tagged protein. For experiments where the amount of donor is held constant and the amount of acceptor is increased,

corresponding increases of the acceptor should be observed in the fluorescence measurement.

8. As stated above, for detection on the TriStar platform, ideal luminescence should be about 100,000–350,000 relative luminescence units (RLUs). Ideal fluorescence should range between 30,000 and 200,000 relative fluorescence units (RFUs). As a corollary, typical acceptor/donor ratios range between 0 and 15; however, this number will vary depending on transfection efficiency and the expression level of the acceptor. In addition, lowering the level of donor expression will also inflate the acceptor/donor ratio.

Chapter 4: Integration of G Protein Alpha (Gα) Signaling by the Regulator of G Protein Signaling 14 (RGS14)[2]

[2]This chapter has been slightly modified from the published manuscript. Brown NE, Goswami D, Branch MR, Ramineni S, Ortlund EA, Griffin PR, Hepler JR (2015) Integration of G protein alpha (Gα) signaling by the regulator of g protein signaling 14 (RGS14). *J Biol Chem*. 290, 9037-49.

4.1 Introduction

Classically defined G protein signaling begins with a heterotrimeric G protein (Gαβγ) bound to a G protein-coupled receptor (GPCR). GPCR activation promotes GDP release and subsequent GTP binding to activate Gα. Activation of Gα leads to dissociation/rearrangement of the heterotrimeric complex and allows Gα and Gβγ to interact with downstream effectors. Intrinsic GTP hydrolysis (GTPase) returns Gα to its basal state (Gα-GDP) where it can bind Gβγ once more and reassociate with a GPCR (210-212). G proteins are further regulated by members of the regulators of G protein signaling (RGS) family. RGS proteins contain a canonical RGS domain of ~120 amino acids which binds activated G proteins and act as GTPase activating proteins (GAPs) to catalyze GTP hydrolysis and accelerate the G protein cycle (213-215).

Our previous research has revealed Regulator of G protein signaling 14 (RGS14), a member of the R12 subfamily of RGS proteins, is highly expressed in the brain (163,170) and is a natural suppressor of CA2 hippocampal synaptic plasticity and learning and memory (169,216). RGS14 has a unique domain structure with an N-terminal RGS domain and a C-terminal G protein regulatory (GPR; also known as GoLoco) motif. GPR motifs consist of ~20 amino acids and bind inactive Gα-GDP subunits (99,128) thereby targeting GPR-containing proteins to the plasma membrane (172,175,205). In addition to its RGS domain and GPR motif, RGS14 also contains two central tandem Raf-like Ras binding domains (RBDs) allowing RGS14 to engage H-Ras signaling pathways (165,166).

Due to its unusual domain structure, RGS14 (together with RGS12) possesses the unique capacity for interacting with distinct forms of Gα subunits. As an RGS protein, RGS14 engages activated forms (Gα-GTP) of the Gαi/o subfamily to stimulate Gα-directed GTP hydrolysis (75,162,163). Through its GPR motif, RGS14 selectively binds either

inactive Gαi1-GDP or Gαi3-GDP to inhibit GDP dissociation and target RGS14 to the plasma membrane (130,164,172). However, it remains unknown which form of Gα (active or inactive) RGS14 engages first in cells and is bound to in its resting state. Potentially, RGS14 may act primarily as an RGS-GAP, recruited first by Gα-GTP following a G protein activation step, and then secondarily interacting with the resulting inactive Gα-GDP to serve as a signaling complex. Alternatively, resting RGS14 may exist as a preformed complex with inactive Gα-GDP in place of Gβγ (as proposed (144,217)), with its RGS domain free to interact with a second active Gα-GTP. We have previously demonstrated that recombinant RGS14 forms a stable complex with inactive Gαi at the plasma membrane (172,173,218). Activation of a Gαi-linked GPCR uncouples the RGS14:Gαi-GDP complex from the receptor, and the non-receptor guanosine exchange factor Ric-8A uncouples RGS14 from Gαi via the GPR motif (167,173). Moreover, removal of the RGS domain does not prevent RGS14 localization to the plasma membrane (172), suggesting that the basal state for RGS14 is in a stable complex with Gαi-GDP.

While we have made great strides in understanding RGS14 protein-protein interactions, studies by our lab and others have not yet established a clear mechanism of action for how RGS14 utilizes the RGS domain and the GPR motif to integrate G protein signaling. Moreover, the structural rearrangements governing RGS14 function as an integrator of G protein signaling remain unknown. Here we explored the intramolecular dynamics of the RGS domain and the GPR motif with the goal of clarifying RGS14's mechanism of action on Gα protein signaling. Our studies sought to distinguish between recruitment of RGS14 to the plasma membrane by the GPR motif and RGS domain. We further explored the intramolecular communication between the GPR motif and RGS domain when bound to Gα, and examined whether RGS14 can engage two distinct forms of

Gα subunits simultaneously. Using a variety of complementary cellular and biochemical approaches, we show that binding of active or inactive Gα subunit differentially affects RGS14 protein conformation, and that RGS14 can bind both an inactive Gα-GDP and an active Gα-GDP-AlF_4^- subunit simultaneously to form a ternary signaling complex at the plasma membrane. Based on these findings, we propose and discuss a working model for RGS14 regulation and integration of G protein signaling at postsynaptic spines of its natural host cell, CA2 hippocampal neurons.

4.2 Experimental Procedures

Cell Culture and Transfection – HeLa cells were maintained in 1X Dulbecco's modified eagle medium with phenol red indicator supplemented with 10% fetal bovine serum, 100 units/mL penicillin, and 100 mg/mL streptomycin. HEK 293 cells were maintained in 1X Dulbecco's modified eagle medium without phenol red indicator supplemented with 10% fetal bovine serum, 2 mM L-glutamine, 100 units/mL penicillin, and 100 mg/mL streptomycin. Cells were incubated at 37°C with 5% CO_2. Transfections were carried out using polyethyleneimine (PEI) as previously described (175).

Immunofluorescence and Confocal Imaging – HeLa cells were used preferentially for confocal imaging because cell morphology allowed for better observation of the boundary between the cytosol and plasma membrane. HeLa cells were transiently transfected with 100 ng RGS14 (pcDNA3.1-FLAG-RGS14) and/or 100 ng Glu-Glu epitope (EE) tagged Gα subunits (pcDNA3.1-Gαi1-EE or pcDNA3.1-Gαo-EE). Transfected cells were washed with PBS and treated with AlF_4^- for 10 minutes in Tyrode's solution (140 mM NaCl, 5 mM KCl, 1 mM $MgCl_2$, 1 mM $CaCl_2$, 0.37 mM NaH_2PO_4, 24 mM $NaHCO_3$, 10 mM HEPES, and 0.1% glucose, pH 7.4) supplemented with 10 mM NaF, 9 mM $MgCl_2$, and 30 μM $AlCl_3$. Cells were

then fixed at room temperature in 4% paraformaldehyde for 10 minutes. Excess paraformaldehyde was quenched with 200 mM Tris pH 7.4 supplemented with 0.75% glycine. Cells were then permeabilized in 0.1% Triton X-100 for 10 minutes and blocked for 1 hour in 8% BSA. Next, cells were incubated for 1 hour at 37°C in a 1:1000 dilution of rabbit anti-FLAG (Sigma) to detect FLAG-RGS14 and/or a 1:1000 dilution of mouse anti-EE (Covance) to detect Gα-EE in 4% BSA. Cells were then washed three times in PBS containing 0.05% Triton X-100 and placed into secondary for 30 minutes at 37°C. Secondary antibodies, Alexa 488 goat anti-mouse and Alexa 594 goat anti-rabbit (Molecular Probes), were diluted 1:500 in PBS with 4% BSA. Cells were then washed twice in PBS and stained with Hoechst 33342 (1:5000) in 4% BSA for 3 minutes. Cells were then washed again in PBS and mounted with ProLong Gold Antifade Reagent (Invitrogen). Confocal images were taken using a 60X oil immersion objective on Olympus FV1000. Images were processed and intensity graphs generated with ImageJ.

Bioluminescence Resonance Energy Transfer (BRET) – BRET experiments were performed in HEK 293 cells as previously described (167,175,205). To generate the Venus-RGS14-Luc cDNA used in current studies, Venus was inserted at XhoI site of the previously described phRLucN2-RGS14 (167). HEK 293 cells were transiently transfected with 5ng Ven-RGS14-Luc and either 0, 50, 100, 250, 500, or 750 ng pcDNA3.1-Gαi1. For BRET experiments characterizing Gαi1(G42R) activity, HEK 293 cells were transfected with 5 ng of either RGS14-WT-Luc, Luc-RGS14-WT, or RGS14-515/516-Luc (GPR-null mutant) plasmid alone or along with 25, 50, 100, 250, or 500 ng of Gαi1(G42R)-YFP or Gαi1-WT DNA where indicated. Twenty-four hours after transfection, cells were resuspended in Tyrode's solution (140 mM NaCl, 5 mM KCl, 1 mM $MgCl_2$, 1 mM $CaCl_2$, 0.37 mM NaH_2PO_4, 24 mM $NaHCO_3$, 10 mM HEPES, and 0.1% glucose, pH 7.4). Cells treated with AlF_4^- were

resuspended in Tyrode's solution supplemented with 10 mM NaF, 9 mM $MgCl_2$, and 30 μM $AlCl_3$. After counting, 10^5 cells were plated into white 96-well Optiplates (PerkinElmer Life Sciences). Acceptor expression was confirmed by measuring fluorescence using the TriStar LB 941 plate reader (Berthold Technologies) with 485 nm excitation and 530 emission filters. BRET was monitored using 485 and 530 emission filters. After a 2 minute application of 5 μM coelenterazine H (Nanolight Technologies), the change in BRET (ΔBRET) was calculated by dividing the 530 signal by the 485 signal (Venus/Luciferase) and subtracting the signal observed from Ven-RGS14-Luc alone. In experiments characterizing Gαi1(G42R)activity, BRET ratios (YFP/Luc) were recorded and net BRET was calculated by subtracting the BRET signal from the luciferase alone. Data was collected using the MikroWin 2000 software and analyzed using Microsoft Excel and GraphPad Prism.

Purification of recombinant proteins – Full-length rat RGS14 was cloned using ligation independent cloning into a pLIC-MBP vector (a gift from John Sondek to EAO) containing a hexa-histidine (H_6) tag, a maltose binding protein (MBP) tag, and a tobacco etch virus (TEV) cleavage site to generate H_6-MBP-TEV-RGS14. H_6-MBP-TEV-RGS14 was expressed in BL21 (DE3) *E. coli* and purified using Ni^{2+}-affinity chromatography. The H_6-MBP tag was cleaved by treatment with purified TEV protease (1:200 TEV:RGS14) overnight at 4°C. Pure RGS14 was isolated with size-exclusion chromatography by FPLC (AKTA Purifier) utilizing tandem superdex S75/S200 columns (GE Healthcare). Purified protein was snap frozen and stored at -80°C. H_6-Gαi1 and H_6-Gαo were prepared and used as previously described (163).

Generation of G42R mutant – An AlF_4^- insensitive mutant of Gαi1 was generated by introducing a glycine to arginine mutation at amino acid 42 using the QuikChange kit (Stratagene). To generate H_6-Gαi1(G42R) (rat) the following oligonucleotide primers were

used: forward 5'CTG CTG CTG CTG GGT GCT CGT GAA TCC GGG AAG AGC3'; reverse 5'GCT CTT CCC GGA TTC ACG AGC ACC CAG CAG CAG CAG3'. To generate Gαi1(G42R)-YFP (human) the following primers were used: forward 5'CTG CTG CTG CTC GGT GCT CGT GAA TCT GGT AAA AGT ACA ATT GTG3'; reverse 5'CAC AAT TGT ACT TTT ACC AGA TTC ACG AGC ACC GAG CAG CAG CAG3'.

Hydrogen/Deuterium Exchange (HDX) Mass Spectrometry – Solution-phase amide HDX was carried out with a fully automated system as described previously (219). Briefly, 4 μL of 10 μM RGS14 was diluted to 25 μL with D_2O-containing HDX buffer and incubated at 4 °C for 10 s, 30 s, 60 s, 900 s or 3,600 s. Following on exchange, back exchange was minimized and the protein was denatured by dilution to 50 μL in a low pH and low temp buffer containing 0.1% (v/v) TFA in 3 M urea (held at 1 °C). Samples were then passed across an immobilized pepsin column (prepared in house) at 50 μl min^{-1} (0.1% v/v TFA, 15 °C); the resulting peptides were trapped on a C8 trap cartridge (Hypersil Gold, Thermo Fisher). Peptides were then gradient-eluted 4% (w/v) CH_3CN to 40% (w/v) CH_3CN, 0.3% (w/v) formic acid over 5 min at 2 °C across a 1 mm × 50 mm C18 HPLC column (Hypersil Gold, Thermo Fisher) and electrosprayed directly into an Orbitrap mass spectrometer (LTQ Orbitrap with ETD, Thermo Fisher). Peptide ion signals were confirmed if they had a MASCOT score of 20 or greater and had no ambiguous hits using a decoy (reverse) sequence in a separate experiment using a 60 min gradient. The intensity-weighted average m/z value (centroid) of each peptide's isotopic envelope was calculated with the in-house developed software (220) and corrected for back-exchange on an estimated 70% recovery and accounting for the known deuterium content of the on-exchange buffer. To measure the difference in exchange rates, we calculated the average percent deuterium uptake for RGS14 following 10, 30, 60, 900 and 3,600 s of on exchange. From this value, we subtracted the

average percent deuterium uptake measured for the activated Gαo or inactive Gαi1 bound RGS14 complex. Negative perturbation values indicate exchange rates are slower for these regions within RGS14 in complex with activated Gαo or inactive Gαi1. Resulting HDX data was mapped onto homologous RGS14 (PDB # 2JNU) or RGS10 (PDB # 2IHB) structures using UCSF Chimera (221). The human RGS14 RGS domain structure utilized for apo-RGS14 map was selected from the solution structure using the ensemble cluster function. Sequence alignments for RGS14 and RGS10 were performed using ClustalΩ (222,223).

GTPase Activating Protein (GAP) assay – Single turnover GTPase assays were performed as previously described (163,218). Gαo was diluted in 10 mM HEPES, 5 mM EDTA, 2 mM DTT, 0.1% Lubrol and loaded with 3500 cpms of γ-labeled ^{32}P-GTP for 20 minutes at room temperature. Gαo was then cooled on ice for 5 minutes prior to the start of the assay. Gαo (1 μM) was added to reaction tubes containing 5 μL 10 mM GTP and 5 μL 1M $MgCl_2$ with RGS14 or RGS14:Gαi1 preformed complex. Proteins were incubated on ice for established time points and then quenched with ice cold activated charcoal. The charcoal was pelleted and the collected supernatant was added to scintillation vials. Released $^{32}P_i$ was then measured with scintillation counting.

4.3 Results

Our previous studies have indicated that native RGS14 exists both in the soluble (cytosolic) and particulate (membrane) fractions of brain lysates (163), and is localized diffusely within the soma, dendrites, and spines and at the postsynaptic density in CA2 neurons of mouse brain (169,170). We also have shown that recombinant RGS14 can bind inactive Gα subunits at the plasma membrane through the GPR motif (172). Here we sought to explore how RGS14 subcellular localization changes in response to G protein activation.

For this, we compared Gαi1, which can bind either the RGS domain or the GPR motif, and Gαo, which can only bind the RGS domain (75,162-164,172). Initial experiments examined subcellular localization of RGS14 in response to G protein activation with aluminum tetrafluoride (AlF_4^-). AlF_4^- activates cellular G proteins by mimicking the G protein transition state. Moreover, AlF_4^- activated G proteins are the preferred binding partner for RGS domains (48,78,224) including RGS14. The RGS domain of RGS14 interacts with Gαo when activated with AlF_4^- but not Gαo activated with the non-hydrolyzable analogue of GTP, GTPγS (data not shown). When expressed in HeLa cells, FLAG-RGS14 is localized diffusely within the cytosol in the absence of Gα subunits when visualized by confocal microscopy (Figure 4.1A). Co-expression of EE-epitope tagged Gαi1 (Gαi1-EE-GDP) was sufficient to recruit FLAG-RGS14 to the plasma membrane. In contrast and as expected co-expression of Gαo-EE did not recruit FLAG-RGS14 to the plasma membrane (Figure 4.1B, 4.1D). Following activation of HeLa cells with AlF_4^-, FLAG-RGS14 remained at the plasma membrane with Gαi1-EE, but translocated from the cytosol to the plasma membrane following activation of Gαo-EE (Figure 4.1C, 4.1D). FLAG-RGS14 translocation to the plasma membrane by Gαo-EE-AlF_4^- took place slowly over 10 minutes (Figure 4.1E), likely reflecting the rate of activation of cellular Gα by AlF_4^-.

To investigate conformational changes of RGS14 in response to G protein binding in live cells, we developed an RGS14 BRET biosensor. An acceptor Venus tag was fused to the N-terminus and a donor *Renilla* luciferase tag to the C-terminus of RGS14 (Ven-RGS14-Luc). Resonant energy transfer is dependent on the proximity and conformation of the Venus and luciferase tags, thus conformational changes in RGS14 can alter the position of the donor and acceptor tags and register a change in the BRET signal. As seen in Figure 4.2,

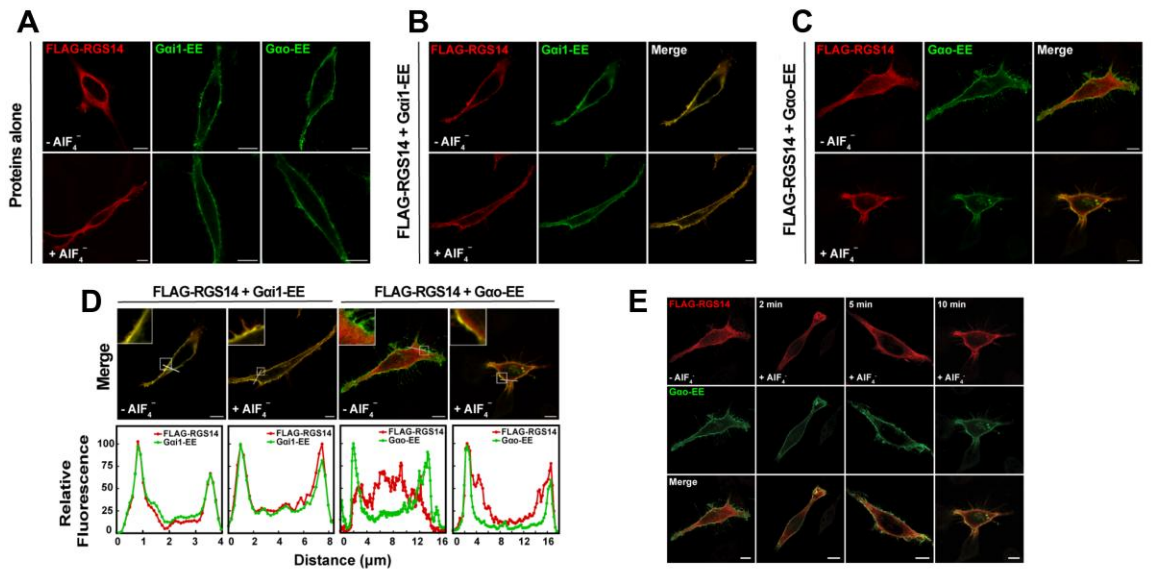

Figure 4.1. RGS14 is Recruited to the Plasma Membrane by Inactive Gαi1-GDP and by Active Gαo-AlF_4^-. *(Panel A)* HeLa cells were transfected with either 100ng FLAG-RGS14 or 100ng of EE-tagged Gα proteins. Transfected cells were treated with AlF_4^- for 10 minutes prior to fixation for immunofluorescence and confocal microscopy as described in experimental procedures. Images are representative of three separate experiments. Scale bar is 10 μm for all panels. *(Panel B)* HeLa cells were co-transfected with 100 ng FLAG-RGS14 and 100 ng Gαi1-EE. Cells were treated with AlF_4^- and fixed as in (A). Images are representative of three separate experiments. *(Panel C)* HeLa cells were co-transfected with 100 ng FLAG-RGS14 and 100 ng Gαo-EE. Cells were treated with AlF_4^- and fixed as in (A). Images are representative of three separate experiments. *(Panel D)* Intensity graphs indicating relative fluorescence from merged images in (B) and (C). Relative fluorescence intensity of FLAG-RGS14 and either Gαi1-EE or Gαo-EE was measured at the plasma membrane as indicated by the white line in merged images. Intensity graphs were generated in ImageJ and are plotted from left to right. Insets highlight the plasma membrane in each image. (*Panel E*) HeLa cells were transfected with 100 ng FLAG-RGS14 (*top row*) and 100 ng EE-tagged Gαo

(*middle row*) and treated with AlF_4^- for 0, 2, 5, and 10 minutes prior to fixation for immunofluorescence and confocal microscopy as described in experimental procedures. Merged overlay images of RGS14 and Gαo is shown (*bottom row*). Scale bar is 10 μm. Note: images for the zero and 10 minute time points are from panel C.

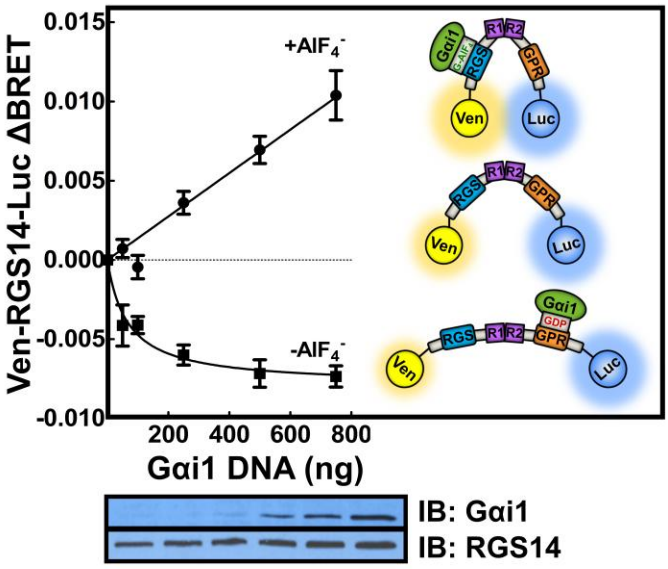

Figure 4.2. RGS14 Adopts Different Conformations in Response to Binding of Gα Proteins in Different Activation States. HEK 293 cells were transfected with 5 ng of plasmid cDNA encoding Venus-RGS14-Luc alone or with 50, 100, 250, 500, or 750 ng of Gαi1. Gαi1 was activated with AlF_4^- for 40 minutes. BRET ratios were recorded and the change in BRET (ΔBRET) was calculated by subtracting the BRET signal from Venus-RGS14-Luc alone. Average basal BRET for Venus-RGS14-Luc in the absence of AlF_4^- was 0.693 while in the presence of AlF_4^- the basal BRET was 0.687. Data shown are the pooled mean +/- SEM of three separate experiments, each with triplicate determinations. The bottom panel shows representative immunoblots for Venus-RGS14-Luc and Gαi1 protein expression. The inset diagrams illustrate the interpreted dynamics of Venus-RGS14-Luc structure in response to binding Gαi1 in different activation states.

the cytosolic Ven-RGS14-Luc biosensor exhibited basal BRET activity when expressed alone in cells. When co-expressed with inactive Gαi1, BRET activity decreased suggesting the BRET tags move away from one another due to the binding of inactive Gαi1-GDP. In stark contrast, application of the non-specific G protein activator AlF_4^- showed a marked increase in BRET signal, suggesting the BRET tags move closer together in the presence of activated Gαi-AlF_4^-. These findings highlight distinct and dynamic structural rearrangements that the RGS14 polypeptide adopts in response to the binding of Gα subunits in different activation states.

We next turned to hydrogen/deuterium exchange (HDX) mass spectrometry to gain a better understanding of the conformational changes occurring in RGS14 in response to interactions with G proteins. HDX measures the incorporation of deuterons from heavy water (D_2O) with mass spectrometry over time to probe secondary structure. HDX has emerged as a sensitive and rapid technique to identify alterations in conformational dynamics in protein-protein or protein-ligand interactions (225-227). The HDX heat map of apo-Gαi1 (data not shown) agrees closely with previous reports of G protein structure and overall stability (228,229) while the HDX heat map of apo-RGS14 indicates RGS14 is highly dynamic in solution (Figure 4.3A). High deuterium exchange was observed in both the N- and C-termini as well as the interdomain regions and the GPR motif. The Ras binding domains (RBDs) and RGS domain were relatively more stable than the GPR motif with increased protection from solvent exchange (as determined by detection of lower levels of deuterium incorporation). The RBD1 region of RGS14 appeared to be a more stable than RBD2.

The most stable regions of apo-RGS14 as indicated by HDX are located in the RGS domain. We modeled the observed solvent exchange onto a solution structure of the RGS

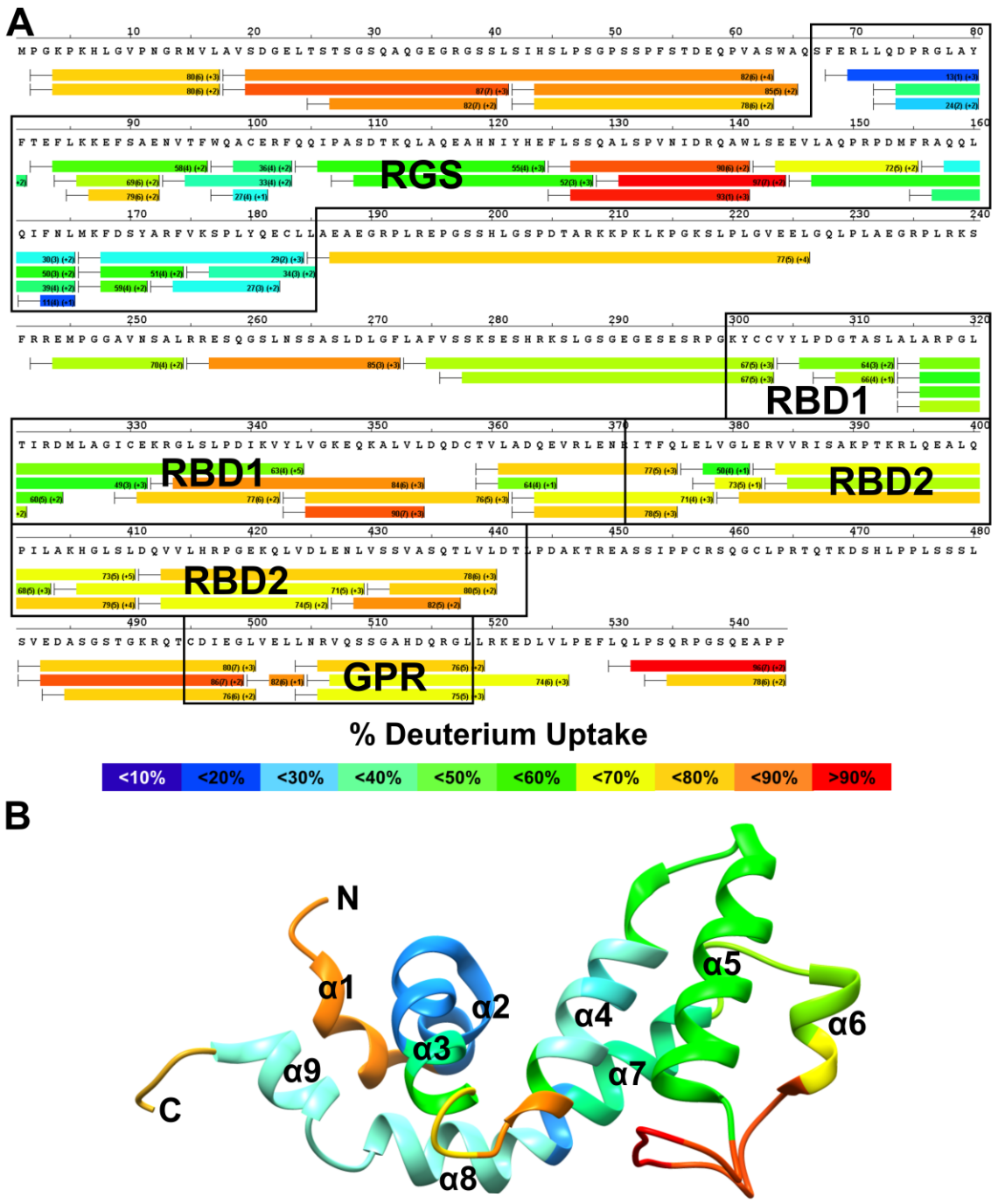

Figure 4.3. RGS14 is a Highly Dynamic Protein. (*Panel A*) HDX heat map for apo-RGS14. Each bar represents an individual peptide with the color corresponding to the average percent deuterium exchange over 6 time points (10, 30, 60, 300, 900, and 3600 seconds). The numbers in the first parentheses indicate the standard deviation for three

replicates. The numbers in the second parentheses indicate the charge of the peptide. Residues corresponding to the RGS domain, Ras binding domains (RBDs), and GPR motif are boxed in black. The percent deuterium exchange is indicated by the colored scale bar. (*Panel B*) Average deuterium incorporation mapped onto the reported solution structure of human RGS14 RGS domain (PDB # 2JNU).

domain of human RGS14 (PDB # 2JNU) (67). As seen in Figure 4.3B, residues 70-185 showed modest deuterium exchange indicating relative stability of the domain. Within the RGS domain, peptide fragments corresponding to the α5-α6 loop (residues 127-142) showed high exchange indicating a highly dynamic region. These results are consistent with the solution structure of RGS domain of RGS10 (PDB # 2I59), a close relative of RGS14 and a member of the R12 subfamily of RGS proteins (67).

We then sought to examine the effects of G protein binding on the dynamics of RGS14 protein structure. To characterize the interaction of RGS14 with activated G proteins, we performed differential HDX with RGS14 and AlF_4^- activated Gαo that binds the RGS domain but not the GPR motif (75,162,163). As seen in the differential HDX heat map (Figure 4.4A), Gαo-AlF_4^- dramatically stabilizes the RGS domain, indicated by a reduced solvent exchange in RGS14 residues 87-96 (28-37%) and 127-174 (8-30%). Also, a modest yet statistically significant decrease in deuterium incorporation was observed in residues 99-126 (2-3%). The RGS domain of RGS14 demonstrates ~50% sequence identity with the RGS domain of RGS10 thus we modeled the changes on to a previously reported crystal structure for RGS10 in complex with AlF_4^- activated Gαi3 (PDB # 2IHB) (67). Significant stabilization was observed in the α3-α4 and α5-α6 loops as well as alpha helices 7 and 8. These regions are responsible for binding and stabilizing the switch regions of the G protein and are consistent with observed interactions between RGS domains and G proteins (51). Notably, no significant change in solvent exchange was observed in the RGS14 polypeptide outside of the RGS domain.

Additionally, we performed HDX experiments with RGS14 bound to inactive Gαi1-GDP. As seen in Figure 4.5A, a significant decrease in deuterium incorporation (9-35%) was observed in residues 502-519 corresponding to the GPR motif. Significant changes in the

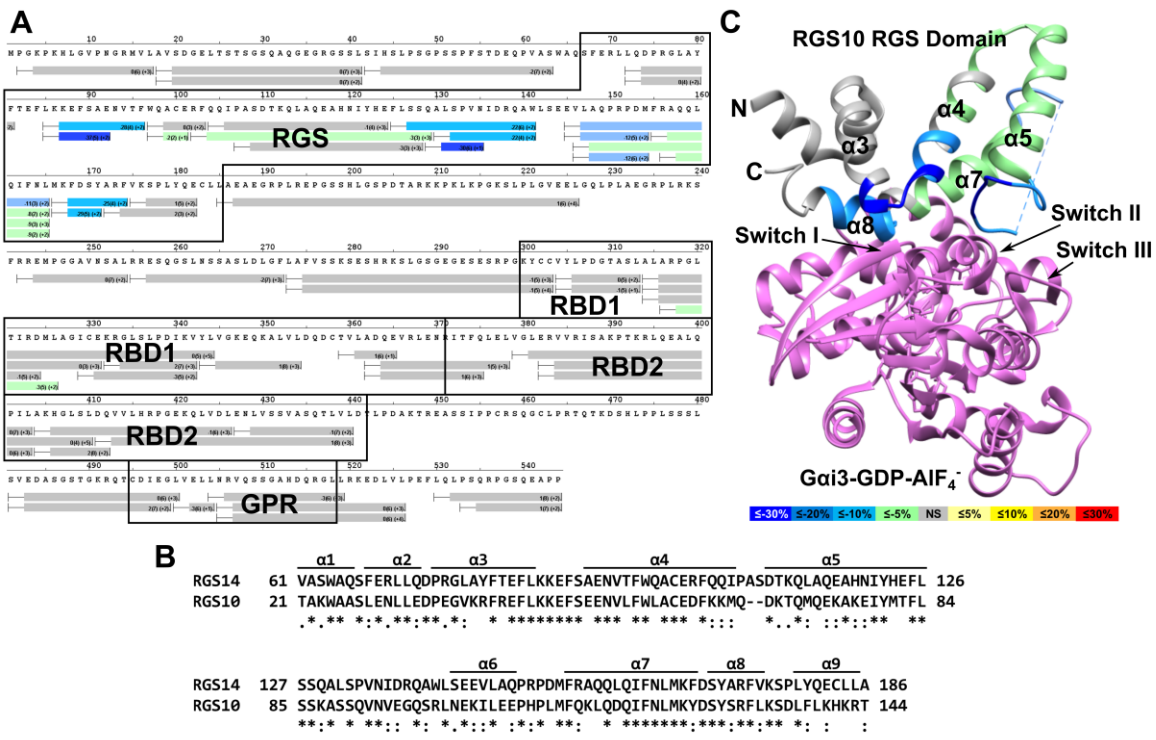

Figure 4.4. Gαo Activated with AlF_4^- Binds and Markedly Stabilizes the RGS Domain of RGS14. (*Panel A*) Differential HDX heat map for the RGS14:Gαo-AlF_4^- complex. Each bar represents an individual peptide with the color corresponding to the average percent change in deuterium exchange between apo-RGS14 and RGS14:Gαo-AlF_4^- over 6 time points (10, 30, 60, 300, 900, and 3600 seconds). The numbers in the first parentheses indicate the standard deviation for three replicates. The numbers in the second parentheses indicate the charge of the peptide. Residues corresponding to the RGS domain, Ras binding domains (RBDs), and GPR motif are boxed in black. Changes in deuterium exchange are indicated by the colored scale bar. (*Panel B*) ClustalΩ sequence alignment of rat RGS14 and human RGS10. Asterisks (*) indicate fully conserved residues, colons (:) indicate conservation of strongly similar properties, periods (.) indicate conservation of weakly similar properties. (*Panel C*) Average percent change in deuterium exchange levels mapped onto the crystal structure of human RGS10 bound to AlF_4^- activated Gαi3 (PDB # 2IHB). Gαi3 is

represented in purple. Differences in percentage of deuterium exchange are indicated by the colored scale bar.

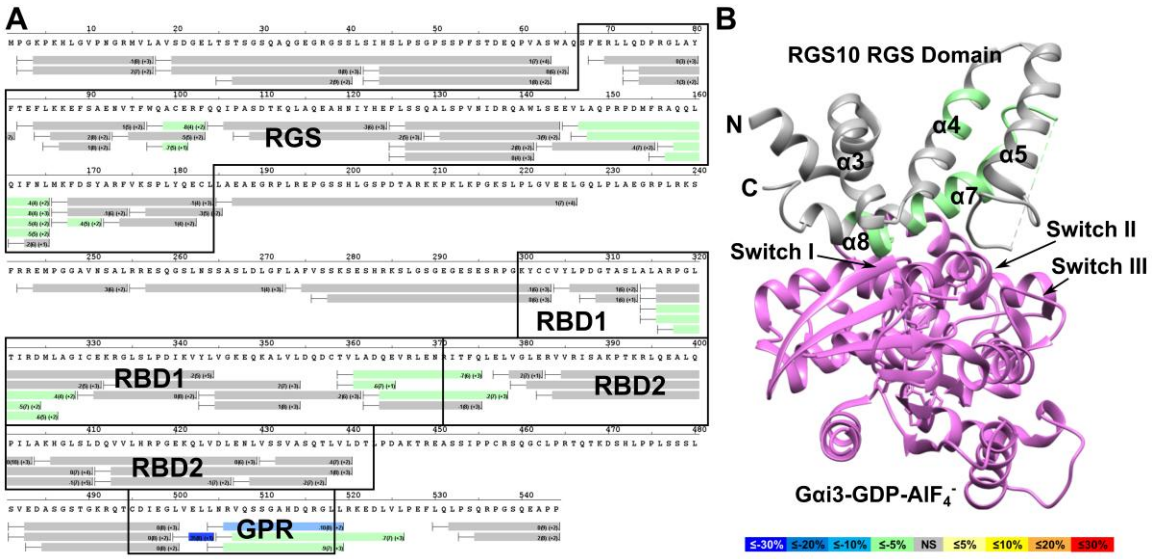

Figure 4.5. Binding of Gαi1-GDP Stabilizes the GPR Motif and Induces Allosteric Stabilization of Other Regions within RGS14. (*Panel A*) Differential HDX heat map for the RGS14:Gαi1-GDP complex. Each bar represents an individual peptide with the color corresponding to the average percent change in deuterium exchange between RGS14-apo and RGS14:Gαi1 over 6 time points (10, 30, 60, 300, 900, and 3600 seconds). The numbers in the first parentheses indicate the standard deviation for three replicates. The numbers in the second parentheses indicate the charge of the peptide. Residues corresponding to the RGS domain, Ras binding domains (RBDs), and GPR motif are boxed in black. Changes in deuterium exchange are indicated by the colored scale bar. (*Panel B*) Average percent change in deuterium exchange for the RGS14:Gαi1 complex mapped onto the crystal structure of human RGS10 bound to AlF_4^- activated Gαi3 (PDB # 2IHB). Gαi3 is represented in purple. Differences in percentage of deuterium exchange are indicated by the colored scale bar.

stability of the RGS domain and RBD1 were also observed, indicating long-range allosteric communication between RGS14 domains. As shown in Figure 4.5B, allosteric stabilization was observed in residues 99-129 and 147-171 corresponding to alpha helices 4 and 6/7 in the RGS domain, each showing a decrease in solvent exchange of approximately 2-8%. Additionally, stabilization was observed in residues 316-328 (3-6%) and 361-378 (2-7%) in RBD1.

Next, we explored if RG14 could bind two different Gα subunits simultaneously, each in different activation states, and the effects of these binding interactions on RGS14 structural stability. For these studies, we generated a Gαi1 mutant (G42R) that is insensitive to activation by AlF_4^- and thereby unable to bind the RGS domain, but is nonetheless capable of binding the GPR motif even in the presence of AlF_4^- (230). Our characterization of the purified mutant protein confirmed these properties showing that Gαi1(G42R) in the presence of AlF_4^- readily bound the GPR motif of a truncated form of RGS14 missing the RGS domain (R14-RBD/GPR) (Figure 4.6A) but failed to bind the isolated RGS domain of RGS14 (H_6-RGS), again in the presence of AlF_4^- (Figure 4.6B). We further characterized Gαi1(G42R) interactions with RGS14 in live cells using BRET analysis. For these studies, we utilized two different RGS14 BRET probes. The first contained a C-terminal tagged luciferase (RGS14-Luc) that is more sensitive to G protein binding at the GPR motif. The second contained an N-terminally tagged luciferase (Luc-RGS14) that is more sensitive to G protein binding at the RGS domain. Using the RGS14-Luc BRET probe, we found that Gαi1(G42R) interacts with the GPR motif in the presence and absence of AlF_4^- (Figure 4.6C). A GPR-null mutant (Q515A/R516A) of RGS14-Luc showed a greatly diminished capacity for binding Gαi1(G42R), both in the presence and absence of AlF_4^- (Figure 4.6C). BRET analysis with the N-terminal tagged Luc-RGS14 showed that Gαi1(G42R) has

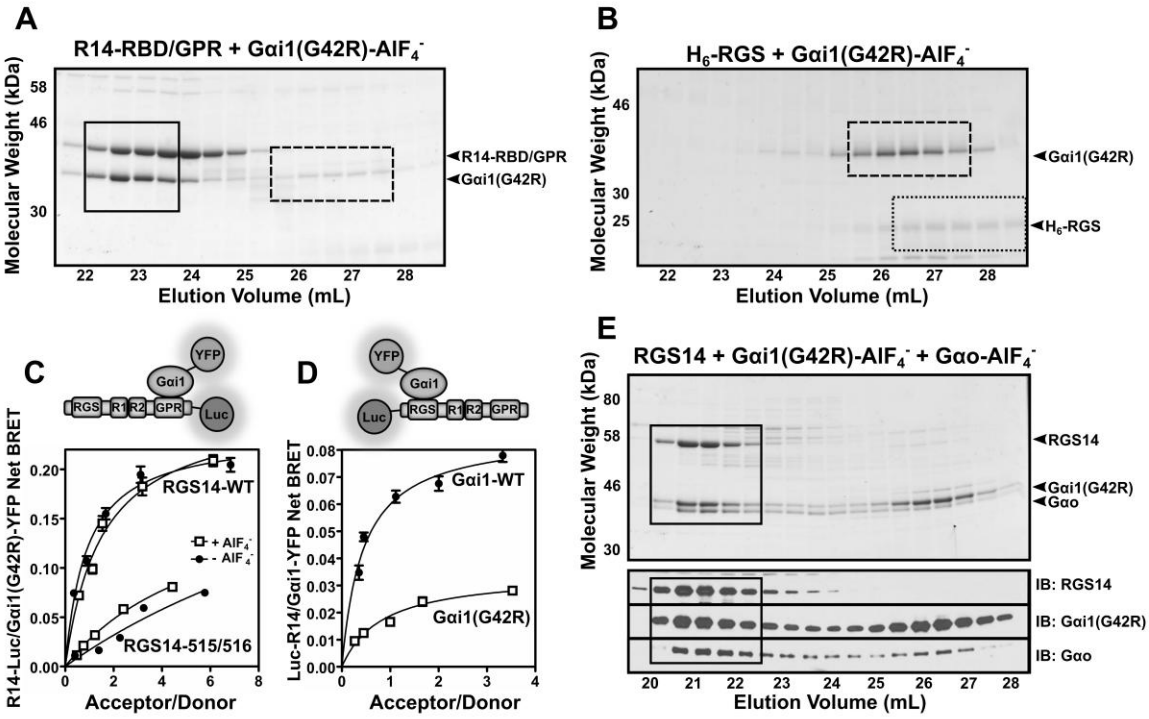

Figure 4.6. RGS14 Forms a Ternary Complex with Gαo-AlF_4^- and Gαi1(G42R). *(Panel A)* Purified truncated RGS14 missing the RGS domain (R14-RBD/GPR) was combined with H_6-Gαi1(G42R) in the presence of AlF_4^- for 1 hour at 4°C and then run over tandem superdex S75/S200 size-exclusion columns. SDS-PAGE of collected fractions were stained with coomassie blue. Boxed in black is the R14-RBD/GPR:Gαi1(G42R) complex while free Gαi1(G42R) is indicated by the dashed box. (*Panel B*) Purified truncated RGS14 expressing solely the RGS domain (H_6-RGS) was combined with H_6-Gαi1(G42R) in the presence of AlF_4^- for 1 hour at 4°C and then run over tandem superdex S75/S200 size-exclusion columns. SDS-PAGE of collected fractions were stained with coomassie blue. Outlined in black dots is the free H_6-RGS protein while free H_6-Gαi1(G42R) is indicated by the dashed box. (*Panel C*) HEK 293 cells were transfected with 5 ng of either RGS14-WT-Luc or RGS14-515/516-Luc (GPR-null mutant) plasmid alone or along with 25, 50, 100, 250, or 500 ng of Gαi1(G42R)-YFP DNA. Gαi1(G42R) was activated with AlF_4^- for 40 minutes.

BRET ratios were recorded and net BRET was calculated by subtracting the BRET signal from the luciferase alone. Data shown are the mean of three separate experiments, each with triplicate determinations. (*Panel D*) HEK 293 cells were transfected with 5 ng of Luc-RGS14 plasmid alone or along with 25, 50, 100, 250, or 500 ng of Gαi1-WT-YFP or Gαi1(G42R)-YFP DNA. Gαi1 was activated with AlF_4^- for 40 minutes. BRET ratios were recorded and net BRET was calculated by subtracting the BRET signal from the luciferase alone. Data shown are the mean of three separate experiments, each with triplicate determinations. (*Panel E*) Purified full-length RGS14, H_6-Gαo, and H_6-Gαi1(G42R) proteins were incubated together in the presence of AlF_4^- for one hour and then run over tandem S75/S200 size-exclusion columns (*Top Panel*). Fractions were collected and SDS-PAGE of collected fractions were stained with commassie blue. (*Bottom Panel*) Immunoblots of each protein corresponding to fractions in the coomassie blue stained gel. Fractions containing the RGS14:Gαi1(G42R):Gαo-AlF_4^- complex are indicated by the black box.

diminished binding to RGS14 in the presence of AlF_4^- than Gαi1-WT (Figure 4.6D). Following confirmation of Gαi1(G42R) properties, we then utilized this unique experimental tool to explore the function of the RGS domain when bound to Gαi1 at the GPR motif. We preincubated purified RGS14 with purified Gαi1(G42R) and Gαo in the presence of AlF_4^-, and then subjected these proteins to size-exclusion chromatography (Figure 4.6E). All three proteins co-eluted together at an elution volume consistent with a ternary protein complex, suggesting binding of Gαi1(G42R) at the GPR motif does not preclude RGS14 interactions with activated Gαo-AlF_4^- at the RGS domain.

We next examined the effects of binding two different Gα subunits simultaneously at the GPR motif and the RGS domain on the RGS14 polypeptide stability using differential HDX (Figure 4.7). Binding of AlF_4^- activated Gαi1(G42R) and Gαo resulted in significant decreases in deuterium incorporation in both the GPR motif and RGS domain. In the RGS domain, significant decreases in solvent exchange were observed for residues 86-92 (24-26%) and 126-174 (3-25%), corresponding to the α3-α4 and α5-α6 loops as well as alpha helices 7 and 8, similar to what was observed for Gαo-AlF_4^- binding (Figure 4.4). Additional stabilizations were observed in the RGS domain in residues 99-124 (2-5%). These residues correspond to the α4-α5 loop and a large portion of the alpha 5 helix of the RGS domain. Significant stabilization was also observed in the GPR motif. Residues 502-519 showed a 10-49% decrease of deuterium uptake consistent with the results observed for the RGS14:Gαi1-GDP complex (Figure 4.5). In addition to the RGS domain and GPR motif, stability was also observed in both Ras binding domains as indicated by decreases in deuterium exchange of 2-14%. These results are consistent with the formation of a ternary complex.

Finally, we tested whether the binding of Gαi1-GDP at the GPR motif affects the capacity of RGS14 to function as a GAP on a second Gα, Gαo-GTP. For this, we

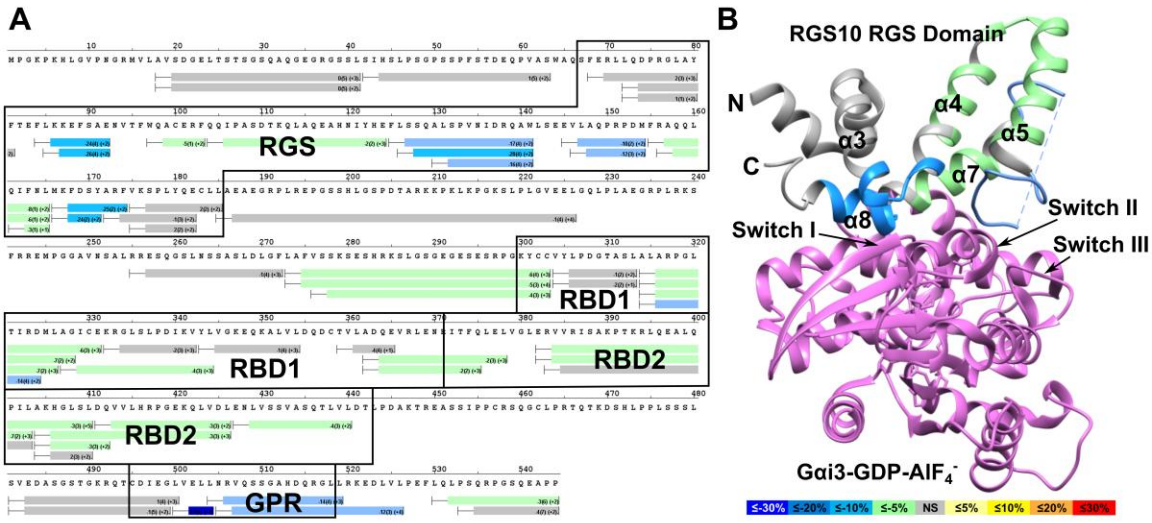

Figure 4.7. Simultaneous Binding of Gαo-AlF_4^- and Gαi1(G42R) Induces Stability throughout RGS14. *(Panel A)* Differential HDX heat map for the RGS14:Gαi1(G42R):Gαo-AlF_4^- complex. Each bar represents an individual peptide with the color corresponding to the average percent change in deuterium exchange between apo-RGS14 and RGS14:Gαi1(G42R):Gαo-AlF_4^- over 6 time points (10, 30, 60, 300, 900, and 3600 seconds). The numbers in the first parentheses indicate the standard deviation for three replicates. The numbers in the second parentheses indicate the charge of the peptide. Residues corresponding to the RGS domain, Ras binding domains (RBDs), and GPR motif are outlined in black. Changes in deuterium exchange are indicated by the colored scale bar. (*Panel B*) Average change in deuterium exchange for the RGS14:Gαi(G42R):Gαo-AlF_4^- complex mapped onto the crystal structure of human RGS10 bound to AlF_4^- activated Gαi3 (PDB # 2IHB). Gαi3 is represented in purple. Differences in percentage of deuterium exchange are indicated by the colored scale bar.

performed single turnover GTPase assays comparing RGS14 alone and a preformed complex of RGS14 bound to Gαi1-GDP (RGS14:Gαi1-GDP). As seen in Figure 4.8, RGS14 alone accelerated the GTPase activity of Gαo, as expected and consistent with previous reports (75,162,163). The preformed RGS14:Gαi1-GDP complex also stimulated Gαo GTPase activity equally well as RGS14 alone (Figure 4.8A), and this was the case across a range of increasing protein concentrations (Figure 4.8B). These results indicate that binding of Gαi1-GDP to RGS14 at the GPR motif does not alter the capacity of the RGS domain to bind Gαo-GTP and serve as a GAP.

4.4 Discussion

RGS14 and its close relative RGS12 are the only identified proteins that contain distinct domains that bind both active (RGS domain) and inactive (GPR motif) forms of Gα subunits. How RGS14 interacts with these two Gα in different activation states to integrate G protein signaling is unknown. Our current understanding of RGS14 biochemistry is limited to the functions of individual domains and motifs in isolation. Here we explored the intramolecular communication between the GPR motif and the RGS domains within full-length RGS14 following G protein binding. Overall, our results indicate that: 1) RGS14 can exist as a preformed stable complex with Gαi1-GDP at the plasma membrane; 2) free cytosolic RGS14 can translocate to the plasma membrane in the presence of Gαo-AlF_4^-; 3) apo-RGS14 is a highly dynamic protein, but adopts different conformations in response to binding of either active or inactive Gα; 4) Gαo-AlF_4^- binding stabilizes the RGS domain but does not alter the stability of other domains; 5) Gαi1-GDP binding stabilizes the GPR motif and also induces allosteric stabilization of the RGS domain and RBD1; 6) RGS14 complex formation with Gαi1-GDP at the GPR motif does not preclude binding of activated Gαo-

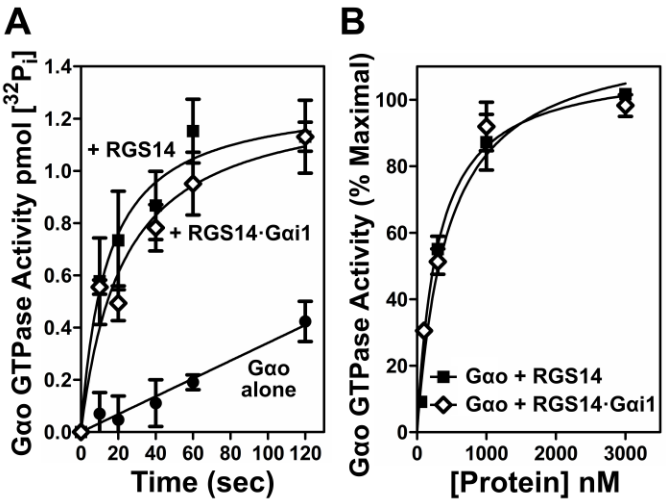

Figure 4.8. Gαi1-GDP Binding at the GPR Motif does not impede the RGS Domain of RGS14 from Binding Gαo-GTP and Exerting GAP Activity. (*Panel A*) Purified recombinant Gαo (1 μM) was loaded with [^{32}P]GTP for 20 minutes at room temperature, cooled on ice for 5 minutes, then incubated with either 1 μM RGS14 or 1 μM RGS14:Gαi1 preformed complex for the times indicated. (*Panel B*) Purified recombinant Gαo (1 μM) loaded with [^{32}P]GTP was incubated with either 100 nM, 300nM, 1μM, or 3μM RGS14 or RGS14:Gαi1 preformed complex for 20 seconds. In both sets of experiments, measurement of t = 0 seconds was performed without magnesium or RGS protein and subtracted from each condition. Each graph (Panel A and Panel B) is representative of three independent experiments.

AlF_4^- at the RGS domain; and 7) binding of Gαi1-GDP at the GPR motif does not disrupt the GAP activity of the RGS domain directed at a Gαo protein. Taken together, these results clarify the interdomain regulation between the RGS domain and GPR motif, and demonstrate that RGS14 can functionally engage two distinct Gα subunits simultaneously. We discuss the implications of these findings on RGS14 function, and propose a working model for RGS14 regulation of G protein signaling in its native environment of CA2 hippocampal neurons.

RGS14 Subcellular Localization – Our previous work has shown that native RGS14 exists as biochemically distinct subpopulations in brain, present both in the cytosol and at membranes (163,172). Consistent with this observation, we also found that native RGS14 in hippocampal CA2 pyramidal neurons is broadly expressed in soma and dendrites, and also in spine necks and post-synaptic densities (PSDs) (169). Together, these findings suggest that RGS14 exists within various subcellular compartments and is dynamically regulated. Unresolved is what form of Gα makes first contact with RGS14 within the cell, i.e., is the RGS domain first recruited to an active Gα-GTP or is the GPR motif first recruited to an inactive Gα-GDP? Here, we found that inactive Gαi1-GDP can preform a stable complex with RGS14 at the plasma membrane that remains there following cell-wide activation with AlF_4^-. In this case, we postulate that different domains of RGS14 simply swap positions with the different activated states of Gα, without falling off the membrane. By contrast, in the absence of Gαi1-GDP, RGS14 remains cytosolic yet can be recruited by activated Gαo-AlF_4^- to the plasma membrane via the RGS domain. Together with previous observations of RGS14 localization in brain and CA2 neurons (169,170), our findings here suggest that RGS14 exists as distinct cellular subpopulations, either bound to the plasma membrane in complex with Gαi-GDP or recruited from the cytosol to the plasma

membrane by active Gα-GTP followed by capture of the Gα-GDP resulting from GAP activity.

RGS14 Protein Conformational Changes – Following RGS14 association with Gα at the plasma membrane, an unresolved question is how Gα binding affects RGS14 protein conformation. As we previously postulated (167), RGS14 may form a clamshell-like structure similar to other GPR scaffolding proteins (154) that closes after binding active Gα-GTP and opens upon binding inactive Gα-GDP. In support of this idea, we found here that an RGS14 biosensor (Ven-RGS14-Luc) exhibited intrinsic BRET activity that increased following binding of active Gαi1-AlF_4^- at the RGS domain, and decreased following binding of inactive Gαi1-GDP at the GPR motif. This suggests that in the absence of Gα, apo-RGS14 exists in a semi-clam shell conformation that opens following binding of inactive Gα-GDP and closes following binding of Gα-AlF_4^-, thus reflecting the N- and C-termini of RGS14 becoming more compact. In either case, Gα binding could alter RGS14 interactions with other known RGS14 partners (e.g. active H-Ras, Rap2 or Ca^{2+}/CaM) and/or put RGS14 in a conformation that is optimal for regulation (e.g., phosphorylation, other).

As a complement to these findings, we utilized HDX to explore the dynamic nature of purified apo-RGS14 as well as dynamic changes that might occur to RGS14 structure following binding Gα subunits. Apo-RGS14 demonstrated considerable intrinsic flexibility, particularly within the interdomain regions and at both termini (Figure 4.3). As a scaffolding protein capable of integrating signals from different Gα proteins and H-Ras, RGS14 flexibility in the interdomain regions would allow for the adoption of different conformations when binding different proteins. The GPR motif exhibited considerable flexibility, consistent with a previous report showing a short peptide corresponding to the RGS14 GPR motif utilizes an α-helix to contact the Ras-like lobe and irregular secondary

structure to contact the α-helical lobe of Gαi1-GDP (67,231). As such, many residues within this motif must remain accessible to solvent in order to bind Gα.

The tandem Ras binding domains (RBD1, RBD2) also showed considerable flexibility. Of these, RBD1 was most stable, particularly within residues 315-330. Based on homologous RBDs (168), these residues correspond to the β2-sheet and α1-helix known to engage small GTPases such as H-Ras and Rap2. The increased stability in RBD1 may reflect the functionality of the domain since H-Ras and Rap2 bind RBD1 but not RBD2 (133,166). At present, there are no known binding partners of RBD2, but in order to engage other binding partners, this domain may require additional stabilization by (as yet unknown) posttranslational modification(s), an adjacent lipid bilayer and/or ancillary binding partners.

Lastly, the RGS domain of apo-RGS14 showed the most stability, consistent with a folded RGS domain. Peptides corresponding to the α2, α3, α4, and α7 helices were most stable, and are known to contribute to the hydrophobic core in homologous RGS domain structures (51). Peptides corresponding to the α3-α4 and α5-α6 loops were least stable reflecting the solvent accessible G protein binding site where the RGS domain contacts and stabilizes the switch regions of the G protein to promote GTP hydrolysis (51,67). In summary, apo-RGS14 exhibited dynamic structural properties typical of scaffolding proteins that integrate signals from many binding partners.

We also examined the effects of Gα binding on RGS14 structural stability by differential HDX. Upon binding Gαo-AlF_4^-, the α3-α4 and α5-α6 loops of the RGS domain show the most stabilization. Additionally, stabilization was observed in helix 7/8, regions known to interact with and stabilize G protein switch regions. These results are consistent with previous reports of G protein interactions with RGS domains (51,67). Somewhat surprisingly, the differential HDX map for RGS14:Gαo-AlF_4^- did not show significant

changes in other protein regions, suggesting RGS14 interactions with activated Gα-GTP does not regulate the function of other RGS14 domains. Conversely, the differential HDX map for RGS14:Gαi1-GDP suggests binding at the GPR motif has effects on other domain stability. Binding of Gαi1-GDP stabilized the GPR motif, as expected. However, stability was also observed in the RGS and RBD1 domains. These changes do not appear to be the result of direct protein binding to the domains but rather allosteric stabilization, suggesting that Gαi1-GDP stabilization of RGS14 could modulate Gα-GTP binding via the RGS domain and H-Ras-GTP binding at RBD1. Consistent with this observation, we previously reported that Gαi1-GDP binding at the GPR motif markedly enhanced H-Ras-GTP interactions with RGS14 (167).

To understand the implications of stabilization of the RGS domain by binding of Gαi1-GDP at the GPR motif, we modeled the stabilized regions onto a previously reported structure of RGS10 bound to Gαi3 (PDB # 2IHB) (67). The observed regions of stabilization were located away from the G protein binding site in α-helices 4 and 6/7. Within the residues identified, a conserved cysteine is present in the α4 helix which has been shown to be palmitoylated in RGS4 (C95) and RGS10 (C66) (232). While RGS14 has not been shown to be palmitoylated to date, the allosteric changes in the RGS domain may allow for such regulation to occur. Additionally, the changes observed in the RGS domain are proximal to identified PIP3 binding sites in other RGS proteins (233,234), suggesting these alterations in domain stability may place RGS14 in a more favorable position to interact with the plasma membrane.

RGS14 complex formation with two G Proteins – We examined if RGS14 could simultaneously interact with an active Gαo-AlF_4^- at the RGS domain and an inactive Gαi1(G42R)-GDP at the GPR motif. By size-exclusion chromatography (Figure 4.6E),

RGS14 appears to form a ternary complex with active Gαo-AlF_4^- and inactive Gαi1(G42R)-GDP. This finding raised two additional questions: 1) how does simultaneous binding of two proteins alter RGS14 protein conformation, and 2) does binding of Gαi1-GDP at the GPR motif affect the GAP activity of RGS14 towards an active Gαo-GTP? Our differential HDX studies indicated that binding of two Gα proteins simultaneously results in overall stability of RGS14. Somewhat surprisingly, binding of Gαi1-GDP at the GPR motif appears to not affect RGS14 GAP activity towards Gαo-GTP. A preformed RGS14:Gαi1-GDP complex retains full and unaltered capacity to directly bind Gαo-GTP and accelerate its GTPase activity by single turnover GTPase assays, irrespective of the conformational changes within the RGS domain indicated by HDX.

Proposed Working Model: Based on our findings here and elsewhere, we propose a working model (Figure 4.9) for how RGS14 integrates G protein signaling in its native environment, CA2 hippocampal neurons. Our data is most consistent with a model where RGS14 is recruited by an activated Gα-GTP and then is captured at the plasma membrane by Gα-GDP. Native RGS14 is most abundant in the cytosol (soma, dendrites and spines) of CA2 hippocampal neurons and in extracts (soluble fraction) of whole brain (163,169). In our proposed model, inactive RGS14 is present in the cytosol unbound to Gα. Following stimulation of a postsynaptic GPCR (Figure 4.9A), RGS14 is initially recruited as a GAP to the plasma membrane by Gαi1-GTP via the RGS domain. Following GAP activity, the resulting Gα-GDP immediately binds the GPR motif, thereby capturing and anchoring RGS14 at the plasma membrane to regulate signaling pathways important for LTP. We propose that this newly formed RGS14:Gα-GDP complex can serve as a nucleating center for the recruitment and clustering of additional RGS14 at the plasma membrane within the immediate vicinity to serve as a signaling hot spot. As illustrated in Figure 4.9A, the RGS

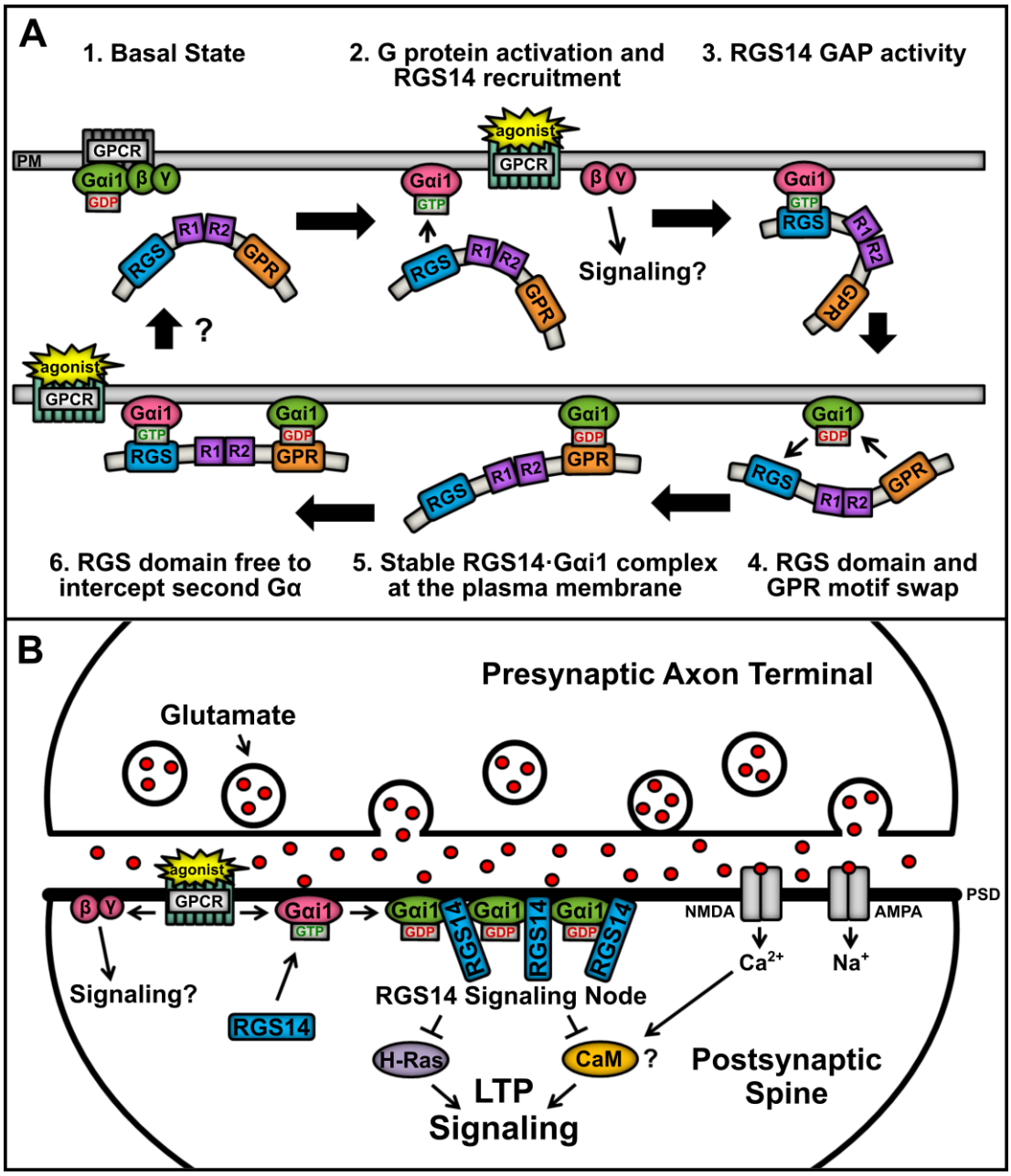

Figure 4.9. Proposed Model Showing RGS14 Binding and Integration of Gα-GDP and Gα-GTP Signaling in Cells. *(Panel A)* The proposed model of RGS14 signaling function proceeds clockwise from the top left. (1) In the basal resting state, Gαi1-GDP in complex with Gβγ is bound to a GPCR at the plasma membrane (PM) while RGS14 remains in the cytosol. (2) Agonist activation of a GPCR induces downstream signaling through Gβγ

while activated Gαi1-GTP recruits RGS14 to the plasma membrane. (3) RGS14 accelerates the GTPase of Gαi1, causing hydrolysis of GTP to GDP. (4) The RGS domain loses affinity for Gαi1-GDP and the GPR motif is free to bind the newly inactivated Gαi1. (5) RGS14 forms a stable complex with inactive Gαi1-GDP at the plasma membrane, which could serve to nucleate local recruitment of other RGS14:Gαi1-GDP complexes. (6) The RGS domain is then free to intercept and "GAP" a second nearby Gαi1-GTP after activation of a nearby GPCR, generating a Gαi1-GDP that could recruit a second RGS14. Unresolved (?) is how the complex is regulated to return to basal state (1). *(Panel B)* In the dendritic spines of CA2 hippocampal neurons, RGS14 is recruited to the post-synaptic density (PSD) by activated Gαi1-GTP following coincident activation of a GPCR (e.g. metabotropic glutamate receptors, others) and iGluRs (AMPA and NMDA receptors). Following RGS domain-catalyzed GTP hydrolysis, RGS14 may remain bound at the membrane by inactive Gαi1-GDP through the GPR domain, thereby concentrating RGS14 at the PSD. This serves to nucleate subsequent recruitment of a collection of RGS14:Gαi1 complexes at the PSD to form a signaling node that can intercept incoming excitatory signals promoting LTP, such as H-Ras and Ca^{2+}/calmodulin (CaM). Clustering of inactive Gαi1-GDP in an RGS14:Gαi1 signaling node may also promote sustained signaling by activated Gβγ.

domain is free to GAP one or more adjacent Gα-GTP subunits to form free Gα-GDP, each capable of recruiting RGS14 to form a cluster of RGS14:Gα-GDP complexes. Within the dendritic spines of CA2 neurons (Figure 4.9B), coincident activation of AMPA receptors and nearby Gαi-linked group II metabotropic glutamate receptors (or other GPCRs) by released glutamate may recruit a cluster of RGS14:Gα-GDP to the plasma membrane (or PSD). As we have reported previously, this complex is capable of interacting with active H-Ras-GTP to inhibit ERK signaling (166) and Ca^{2+}/CaM (235), both key regulators of LTP and synaptic plasticity (236,237). Recruitment of RGS14 would limit Gαi1-GTP signaling, and the newly formed RGS14:Gαi-GDP complex is now well positioned to sequester H-Ras-GTP and/or CaM activated by Ca^{2+}-influx from NMDA receptors, and thereby inhibit downstream signaling events essential for LTP.

An implicit prediction of this model is that RGS14 sequestering of Gα-GDP would enhance/prolong the signaling of the Gβγ abandoned by the Gα-GDP bound to RGS14. Therefore, the purpose of this GPCR signaling event in dendrites/spines of CA2 neurons may be to nucleate a localized cluster of RGS14:Gα-GDP to serve as a signaling center, block LTP, and enhance Gβγ signaling (for as yet unknown purposes). Cellular mechanisms that regulate and reverse this complex are poorly understood at this time, though the RGS14:Gα-GDP complex is phosphorylated (178,238) and can be regulated by a GPCR and the non-receptor guanine nucelotide exchange factor Ric8A (173,218), suggesting possible modes of regulation for further investigation. While speculative, this model is entirely consistent with existing data, and makes predictions that are testable and under investigation. In this way, RGS14 may act to suppress LTP and synaptic plasticity in CA2 hippocampal neurons.

Chapter 5: RGS14 Regulates the Lifetime of Gα-GTP Signaling but does not Prolong Gβγ Signaling Following Receptor Activation in Live Cells

5.1 Introduction

Canonical G Protein-coupled receptor (GPCR) signaling begins with binding of an extracellular ligand to the receptor. Upon conformational rearrangement of the GPCR, the receptor is able to stimulate the exchange of GDP for GTP in the Gα subunit of the heterotrimeric G protein (Gαβγ) (239). Binding of GTP by Gα results in rearrangement and sometimes dissociation of the Gαβγ heterotrimer, allowing both Gα and Gβγ to signal to downstream effector molecules (210-212). Regulators of G protein signaling (RGS) proteins negatively regulate G protein signaling by serving as GTPase activating proteins (GAPs) that stimulate the intrinsic GTPase of the Gα subunit. Upon hydrolysis of GTP to GDP, Gα rebinds Gβγ thereby terminating the G protein signaling event (213-215).

Many RGS proteins have a relatively simple structure, lacking domains outside the canonical RGS domain. However, other RGS proteins have a more complicated structure. One such protein, RGS14, is a multifunctional scaffold that is highly expressed in the brain (162,169,170), and has been identified as a natural suppressor of synaptic plasticity in CA2 hippocampal neurons and of hippocampal-based learning and memory (169). As a member of the R12 family of RGS proteins, RGS14 possesses an N-terminal RGS domain that engages Gαi/o family members (75,162,163). In addition, RGS14 has a C-terminal G protein regulatory (GPR) motif (130,163) and two tandem Ras/Rap binding domains (RBDs) (162). The GPR motif binds inactive Gαi1/3 proteins while the first RBD binds activated H-Ras/Rap2 proteins (162,164-167).

Given its unique molecular architecture, RGS14 is primed to intercept incoming Gα signals. Previously we showed that activation of Gαi/o proteins can recruit cytosolic RGS14 to the plasma membrane through the RGS domain (177). Moreover, co-expression of inactive Gαi1 targets RGS14 to the plasma membrane through the GPR motif (172,177)

where RGS14 can form a Gα-dependent complex with GPCRs (167). Considering these two distinct Gα interacting sites, we have proposed a model of RGS14 function (177) in which the RGS domain 'senses' G protein activation, thereby recruiting cytosolic RGS14 to the plasma membrane. At the membrane, RGS14 accelerates the GTPase of the Gα to hydrolyze GTP to GDP. At this time, RGS14 would then be optimally positioned to bind the newly formed Gα-GDP through its GPR motif and form a stable complex at the plasma membrane.

Previous studies have indicated that the binding of Gα by Gβγ and the GPR motif of RGS14 are mutually exclusive (133,172). In support of this idea, structural characterization of the RGS14 GPR motif demonstrated that the binding site on Gα of the RGS14 GPR motif overlaps with that of Gβγ (132). While biochemical studies have suggested the RGS14 GPR motif cannot disrupt preformed Gαβγ heterotrimers (133), other studies have suggested the GPR motif may prevent heterotrimer re-assembly after GPCR stimulation (136). As such, RGS14 interference with the re-association of Gα with Gβγ may prolong Gβγ signaling. To test the idea that RGS14 might prolong Gβγ signaling more than conventional RGS proteins, we utilized a bioluminescence resonance energy transfer (BRET) based biosensor for Gβγ release to monitor the activation and deactivation of heterotrimeric G proteins that interact with RGS14 (Gαo and Gαi1). Using this biosensor, we compared RGS4, a conventional RGS protein, with the unconventional RGS14 to understand the regulation of G protein heterotrimers. We examined whether RGS14 interrupts formation of Gαβγ heterotrimers by examining basal BRET ratios prior to agonist addition. Additionally, we examined whether BRET signals returned to baseline after antagonist addition to assess whether RGS14 disrupts heterotrimer re-assembly after a signaling event.

Here we show that co-expression of RGS4 or RGS14 each limits the release of free Gβγ as well as stimulates the deactivation rate of G proteins in live cells. RGS14 does not appear to interfere with formation of Gαβγ heterotrimers either before or after receptor stimulation. Co-expression of inactive Gαi1 with RGS14 did not alter the GAP effect on Gαo proteins. Based on these findings, we propose that the RGS domain and the GPR motif of RGS14 function independently in live cells.

5.2 Experimental Procedures

Cell Culture and Transfection

HEK 293 cells were maintained in 1X Dulbecco's Modified Eagle's Medium without phenol red indicator supplemented with 10% fetal bovine serum (5% after transfection), 2 mM L-glutamine, 100 units/ml penicillin, and 100mg/ml streptomycin. Cells were kept in a 37 °C incubator supplied with 5% CO_2. Transfections were carried out using polyethyleneimine (PEI) as described previously (240).

Constructs and Reagents

The hemagglutinin (HA) epitope-tagged α2a-adrenergic receptor (HA-α2a-AR) used in this study was kindly provided by Dr. Joe Blumer (Medical University of South Carolina). Hemagglutinin epitope-tagged RGS4 (HA-RGS4) and FLAG-tagged RGS14 (FLAG-RGS14) were generated as described previously (172,241). The pertussis-resistant mutants (C351G) of Gαo and Gαi1 were purchased from the cDNA Resource Center (cDNA.org, Bloomsberg, PA). Mas-GRK3ct-Luc and Ven-Gβγ were described previously (242). UK 14,304 was obtained from Sigma-Aldrich (St. Louis, MO) while rauwolscine was purchased from Tocris Bioscience (Bristol, United Kingdom). Pertussis toxin was purchased from List Biological Laboratories, Inc (Campbell, CA).

Kinetic BRET Assay

For kinetic BRET experiments, HEK 293 cells seeded in six-well plates, were transfected with 25 ng mas-GRK3ct-Luc, 200 ng HA-α2A-AR, 200 ng Ven-Gβ1, 200 ng Ven-Gγ2, and 400 ng of either Gαo-C351G or Gαi1-C351G. HA-RGS4 or FLAG-RGS14 was also transfected in 3, 10, 30, and 100 ng amounts. For each experiment, a control using pertussis-sensitive Gαo or Gαi1 was included to record any noise within the system. Pertussis toxin (100 ng/ml) was added at the time of transfection to limit activation of endogenous G proteins. Twenty-four hours after transfection, cells were resuspended in Tyrode's solution (140mM NaCl, 5mM KCl, 1mM $MgCl_2$, 1 mM $CaCl_2$, 0.37mM NaH_2PO_4, 24mM $NaHCO_3$, 10mM HEPES, and 0.1% glucose, pH 7.4) and plated on white 96-well Optiplates (Perkin Elmer Life Sciences, Waltham, MA). Fluorescence measurements to confirm acceptor expression were made using the TriStar LB 941 plate reader (Berthold Technologies, Bad Wildbad, Germany) with 485-nm excitation and 530-nm emission filters. After a 5 minute application of 5 μM coelenterazine H (Nanolight Technologies, Pinetop, AZ), kinetic BRET was monitored using sequential measurements through 485- and 530-nm emission filters. BRET was recorded for 30 seconds with no stimulation to establish basal BRET. After basal BRET measurements, agonist was applied for 60 seconds followed by 90 seconds of antagonist application. The change in BRET (ΔBRET) was calculated by dividing the mas-GRK3ct-Luc signal (530 nm) by the Ven-Gβγ signal (485 nm) and subtracting the average BRET signal observed from the first 30 seconds of observation (basal BRET). With each experiment, a kinetic BRET control was performed utilizing pertussis-sensitive Gα to ensure the effectiveness of the pertussis toxin. Any signal recorded in these controls was regarded as noise and subtracted from experimental kinetic BRET recordings. Data were collected using the MikroWin 2000 software and analyzed using Microsoft Excel and

GraphPad Prism 5. Deactivation curves were fitted to a single phase decay exponential function. Statistical data analysis was performed using a one way analysis of variance (ANOVA) with Tukey's or Dunnett's post-hoc test where indicated.

5.3 Results

Activation of α2A-AR releases free Gβγ from Gαo and Gαi1 proteins

The goal of these studies was to compare the regulation of G protein activation and deactivation in live cells by a conventional RGS protein (RGS4) and an un-conventional RGS protein containing a second G protein binding GPR motif (RGS14). In order to assess signaling in live cells, we transfected a GPCR, Gα protein, Gβγ, and a biosensor for Gβγ activation (Figure 5.1A). The biosensor for Gβγ activation, designated as mas-GRK3ct-Luc (242), features the C-terminal Gβγ binding region of G protein coupled receptor kinase 3 (GRK3). A myristate attachment sequence (mas) was attached to the N-terminus of the GRK3 Gβγ binding domain while Renilla Luciferase (RLuc8) was attached to the C-terminus. The mas sequence allows the Gβγ biosensor to be targeted to the plasma membrane where the Luciferase tag serves as a BRET donor. A bimolecular fluorescence complementation technique was employed to generate a Venus-Gβ1γ2 BRET acceptor. Residues 156-239 of Venus were fused to the N-terminus of Gβ1 while residues 1-155 of Venus were fused to the N-terminus of Gγ2. Upon heterodimerization, the Venus-tagged Gβ1γ2 constructs form a functional Gβγ subunit (242,243). We chose this Gβγ biosensing system because the mas-GRK3ct-Luc biosensor provides a clear indication of heterotrimer activation (242,244,245). Additionally, we chose the α2A-adrenergic receptor as we have studied it previously and demonstrated that RGS14 can associate with the receptor in a Gαi1-dependent manner (167,173).

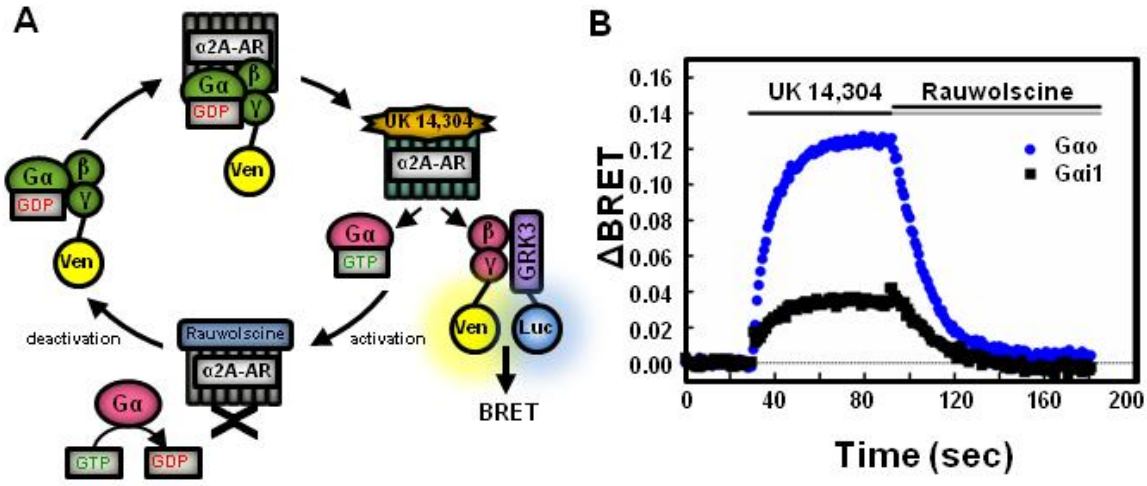

Figure 5.1. Gαo Releases More Free Gβγ than Gαi1 Following Receptor Activation. **(A)** Schematic representation of kinetic BRET experiment. Venus-tagged Gβ1 and Gγ2 form a dimer that binds inactive Gα-GDP. Addition of α2A-adrenergic receptor agonist UK 14,304 stimulates Gα to bind GTP and releases Venus-Gβγ. During the activation phase, free Venus-Gβγ binds the mas-GRK3ct-Luc to produce a rise in BRET. Addition of rauwolscine halts the activation of Gα proteins. During the deactivation phase, Gα hydrolyzes GTP to GDP and reforms a heterotrimer with Gβγ, quenching the BRET signal. **(B)** HEK 293 cells were transfected with 200 ng of α2A-adrenergic receptor, 200 ng of Venus-Gβ1, 200 ng of Venus-Gy2, 25 ng of mas-GRK3ct-Luc, and 400 ng of either Gαo or Gαi1. Baseline BRET was measured for 30 seconds prior to addition of agonist. Alpha2A-AR agonist (1 μM UK 14,304) was added for 60 seconds followed by a 90 second application of antagonist (100 μM rauwolscine). Data is expressed as average whole traces of BRET in cells expressing Gαo (blue, n=3) and Gαi1 (black, n=4).

HEK 293 cells were transfected with the α2A-adrenergic receptor (α2A-AR), mas-GRK3ct-Luc, Venus-Gβγ and either Gαo or Gαi1, each containing a mutation conferring pertussis toxin-resistance (C351G) and then treated with pertussis toxin to eliminate signaling contributions from endogenous G proteins. Addition of α2A-AR agonist UK 14,304 (1 μM) activates the G protein heterotrimer and produces dissociation of the Gα and Gβγ subunits. Free Gβγ binds the Gβγ activation biosensor as indicated by the rise in ΔBRET (Figure 5.1B). After 60 seconds of agonist application, addition of α2A-AR antagonist rauwolscine (100 μM) rapidly halts activation of G proteins and allows Gα proteins to hydrolyze GTP to GDP. Gβγ dissociates from the Gβγ biosensor to reform a heterotrimer with Gα as indicated by a decrease in ΔBRET.

Agonist-induced activation of Gαo proteins generated a larger ΔBRET than Gαi1. Cells expressing Gαo produced a maximum ΔBRET of 0.129 (± 0.020 SE) while cells expressing Gαi1 produced a maximum ΔBRET of 0.040 (± 0.002 SE) (Figure 5.1B). These results are consistent with other reports suggesting Gαi1 proteins do not release as much free Gβγ as Gαo proteins (245,246).

Expression of RGS4 reduces the release of free Gβγ and accelerates the deactivation rate of G proteins

To determine the effect of an RGS protein on free Gβγ release, we co-expressed increasing amounts of RGS4 (Figures 5.2A, 5.3A). We chose RGS4 because it is a well studied RGS protein that features a relatively simple protein structure, lacking domains outside the RGS domain. In cells expressing Gαo, expression of 100 ng of RGS4 significantly reduced the maximum ΔBRET from 0.112 (± 0.010 SE) to 0.078 (± 0.003 SE, $p < 0.01$) (Figure 5.2B). In cells expressing Gαi1, co-expression of RGS4 did not result in a

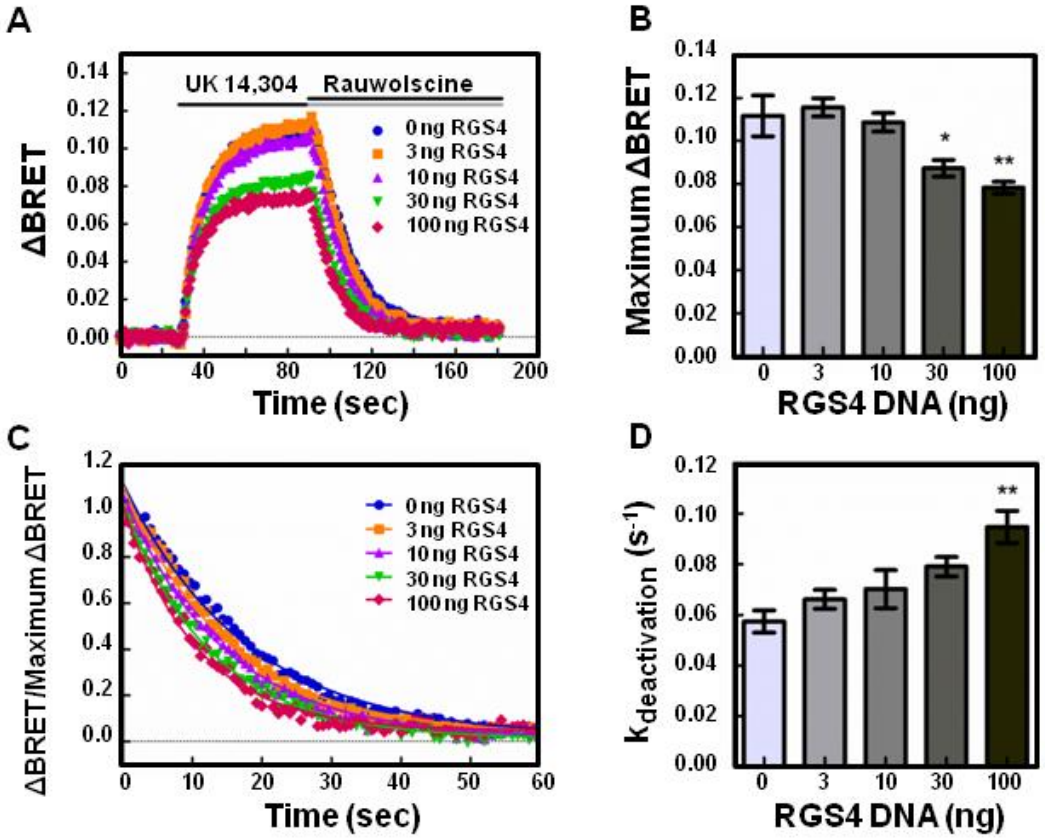

Figure 5.2. RGS4 Reduces the Release of Free Gβγ and Accelerates the Deactivation of Gαo Proteins Following Receptor Activation. **(A)** HEK 293 cells were transfected with 200 ng of α2A-adrenergic receptor, 200 ng of Venus-Gβ1, 200 ng of Venus-Gγ2, 25 ng of mas-GRK3ct-Luc, and 400 ng of Gαo and monitored for kinetic BRET as in Figure 1. Average whole traces of BRET signal over time are shown from cells expressing Gαo alone and 3, 10, 30, or 100 ng of HA-RGS4 (n=3). **(B)** Maximum ΔBRET observed from data presented in (A). **(C)** Deactivation curves normalized to Maximum BRET and fit using a single exponential decay function. **(D)** Deactivation rates ($k_{deactivation}$) determined from curves fit in (C). Error bars represent ± S.E. Statistical analysis was performed using a one-way analysis of variance (ANOVA) with Tukey's post-hoc test (*$p<0.05$, **$p<0.01$).

significant decrease in maximum ΔBRET though a trend appears to be present (Figure 5.3B).

We then examined the effect of an RGS on Gα GTPase activity. The association of Gβγ with the biosensor is governed by the activation state of Gα. Upon heterotrimer activation and formation of Gα-GTP, Gβγ is released and binds the Gβγ biosensor. Upon hydrolysis of GTP to GDP, Gα-GDP regains affinity for Gβγ and Gβγ dissociates from the biosensor to reassociate with Gα-GDP. As Gβγ association with the biosensor is directly tied to the activation state of Gα, the deactivation rate serves as an indirect measure of the Gα GTPase rate (93). To determine the deactivation rate, we fit the BRET curve dissociation phase with a single phase exponential decay function (Figures 5.2C, 5.3C).

In cells expressing Gαo alone, the deactivation rate was determined to be 0.057 s^{-1} (± 0.004 SE) (Figure 5.2D). In cells expressing 100 ng RGS4, the deactivation rate increased significantly to 0.095 s^{-1} (± 0.006 SE, $p < 0.01$). In cells expressing Gαi1, 100 ng of RGS4 expression significantly increased the deactivation rate from 0.044 s^{-1} (± 0.001 SE) to 0.083 s^{-1} (± 0.005 SE, $p < 0.01$) (Figure 3D). These results correspond with the decreased maximum ΔBRET observed in Figures 5.2B and 5.3B and highlight the utility of the Gβγ biosensor in detecting free Gβγ release and inferred GTPase rates of Gα proteins.

Expression of RGS14 reduces the release of free Gβγ and accelerates the deactivation rate of G proteins

We then sought to compare the effects of RGS14 with RGS4 on the release of Gβγ and deactivation rate. Unlike most RGS proteins including RGS4, RGS14 contains tandem Ras binding domains (RBDs) and a GPR motif in addition to the RGS domain that could regulate the RGS14 effects on G protein heterotrimer activity. Similar to RGS4 (Figures 5.2

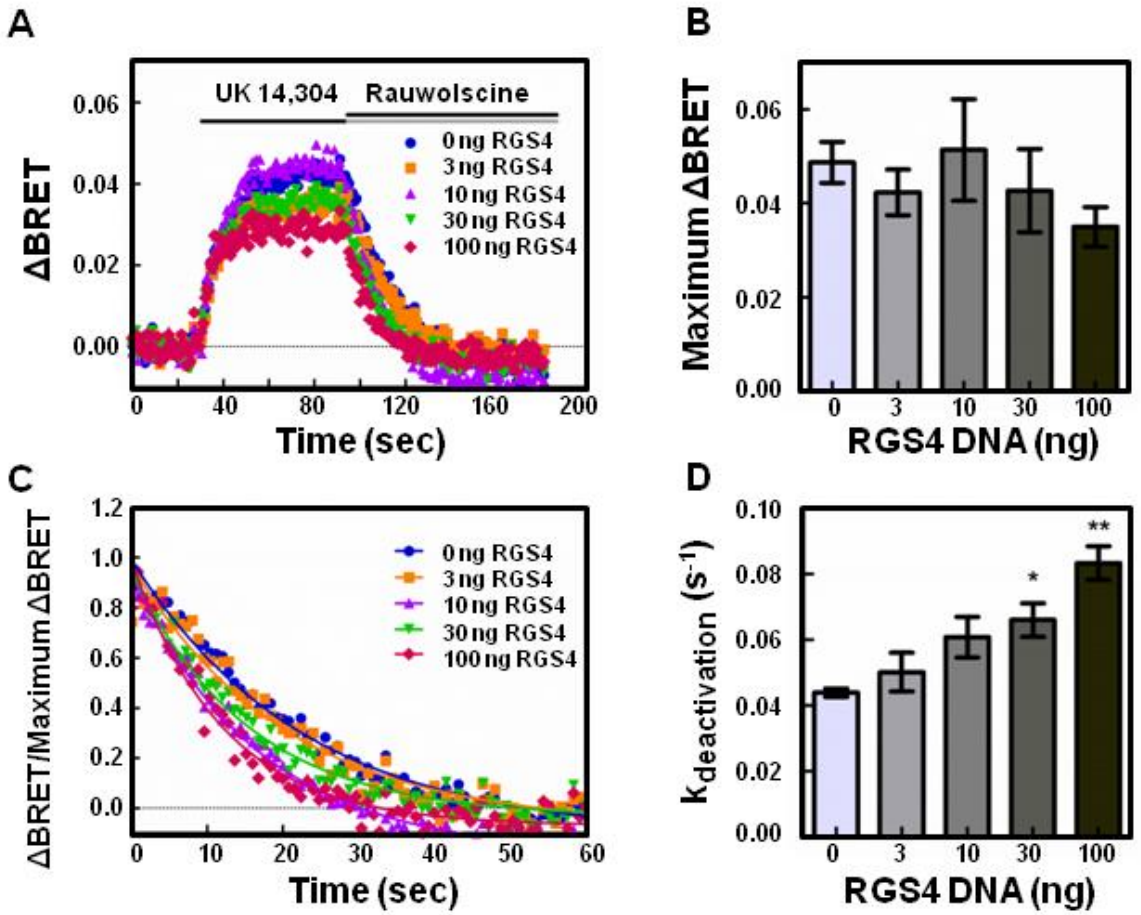

Figure 5.3. RGS4 Accelerates the Deactivation of Gαi1 Proteins Following Receptor Activation. **(A)** HEK 293 cells were transfected with 200 ng of α2A-adrenergic receptor, 200 ng of Venus-Gβ1, 200 ng of Venus-Gγ2, 25 ng of mas-GRK3ct-Luc, and 400 ng of Gαi1 and monitored for kinetic BRET as in Figure 1. Average whole traces of BRET signal over time are shown from cells expressing Gαi1 alone and 3, 10, 30, or 100 ng of HA-RGS4 (n=3). **(B)** Maximum ΔBRET observed from data presented in (A). **(C)** Deactivation curves normalized to Maximum BRET and fit using a single exponential decay function. **(D)** Deactivation rates ($k_{deactivation}$) determined from curves fit in (C). Error bars represent ± S.E. Statistical analysis was performed using a one-way analysis of variance (ANOVA) with Tukey's post-hoc test (*$p<0.05$, **$p<0.01$).

and 5.3), increasing expression of RGS14 reduced the maximum ΔBRET observed in both Gαo and Gαi1 expressing cells (Figures 5.4A, 5.5A). In cells expressing Gαo, co-expression of 100 ng of RGS14 decreased the maximum ΔBRET from 0.129 (± 0.020 SE) to 0.023 (± 0.009 SE, $p < 0.01$) (Figure 5.4B). Similar results were obtained in cells expressing Gαi1 where the maximum ΔBRET recorded for Gαi1 decreased from 0.040 (± 0.002 SE) to 0.014 (± 0.001 SE $p < 0.05$) in cells co-expressing 100 ng of RGS14 (Figure 5.5B). These results indicate that RGS14 limits the release of free Gβγ from both Gαo and Gαi1 proteins.

Next we determined the deactivation kinetics of G proteins in response to RGS14 expression (Figure 5.4C, 5.5C). In conditions transfected with 100 ng of RGS14, the ΔBRET was not large enough to reliably fit the deactivation curve, thus we limited this analysis to conditions transfected with 0, 3, 10, and 30 ng of RGS14. In cells expressing Gαo, the deactivation rate was 0.067 s^{-1} (± 0.006 SE) (Figure 5.4D). Co-expression of 30 ng of RGS14 significantly increased the deactivation rate to 0.120 s^{-1} (± 0.006 SE, $p < 0.05$), indicative of RGS14 GAP activity. In cells expressing Gαi1, the deactivation rate was 0.049 s^{-1} (± 0.003 SE) which increased to 0.080 s^{-1} (± 0.004 SE) upon co-expression of 30 ng of RGS14 (Figure 5.5D).

RGS14 does not interrupt formation of Gαβγ heterotrimers

To assess whether RGS14 alters the formation of Gαβγ heterotrimers prior to agonist stimulation we then examined the basal BRET. As the GPR motif only interacts with Gαi1/3, we did not expect RGS14 to alter basal BRET of Gαo proteins. Prior to activation with receptor agonist, we recorded a basal ΔBRET value of 0.00 (± 0.003 SE). Upon expression of RGS14, no significant difference in basal ΔBRET values was observed across a range of increasing RGS14 amounts (Figure 5.4E). For Gαi1, we observed a basal ΔBRET

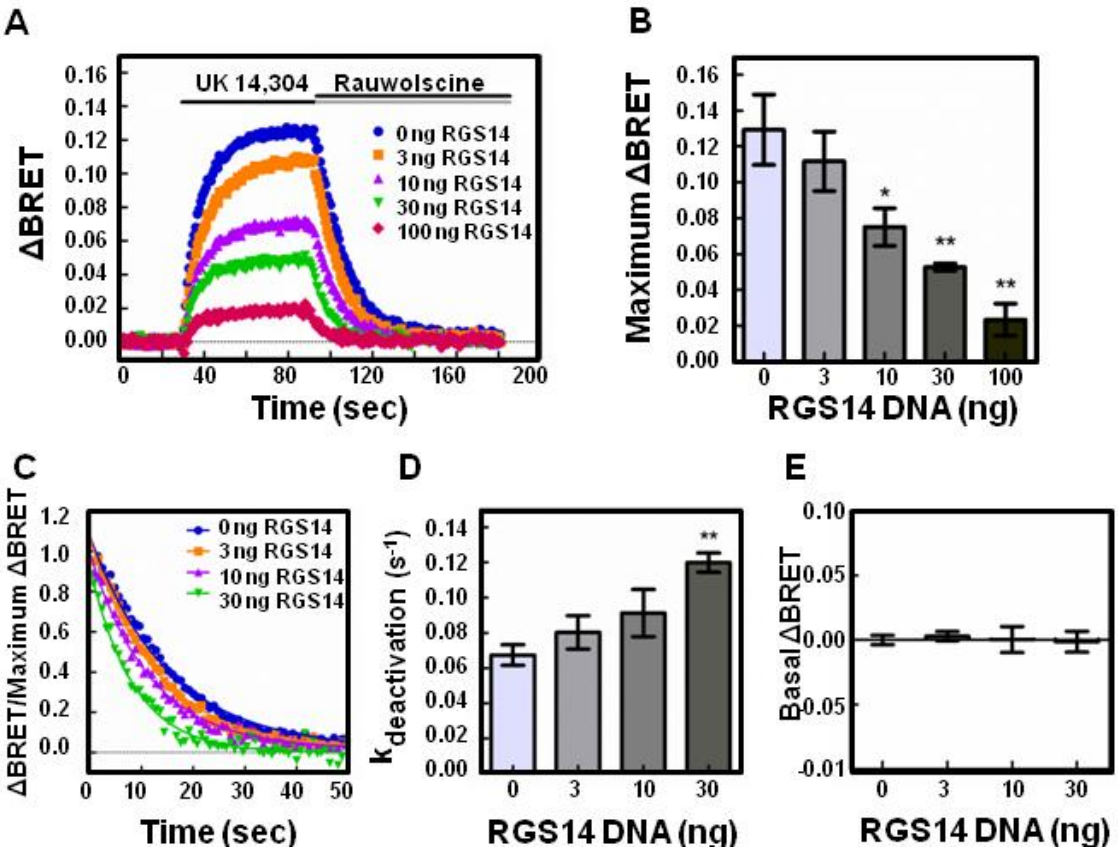

Figure 5.4. RGS14 Reduces the Release of Free Gβγ and Accelerates the Deactivation of Gαo Proteins Following Receptor Activation. **(A)** HEK 293 cells were transfected with 200 ng of α2A-adrenergic receptor, 200 ng of Venus-Gβ1, 200 ng of Venus-Gγ2, 25 ng of mas-GRK3ct-Luc, and 400 ng of Gαo and monitored for kinetic BRET as in Figure 1. Average whole traces of BRET signal over time are shown from cells expressing Gαo alone and 3, 10, 30, or 100 ng of FLAG-RGS14 (n=3). **(B)** Maximum ΔBRET observed from data presented in (A). **(C)** Deactivation curves normalized to Maximum ΔBRET and fit using a single exponential decay function. **(D)** Deactivation rates ($k_{deactivation}$) determined from curves fit in (C). **(E)** Average BRET measured for 30 seconds at baseline, prior to agonist stimulation. Error bars represent ± S.E. Statistical analysis was performed using a one-way analysis of variance (ANOVA) with Tukey's post-hoc test (*$p<0.05$, **$p<0.01$).

value of 0.00 (± 0.004 SE) and no significant difference was observed upon expression of increasing amounts of RGS14 (Figure 5.5E). These results suggest co-expression of RGS14 does not alter the basal formation of Gαβγ heterotrimers.

Additionally, based on previous observations (133,136), we predicted RGS14 may be able to interfere with the capacity of the Gαi1 and Gβγ subunits to reform a heterotrimer. If RGS14 binding to Gαi1 through the GPR motif prevented Gβγ from rebinding Gαi1, we would expect that the ΔBRET to not return to baseline after addition of antagonist. Upon examination of deactivation curves, we did not observe any significant difference in the return to baseline after addition of antagonist. These results suggest RGS14 does not interfere with heterotrimer reformation after receptor stimulation.

RGS-null mutant of RGS14 cannot accelerate GTPase while the GPR-null RGS14 mutant retains GAP activity

Next, to elucidate the roles of the RGS domain and GPR motif on heterotrimer kinetics we employed RGS-null and GPR-null mutants of RGS14 (Figure 5.6). To examine whether the accelerated deactivation rates were due to the RGS domain, we employed an RGS-null mutation of RGS14 (E92A/N93A). In cells expressing Gαo, co-expression of 30 ng the RGS-null RGS14 resulted in a deactivation rate of 0.065 s^{-1} (± 0.009 SE), which did not differ from Gαo alone. Moreover, expression of a GPR-null mutant of RGS14 (Q515A/R516A) increased the deactivation rate to 0.132 s^{-1} (± 0.012 SE), which did not differ from RGS14-WT.

Similar results were obtained in cells expressing RGS14 mutants with Gαi1 proteins (Figure 5.7). Expression of 30 ng of RGS-null RGS14 resulted in a deactivation rate of 0.052 s^{-1} (± 0.004 SE), which did not differ from the deactivation rate in cells expressing Gαi1

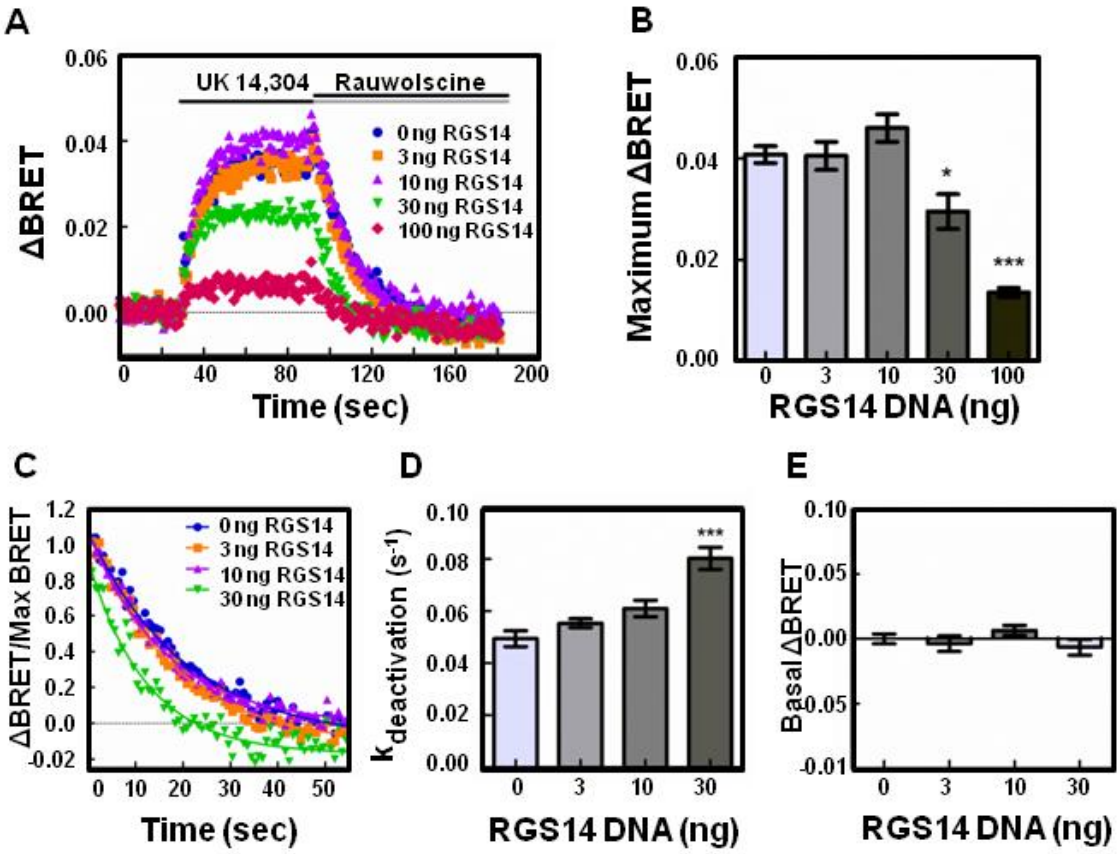

Figure 5.5. RGS14 Reduces the Release of Free Gβγ and Accelerates the Deactivation of Gαi1 Proteins Following Receptor Activation. **(A)** HEK 293 cells were transfected with 200 ng of α2A-adrenergic receptor, 200 ng of Venus-Gβ1, 200 ng of Venus-Gγ2, 25 ng of mas-GRK3ct-Luc, and 400 ng of Gαi1 and monitored for kinetic BRET as in Figure 1. Average whole traces of BRET signal over time are shown from cells expressing Gαi1 alone and 3, 10, 30, or 100 ng of FLAG-RGS14 (n=4). **(B)** Maximum ΔBRET observed from data presented in (A). **(C)** Deactivation curves normalized to Maximum BRET and fit using a single exponential decay function. **(D)** Deactivation rates ($k_{deactivation}$) determined from curves fit in (C). **(E)** Average BRET measured for 30 seconds at baseline, prior to agonist stimulation. Error bars represent ± S.E. Statistical analysis was performed using a one-way analysis of variance (ANOVA) with Tukey's post-hoc test (*$p<0.05$, ***$p<0.001$).

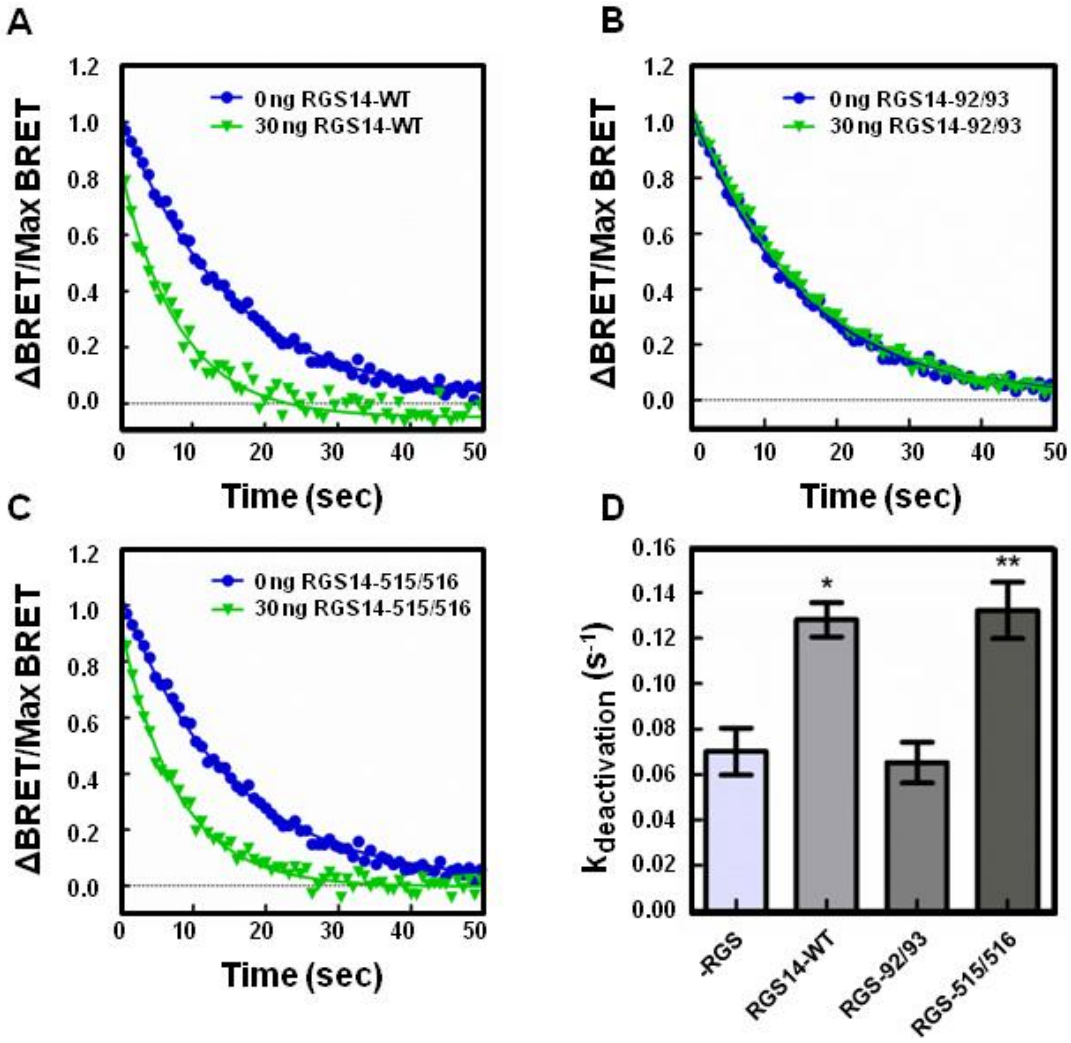

Figure 5.6. RGS14 Accelerates the Deactivation of Gαo Proteins through its RGS Domain Following Receptor Activation. **(A)** HEK 293 cells were transfected with 200 ng of α2A-adrenergic receptor, 200 ng of Venus-Gβ1, 200 ng of Venus-Gγ2, 25 ng of mas-GRK3ct-Luc, and 400 ng of Gαo and monitored for kinetic BRET as in Figure 1. Deactivation curves were normalized to Maximum BRET and fit using a single exponential decay function in cells expressing Gαo and either 0 ng or 30 ng FLAG-RGS14-WT (n=3). **(B)** Deactivation curves as in (A) in cells expressing Gαo and either 0 ng or 30 ng FLAG-RGS14-E92A/N93A (n=3). **(C)** Deactivation curves as in (A) in cells expressing Gαo and either 0 ng or 30 ng FLAG-RGS14-Q515A/R516A (n=3). **(D)** Deactivation rates ($k_{deactivation}$)

determined from curves fit in (A, B, and C). Error bars represent ± S.E. Statistical analysis was performed using a one-way analysis of variance (ANOVA) with Dunnett's post-hoc test (*$p<0.05$, **$p<0.01$).

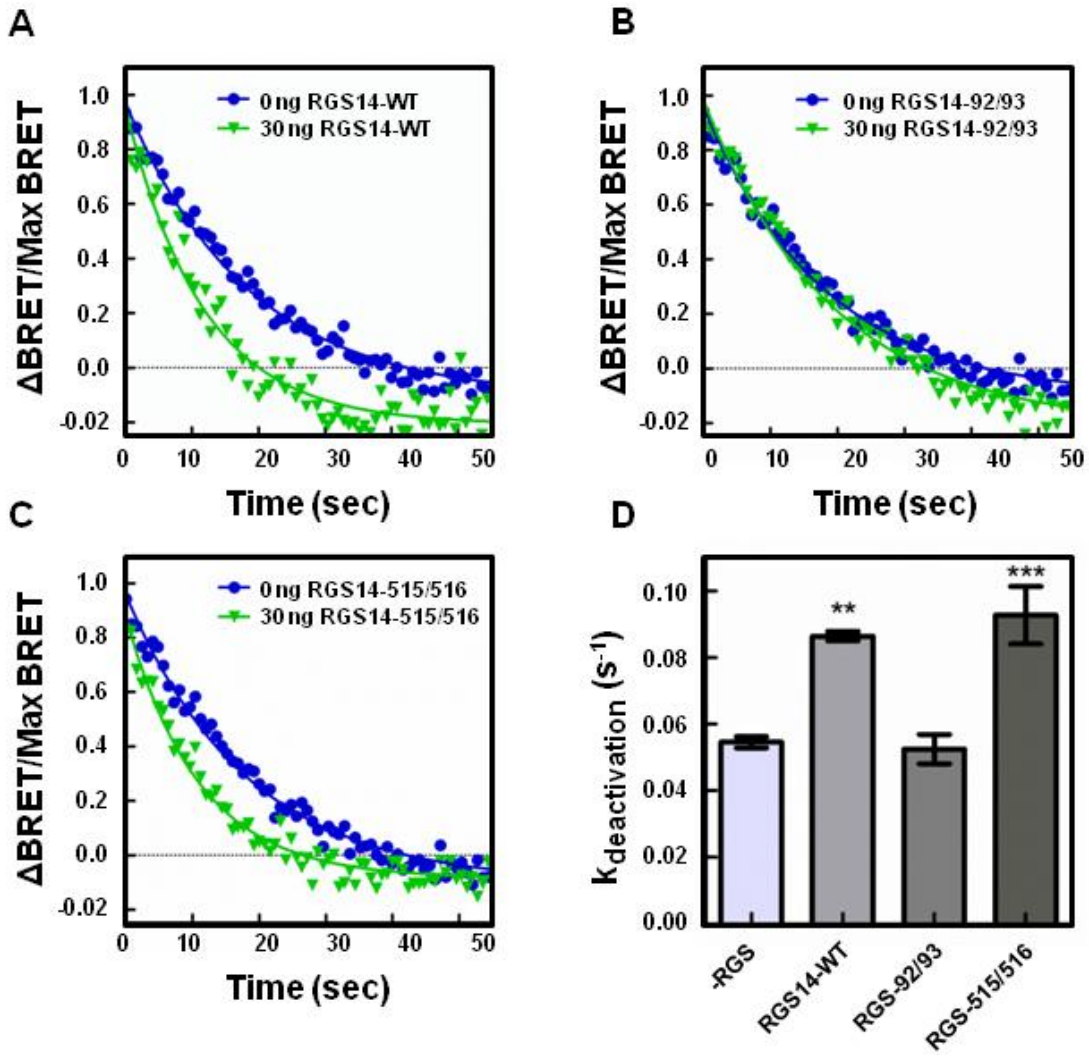

Figure 5.7. RGS14 Accelerates the Deactivation of Gαi1 Proteins through its RGS Domain Following Receptor Activation. **(A)** HEK 293 cells were transfected with 200 ng of α2A-adrenergic receptor, 200 ng of Venus-Gβ1, 200 ng of Venus-Gγ2, 25 ng of mas-GRK3ct-Luc, and 400 ng of Gαi1 and monitored for kinetic BRET as in Figure 1. Deactivation curves were normalized to Maximum BRET and fit using a single exponential decay function in cells expressing Gαi1 and either 0 ng or 30 ng FLAG-RGS14-WT (n=3). **(B)** Deactivation curves as in (A) in cells expressing Gαi1 and either 0 ng or 30 ng FLAG-RGS14-E92A/N93A (n=3). **(C)** Deactivation curves as in (A) in cells expressing Gαi1 and either 0 ng or 30 ng FLAG-RGS14-Q515A/R516A (n=3). **(D)** Deactivation rates ($k_{deactivation}$)

determined from curves fit in (A, B, and C). Error bars represent ± S.E. Statistical analysis was performed using a one-way analysis of variance (ANOVA) with Dunnett's post-hoc test (**$p<0.01$, ***$p<0.001$).

alone. Expression of 30 ng of GPR-null RGS14 resulted in a deactivation rate of 0.093 s^{-1} (± 0.009 SE), which did not differ from RGS14-WT.

RGS14 GAP function on Gαo is unaltered by GPR binding of Gαi1

Our previous investigations of RGS14 revealed that, when bound to an inactive Gα at the GPR motif, RGS14 undergoes conformational rearrangements within the RGS domain (177). Upon measurement of RGS domain function utilizing *in vitro* GTPase assays, the preformed RGS14:Gαi1-GDP complex showed no difference in its ability to catalyze GTPase activity in Gαo when compared to apo-RGS14 (177). Thus, despite binding an inactive G protein to the GPR motif, RGS14 retained RGS function to stimulate the GTPase of a second Gα at the RGS domain (177). Moreover, we were able to demonstrate the capacity of RGS14 to form a ternary complex with an inactive Gα at the GPR motif and an active Gα at the RGS domain (177).

To further demonstrate the role of the GPR motif in regulating RGS function in live cells, we examined whether co-expression of Gαi1 altered RGS14 effects on Gαo heterotrimers (Figure 5.8A). For these experiments we utilized pertussis-resistant Gαo and pertussis-sensitive Gαi1 proteins to ensure the recorded signal was due to Gαo activation. As a control, we examined the interaction with RGS14 and Gαi1 in the presence and absence of pertussis toxin. While treatment with pertussis toxin uncouples G proteins from GPCRs, pertussis toxin treatment did not alter the interaction between Gαi1 and the GPR motif of RGS14 (Figure 5.8B).

In cells expressing Gαo, co-expression of 10 ng of RGS14 resulted in a maximum ΔBRET of 0.0862 (± 0.006 SE). Upon co-expression of RGS14 and 300 ng of pertussis-sensitive Gαi1, the observed maximum ΔBRET was 0.0830 (± 0.007 SE) (Figure 5.8C,

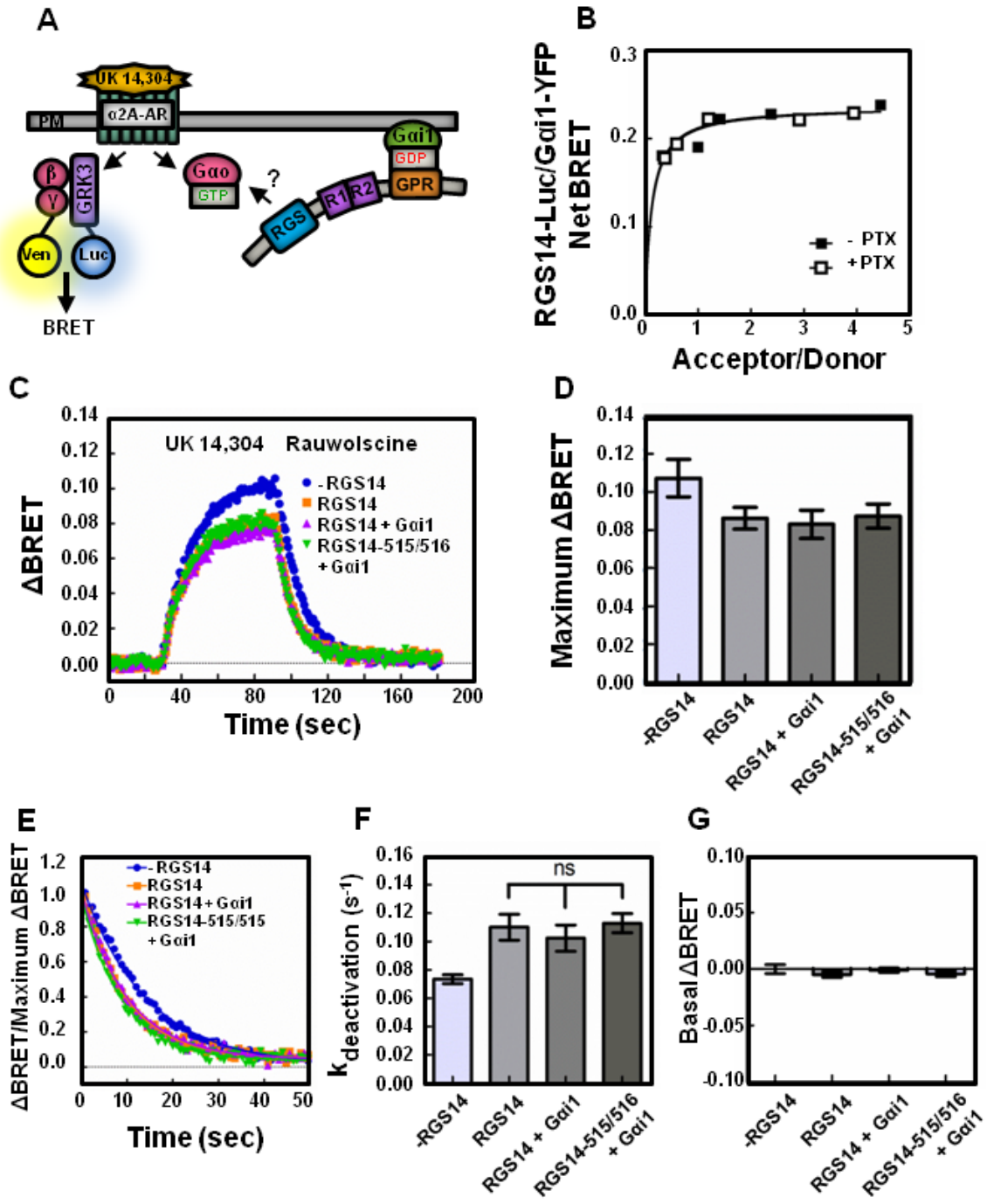

Figure 5.8. RGS14 GAP Function on Gαo is Unaltered by GPR Binding of Gαi1. (A) Schematic representation of BRET experiment. Expression of inactive Gαi1 recruits RGS14 to the plasma membrane through the GPR motif. Agonist binding of the α2A-adrenergic receptor activates the heterotrimeric G protein. Venus-Gβ1γ2 binds mas-GRK3ct to

produce a rise in the BRET signal. RGS14 placement at the plasma membrane may accelerate GTP hydrolysis by Gαo. **(B)** HEK 293 cells were transfected with 10 ng RGS14-Luc and 0, 50, 100, 250, 500, or 750 ng of Gαi1-YFP in the presence or absence of 100 ng/mL of pertussis toxin. BRET ratios were recorded, and net BRET was calculated by subtracting the BRET signal from the luciferase alone (n=3). **(C)** HEK 293 cells were transfected with 200 ng of α2A-adrenergic receptor, 200 ng of Venus-Gβ1, 200 ng of Venus-Gγ2, 25 ng of mas-GRK3ct-Luc, 400 ng of pertussis resistant Gαo as well as 10 ng of FLAG-RGS14/FLAG-RGS14-515/516 and 300 ng of pertussis-sensitive Gαi1 where indicated. Kinetic BRET was monitored for as in Figure 1 (n=4). **(D)** Maximum ΔBRET observed from data presented in (C). **(E)** Deactivation curves were normalized to Maximum BRET and fit using a single exponential decay function (n=4). **(F)** Deactivation rates ($k_{deactivation}$) were determined from curves fit in (C). **(G)** Average BRET measured for 30 seconds at baseline, prior to agonist stimulation. Error bars represent ± S.E. Statistical analysis was performed using a one-way analysis of variance (ANOVA) with Tukey's post-hoc test.

5.8D), demonstrating no difference from RGS14 expressed alone. Co-expression of a GPR-null (RGS14-515/516) confirmed the observed effect on ΔBRET was due to an intact RGS domain (Figure 5.8D). Additionally, the enhanced deactivation rate observed with expression of RGS14 was unchanged with co-expression of Gαi1. In cells expressing RGS14 alone, the observed deactivation rate was 0.110 s^{-1} (± 0.009 SE) while cells expressing RGS14 and 300ng of pertussis-sensitive Gαi1 demonstrated an observed deactivation rate of 0.1023 s^{-1} (± 0.009 SE) (Figure 5.8E, 5.8F). Co-expression of either RGS14 or RGS14 and Gαi1 did not alter the basal BRET (Figure 5.8G). These results suggest that Gα interactions at the GPR motif do not alter RGS domain function on a separate G protein.

5.4 Discussion

The primary goal of this work was to compare the effects of a conventional RGS protein (RGS4) and an unconventional RGS protein (RGS14) on G protein activation/deactivation kinetics and Gβγ signaling. Many conventional RGS proteins interact directly with the receptor/G protein complex by one or more mechanisms to deactivate both Gα and Gβγ signaling (247). RGS14, by contrast, with both a GPR motif and an RGS domain, exerts unique regulation of G protein signaling that has yet to be fully elucidated. Our previous work revealed RGS14 can bind two G proteins simultaneously, one active Gα-GTP at the RGS domain and one inactive Gα-GDP at the GPR motif (177). *In vitro* GTPase assays showed that binding of inactive Gα-GDP to the GPR motif does not alter the GAP function of the RGS domain (177). While this biochemical assessment provided key insights into the mechanics of RGS14 function, how this information would translate to a cellular environment remained unclear. Moreover, these previous findings were unable to clarify the effects RGS14 regulation of Gα would have on Gβγ signaling. Two possible models exist: 1)

The RGS domain of RGS14 could operate independently of the GPR motif and serve as a dedicated GAP that deactivates both Gα and Gβγ signaling, similar to other conventional RGS proteins, or 2) the RGS domain and the GPR motif could work cooperatively to deactivate and capture inactive Gαi-GDP, thereby preventing G protein heterotrimer reassociation and prolonging Gβγ signaling. Our findings in this study are most consistent with the former model, and suggest that the GPR motif is functionally silent in regulating RGS14 GAP activity in a cellular context.

Gαo releases more free Gβγ than Gαi1

Upon examining ΔBRET in our reconstituted GPCR/G protein signaling system, an apparent difference in free Gβγ released by Gαo and Gαi1 emerged. Activation of Gαo-containing heterotrimers resulted in an approximately 3-fold greater increase in Gβγ BRET activity indicative of release of free Gβγ than activation of Gαi1-containing heterotrimers. This difference observed in free Gβγ release could be due to differential delivery of Gαo heterotrimers to the plasma membrane than Gαi1. Similar studies have also demonstrated larger maximum ΔBRET signals in HEK cells expressing Gαo than Gαi1 transfected with similar Gα:Gβγ ratios as we present here (245). Alternatively, the observed difference in free Gβγ release could be due to differences in coupling efficiency of heterotrimers with the GPCR or differential dissociation of heterotrimers after activation. These possibilities are not mutually exclusive and both may contribute to the phenomena observed. In a study examining the release of free Gβγ dimers from Gαo and Gαi1, Gβγ was more readily released from Gαo activation suggesting Gαi1 may have a higher affinity for Gβγ than Gαo (246). *In vitro* analysis of G protein affinities revealed Gαi1 has a higher affinity for Gβγ than Gαo (248). Thus the differences we observe in free Gβγ release may be due to the higher

affinity of Gαi1 for Gβγ than Gαo.

RGS proteins limit the release of free Gβγ and accelerate the deactivation rates of Gαo and Gαi1 proteins

We examined the effects of a conventional RGS protein, RGS4, and an unconventional RGS protein, RGS14, on the kinetics of G protein heterotrimer dissociation and reassociation. Somewhat surprisingly, RGS14 exhibited similar effects as RGS4 on G protein kinetics, despite having a distinct G protein binding domain in addition to the RGS domain. Increased expression of either RGS protein inhibited the release of free Gβγ. Moreover, increased RGS expression resulted in increased rates of deactivation for both Gαo and Gαi1 proteins. These results highlight the roles of RGS4 and RGS14 as negative regulators of Gαi/o signaling.

We determined whether the increase in rate of G protein deactivation by RGS14 was due solely to the RGS domain or had contributions from the GPR motif. Expression of an RGS-null mutant of RGS14 (E92A/N93A) abolished the increase in deactivation rate observed with RGS14-WT, whereas expression of a GPR-null mutant of RGS14 did not alter the deactivation rate observed with RGS14-WT. These results highlight that the deactivation of G protein signaling by RGS14 is due solely to the RGS domain and that the GPR motif does not slow reassociation of heterotrimers.

RGS14 does not alter the formation of Gαi1 heterotrimers with Gβγ

Binding of Gαi1 by the RGS14 GPR motif and Gβγ are mutually exclusive (132,164,172). Previous *in vitro* studies have suggested that the RGS14 GPR motif cannot displace Gβγ from a preformed Gαβγ heterotrimer (133). However, other studies have

suggested that an isolated RGS14 GPR motif peptide can prevent heterotrimer assembly *in vitro*, and alter Gβγ signaling to GIRK channels in response to D2S dopamine receptor activation (136). To examine whether co-expression of RGS14 alters the basal formation of Gαβγ heterotrimers in cells, we examined basal BRET prior to agonist stimulation. Since the RGS14 GPR motif is selective for Gαi1 (163), we expected co-expression of RGS14 to disrupt basal BRET in Gαi1 expressing cells, but not Gαo expressing cells. However, in cells expressing either Gαi1 or Gαo, we saw no difference in basal BRET upon co-expression of RGS14. These results suggest that RGS14 does not alter the assembly of Gαβγ heterotrimers in live cells, consistent with previous observations with purified proteins (133).

Whereas RGS14 does not appear to disrupt the basal formation of Gαβγ heterotrimers, it may be able to bind Gα-GDP following a GPCR-mediated signaling event. As the GPR motif does not bind Gαo (163), we did not see a difference in return to baseline BRET in cells expressing Gαo (Figure 5.4). Surprisingly, we also did not see a difference in return to baseline in cells expressing Gαi1 (Figure 5.5). These results suggest that RGS14 does not interfere with heterotrimer assembly prior to or after agonist stimulation, and does not prolong Gβγ signaling, suggesting that RGS14 may be prebound to the plasma membrane by a distinct Gαi that is bound to the GPR motif and uninvolved with the receptor signaling event.

Interactions of the GPR motif with Gαi1 does not alter RGS14 RGS domain GAP activity towards Gαo

The presence of a second G protein binding motif (GPR) in RGS14 presents a unique mechanism for further regulation of G protein signaling in addition to the RGS domain. Previously we have demonstrated that upon co-expression of inactive Gαi1, RGS14

is targeted to the plasma membrane (172,177) where it can associate with GPCRs via Gα (173). We previously proposed that GPR associations with membrane bound G proteins could facilitate RGS14 RGS GAP activity by physically bringing RGS14 to the site of G protein signaling (177). Recent evidence suggests that membrane association of R7 RGS family members, specifically RGS7 and RGS9-2, potentiated the GAP effect of the RGS domain (249). Results obtained in the current study suggest that RGS14 association with the plasma membrane via the GPR motif does not enhance the deactivation kinetics of RGS14-accelerated G protein deactivation (Figure 5.8). Taken together, these results suggest that the RGS domain and GPR motif function independently from one another, perhaps on distinct Gα - one involved with receptor signaling and a second that anchors RGS14 to the plasma membrane.

While we did not observe a change in Gαo kinetics upon co-expression of Gαi1, our studies do not address the possibility that treatment with pertussis toxin may have altered the ability of Gαi1 to recruit RGS14 to the site of G protein activation. Previously, we and others have shown that GPR-containing proteins can associate with GPCRs (173,174), an association that is dependent on Gα. Pertussis toxin-mediated uncoupling of receptor/Gαi1 may not optimally position RGS14:Gαi1 complexes to favor interaction with GPCRs. However, given that these studies were completed with expressed recombinant proteins, the density of G proteins at the plasma membrane likely favored RGS14:Gαi1 complex placement near GPCRs.

Concluding remarks

Here we compared the effects of distinct RGS proteins on Gαi/o heterotrimeric signaling. Our results indicate that the conventional RGS protein RGS4 and the

unconventional RGS14 each similarly limit the release of free Gβγ and accelerate the deactivation rate of Gα. The GAP effect of RGS14 is solely due to the RGS domain as binding of an inactive G protein to the GPR motif does not alter the GAP effect of the RGS domain. The results presented here suggest the RGS domain and GPR motif do not coordinate to regulate G protein signaling. We propose that despite containing two Gα interaction sites, the GPR motif serves to anchor RGS14 in complex with Gαi-GDP at membranes and is functionally silent with regard the RGS domain-mediated GAP activity with no direct effect on Gβγ signaling.

Chapter 6: Discussion

6.1 Introduction

The overall goal of this dissertation project was to understand how RGS14 integrates heterotrimeric G protein signaling. Previous biochemical characterization demonstrated RGS14 engages G proteins at two different sites, the RGS domain and GPR motif. By examining the structure and function of RGS14 with complementary biochemical and cellular techniques, I further clarified roles of these structural features. Additionally, previous physiological characterization of RGS14-KO mice suggested RGS14 regulates synaptic signaling in the form of long term potentiation (LTP) as well as learning and memory. However, how regulation of G protein signaling by RGS14 relates to synaptic signaling remains unknown. Possible roles for RGS14 function in regulating synaptic plasticity are discussed in sections below.

6.2 RGS14 is a Dynamic Scaffolding Protein

The presence of multiple G protein interaction sites in RGS14 provides a unique mechanism for G protein regulation. Previous characterizations of RGS14 examined the function of each domain in isolation. My studies here, however, sought to explore whether binding at one site could affect activity at another site. In order to examine the complex regulation of signaling by RGS14 I embarked on developing protocols for purification of untagged RGS14 from *Escherichia coli* and bioluminescence resonance energy transfer (BRET), detailed in Chapters 2 and 3, respectively.

As described in Chapter 4, I examined the effect of Gα binding with a dual-tagged RGS14 BRET sensor (Venus-RGS14-Luciferase). Co-expression with Gαi/o proteins suggested RGS14 adopts different conformations depending on whether a G protein is bound to the RGS domain or GPR motif. This was expected as conformational flexibility is

inherent to scaffolding proteins and allows the accommodation of different binding partners. Moreover, *in vitro* characterization of purified RGS14 with hydrogen-deuterium exchange (HDX) further highlighted the role of RGS14 as a scaffolding protein. While the RGS domain exhibited the most stable portions of the protein, the RBDs and GPR motif appeared less stable with the interdomain regions appearing the most flexible.

I expected that upon binding G proteins at either the RGS domain or the GPR motif, RGS14 might adopt a more stable conformation. Interestingly, allosteric stabilization was not observed with G protein binding at the RGS domain. However, I did observe increased allosteric stability upon binding of a G protein at the GPR motif. These results suggested that binding of a G protein at the GPR motif may regulate the RGS domain.

6.3 RGS14 Binds Two G Proteins Simultaneously

After observing allosteric changes in the RGS domain upon binding of a G protein at the GPR motif, I sought to examine whether RGS14 could bind a second G protein at the RGS domain. The capacity of RGS14 to engage two G proteins simultaneously had been proposed previously (217) however, the formation of the complex had never been demonstrated experimentally. Utilizing a mutant of Gαi1 that was insensitive to the activating effects of AlF_4^- (Gαi1-G42R), I demonstrated RGS14 could form a trimeric complex with activated Gαo bound to the RGS domain and Gαi1-G42R bound to the GPR motif. Upon forming a trimeric complex, RGS14 exhibited stabilization in the interdomain regions that was not observed when bound to a single G protein. These results are consistent with RGS14's role as a scaffolding protein and suggest that RGS14 may adopt a different conformation when bound to two G proteins.

6.4 Binding of Gα at the GPR Motif Does Not Prevent RGS GAP Function

As I observed that binding of a G protein at the GPR motif resulted in allosteric stabilization of the RGS domain, I then sought to determine if GAP function was altered utilizing purified proteins in a single-turnover GTPase assay. Though RGS14 could bind two G proteins simultaneously, binding of Gα at the GPR motif may positively or negatively influence the capacity of RGS14 to act as a GAP. Surprisingly, despite being bound by Gα at the GPR motif, no difference was observed in the GAP activity of the RGS14:Gαi1 complex from RGS14 alone. These results suggested that despite the allosteric stabilization observed in the RGS domain, binding of a G protein at the GPR motif and GAP activity at the RGS domain are independently regulated events.

6.5 Binding of Gα at the GPR Motif Does Not Alter RGS GAP Function in Live Cells

While single turnover GTPase assays with purified proteins suggested the GPR motif does not alter the function of the RGS domain, I also sought to examine whether the GPR motif regulated the GAP activity of RGS14 in live cells using kinetic BRET in Chapter 5. Consistent with *in vitro* results reported in Chapter 4, upon examination of deactivation kinetics in live cells expressing Gαo with RGS14, co-expression of inactive Gαi1 to recruit RGS14 to the plasma membrane did not alter the deactivation rate from cells expressing RGS14 alone. As the RGS domain and GPR motif appear to function independently in single turnover GTPase assays with purified proteins, these results further suggest the RGS domain and GPR motif function independently in a cellular context. Moreover, these results suggest that recruitment of RGS14 to the plasma membrane by inactive Gαi1 neither inhibits nor promotes RGS14 GAP activity.

Unlike RGS14, RGS7 and RGS9-2 were recently shown to exhibit increased

deactivation of G protein heterotrimers upon plasma membrane localization by R7BP (249). Potentially, R7BP positions RGS7 and RGS9-2 at the site of GPCR/G protein activation in a manner that did not occur in the present studies with RGS14. It is possible that the formation of an RGS14:Gαi:GPCR complex is necessary to potentiate RGS14 GAP activity on Gα proteins. Nevertheless, the results presented in Chapter 5 suggest that in a cellular context, the GPR motif does not interfere with the capacity of the RGS domain of RGS14 to exert GAP activity.

6.6 RGS14 Does Not Alter G Protein Heterotrimer Formation

Kinetic BRET assays were also used to assess RGS14 effects on Gαβγ heterotrimer formation. Proteins containing GPR motifs were originally identified as activators of G protein signaling (99). Moreover, as GPR motif binding of Gα is mutually exclusive with binding by Gβγ, GPR motif proteins were presumed to activate G protein signaling by enhancing Gβγ signaling to effectors (129,134). Previous studies have suggested the RGS14 GPR motif cannot disrupt preformed Gαβγ heterotrimers (133) but may interfere with heterotrimer re-assembly after receptor stimulation (136).

To examine whether RGS14 altered heterotrimer formation, I compared the unconventional RGS14 to a conventional RGS protein, RGS4. As RGS4 lacks a GPR motif, RGS4 acts solely as a dedicated GAP. RGS4 expression limited release of free Gβγ dimers and accelerated the deactivation rate after addition of antagonist, consistent with its role as a dedicated GAP. Similarly, RGS14 limits release of free Gβγ dimers and accelerated the deactivation rate after addition of antagonist suggesting RGS14 acts as a dedicated GAP in live cells. RGS14 did not appear to alter the formation of Gαβγ heterotrimers prior to agonist addition or after the addition of antagonist. These results suggest that RGS14 does

not function to modulate Gαβγ heterotrimer assembly or promote Gβγ signaling.

GPR motif containing proteins were initially characterized for their capacity to activate G proteins through release of Gβγ (99). While other GPR motif proteins can disrupt preformed Gαβγ heterotrimers (99,134), data presented in Chapter 5 suggests RGS14 cannot. Recent structural models of LGN GPR motifs may provide insight into the different interactions with G proteins between LGN and RGS14 GPR motifs. The original structural models of RGS14 GPR motif interactions with Gα highlighted the formation of a acidic-glutamine-arginine, (D/E)QR, triad that forms an "arginine finger" to facilitate binding of Gα (132). Recent structural work with LGN suggests its GPR motif proteins contain two "arginine fingers." This double "arginine finger" contains the consensus sequence (RΨ(D/E)(D/E)QR) and is conserved in all other GPR motif proteins except RGS14 (143). Moreover, while a GST-fused RGS14 GPR motif peptide has an affinity of 65 nM for Gαi1, a similar GST-fused RGS12 GPR motif has a higher affinity of 19 nM (130). Furthermore, the presence of additional GPR motifs in proteins such as AGS3 and LGN (four GPR motifs each) may have a cooperative effect on Gα binding. Peptides expressing multiple GPR motifs from LGN have an increased affinity for Gαi3 over peptides expressing each GPR motif alone (143). The increased affinity of LGN GPR motifs for Gα may allow LGN to interfere with heterotrimer formation while RGS14 does not.

6.7 Working Model

The data presented here helps elucidate the roles of the RGS14 RGS domain and GPR motif in regulating heterotrimeric G protein signaling. Previous data suggested RGS14 can bind Gαi1/3 proteins through the GPR motif and form a stable complex at the plasma membrane. My current data shows RGS14 can also be recruited through the RGS domain

which may position RGS14 in an ideal position to capture newly inactivated Gα proteins (Figure 6.1). Once bound to an inactive Gα through the GPR motif, the RGS domain is not precluded from binding and acting as a GAP on a second Gα to limit both Gα and Gβγ signaling pathways. My findings here suggest the role of the GPR motif may be to position RGS14 at the plasma membrane where RGS14 is free to engage a second G protein.

While I hypothesized RGS14 may disrupt heterotrimer formation, I did not observe any alterations in the ability of Gαβγ heterotrimers to form in the basal state or re-assemble after receptor stimulation. These findings suggest RGS14 cannot outcompete Gβγ for Gα binding. As Gα and Gβγ protein expression levels are known to be tightly regulated, it remains unclear how RGS14 fits within the heterotrimeric G protein paradigm. Potentially, RGS14 exists as a complex with Gα completely independent of Gβγ, utilizing a separate pool of Gα not destined for Gαβγ heterotrimer formation. As the stoichiometry of Gα, Gβγ, and RGS14 in native CA2 hippocampal neurons remains unknown, it not yet known whether this occurs *in vivo*.

6.8 Future Directions

Structural Characterization – One major aspect of RGS14 biochemistry that we were unable to resolve here is the structure of RGS14. How RGS14 structurally engages G proteins would provide crucial information to understanding the mechanistic function of RGS14. While HDX revealed purified RGS14 is a highly dynamic protein, binding of G proteins at the RGS domain and GPR motif resulted in significant stabilization of not only the RGS domain and GPR motif but also both Ras binding domains (R1 and R2) and interdomain regions. The purification scheme detailed in Chapter 2 provides high quality pure RGS14 that may be utilized for crystallization. Since the RGS14:Gαo:Gαi1-G42R

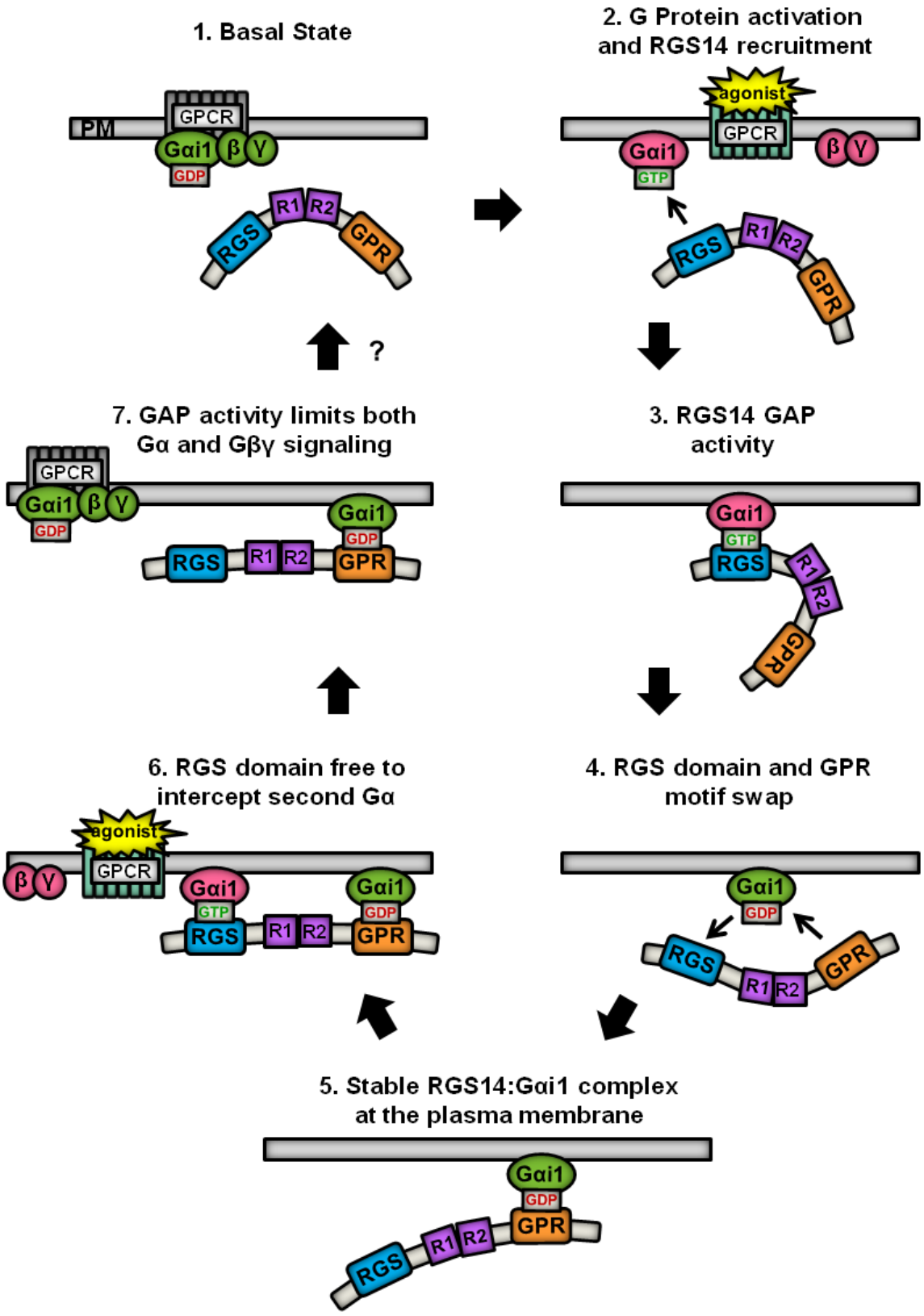
1. Basal State
PM
GPCR
Gαi1
β
γ
GDP
R1
R2
RGS
GPR
?
2. G Protein activation and RGS14 recruitment
agonist
GPCR
Gαi1
GTP
β
γ
RGS
R1
R2
GPR
3. RGS14 GAP activity
Gαi1
GTP
RGS
R1
R2
GPR
4. RGS domain and GPR motif swap
Gαi1
GDP
RGS
R1
R2
GPR
5. Stable RGS14:Gαi1 complex at the plasma membrane
Gαi1
GDP
GPR
R1
R2
RGS
6. RGS domain free to intercept second Gα
agonist
GPCR
β
γ
Gαi1
GTP
Gαi1
GDP
RGS
R1
R2
GPR
7. GAP activity limits both Gα and Gβγ signaling
GPCR
Gαi1
β
γ
GDP
Gαi1
GDP
RGS
R1
R2
GPR

Figure 6.1. Working Model of RGS14 Function. The proposed model of RGS14 signaling function proceeds clockwise from the top left. (1) In the basal resting state, Gαi1-GDP in complex with Gβγ is bound to a GPCR at the plasma membrane (PM) while RGS14 remains in the cytosol. (2) Agonist activation of a GPCR induces activation of the Gαβγ heterotrimer resulting in separation of the Gα and Gβγ subunits. Activated Gαi1-GTP recruits RGS14 to the plasma membrane. (3) RGS14 accelerates the GTPase of Gαi1, causing hydrolysis of GTP to GDP. (4) The RGS domain loses affinity for Gαi1-GDP and the GPR motif is free to bind the newly inactivated Gαi1. (5) RGS14 forms a stable complex with inactive Gαi1-GDP at the plasma membrane, which could serve to nucleate local recruitment of other RGS14:Gαi1-GDP complexes. (6) The RGS domain is then free to intercept and GAP a second Gαi1-GTP after activation of a nearby GPCR. (7) RGS domain-mediated GAP activity of Gα limits both Gα and Gβγ signaling to effectors. Unresolved (?) is how the RGS14:Gαi1 complex is regulated to return to basal state (1).

complex demonstrated the most stability by HDX, it is the best candidate for crystallization of a full length RGS14 protein. Alternatively, this protein complex may be better suited for Cryo-EM which allows for structural analysis of large and dynamic protein complexes. Either way, determination of the RGS14 structure in complex with its G protein binding partners would provide important information on the mechanics of G protein signaling integration by RGS14.

Establishing the Mechanism of RGS14 Function in CA2 Physiology – RGS14 is natively enriched in hippocampal CA2 pyramidal neurons, specifically in dendritic spines, shafts, and postsynaptic densities (PSDs) (169). Due to technical limitations of working with primary CA2 neurons, my studies relied heavily on purified proteins and heterologous transfection systems to explore RGS14 function. As RGS14 is not natively expressed in *E. coli* or HEK 293 cells, RGS14 likely does not receive the same post-translational modifications as RGS14 expressed in CA2 neurons. As a result, the function of purified and transfected RGS14 may differ from natively expressed RGS14. Moreover, given the native localization of RGS14, it is possible that RGS14 participates in a highly structured signaling complex or microdomain *in vivo* that is not observed in a reconstituted GPCR/G protein signaling system. Such a structured signaling complex may dictate how RGS14 engages Gα proteins through its RGS domain and GPR motif. Future experiments in CA2 neurons are required to define whether RGS14 participates in a structured signaling complex and receives function-altering post-translational modifications *in vivo*. Such data is imperative to determine the mechanism by which RGS14 regulates synaptic plasticity, learning, and memory.

Potential Unconventional Role of RGS14 in CA2 Hippocampal Neurons – The biggest challenge to understanding the role of RGS14 in native CA2 neurons is elucidating the molecular mechanisms by which RGS14 regulates synaptic signaling. *In vitro* characterization of the RGS domain reveals RGS14 functions as a GAP to limit Gαi/o signaling. *In vitro* characterization of the GPR motif reveals RGS14 functions as a GDI to prevent activation of Gαi1/3. Thus, RGS14 possesses two G protein interaction sites that would be predicted to coordinate its functions to limit canonical Gαi/o signaling *in vivo*.

Canonical Gαi/o signaling at excitatory synapses is strongly implicated in limiting LTP (Figure 6.2) (250). Gαi proteins are widely accepted to function by inhibiting adenylyl cyclase to decrease cAMP production. Cyclic AMP is vital to the production of LTP as it activates PKA to promote AMPA receptor delivery to the PSD and downstream gene expression necessary for maintenance of LTP (251,252). Additionally, canonical Gαo function in the brain is characterized by Gβγ signaling to GIRK channels. GIRK channels can contribute to the resting membrane potential of neurons. Enhanced GIRK signaling lowers the resting membrane potential preventing induction of LTP (253).

Given this information, loss of RGS14 would be predicted to enhance Gαi/o signaling and subsequently suppress LTP. Accordingly, loss of other Gαi/o selective RGS proteins, specifically RGS7, at excitatory synapses in CA1 hippocampal neurons results in suppressed LTP (91). These results are in accordance with the role of RGS7 as a dedicated GAP for Gαi/o proteins. Inconsistent with a role in canonical G protein signaling, loss of RGS14 results in *enhanced* LTP, suggesting that RGS14 may not function as a GAP protein in

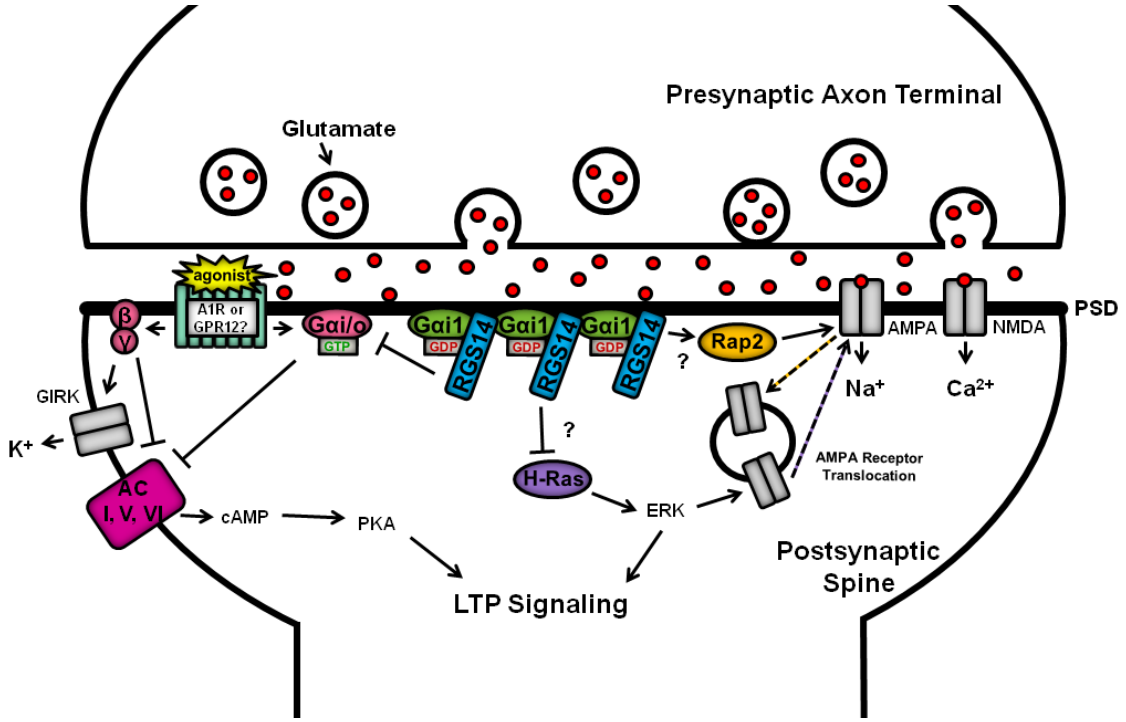

Figure 6.2. Working Model of RGS14 Function at Excitatory CA2 Synapses. Long term potentiation (LTP) signaling at excitatory hippocampal synapses is characterized by glutamate release from a presynaptic axon terminal and concomitant Na^+ and Ca^{2+} influx into the postsynaptic spine. Influx of Ca^{2+} initiates signaling cascades giving rise to cAMP production and subsequent PKA activation as well as Ras/Raf/MEK/ERK signaling. In the dendritic spines of CA2 hippocampal neurons, RGS14 may regulate LTP through intersecting with Gβγ, cAMP, and/or Ras/Rap signaling pathways. RGS14 is localized to the postsynaptic density (PSD) through the GPR motif with inactive Gαi-GDP. RGS14 recruitment to the PSD may be solely mediated by the GPR motif or alternatively, RGS14 may be recruited by activated Gαi-GTP through the RGS domain and anchored upon subsequent GAP-mediated deactivation (as shown in Figure 6.1). Upon forming a stable complex with inactive Gαi-GDP, RGS14 may then regulate heterotrimeric G protein signaling as a GAP downstream of CA2 enriched GPCRs such as the A1 adenosine receptor and GPR12, an orphan GPCR. Gαo activation and subsequent release of Gβγ can signal to

GIRK channels to lower the resting membrane potential or Gβγ binding of CA2 enriched adenylyl cyclases (ACs) I, V, and VI can inhibit the production of cAMP. Additionally, activated Gαi proteins can bind AC to inhibit cAMP production. Alternatively, RGS14 may regulate Ras/Rap signaling through its RBDs. Binding and inhibiting Ras signaling may prevent ERK phosphorylation-mediated translocation of AMPA receptors to the PSD to facilitate LTP. Conversely, promotion of Rap2 signaling may promote internalization of AMPA receptors to depotentiate LTP.

native CA2 neurons. Alternatively, RGS14 may engage in unconventional signaling mechanisms through G proteins and/or Ras/Rap proteins.

One possible mechanism for RGS14 function is that, upon binding Gαi through the GPR motif, RGS14 forms a stable complex located within dendritic spines and at the postsynaptic density (PSD), as shown in Figure 6.2. Upon binding Gαi, RGS14 may alter synaptic plasticity through release of free Gβγ, a hypothesis I explored in the present work. Binding of Gαi proteins and consequent release of free Gβγ may increase GIRK channel activity to lower the resting membrane potential. Of note, the resting membrane potential of CA2 pyramidal neurons is lower than neighboring CA1 pyramidal neurons (171). Alternatively, Gβγ could bind and inhibit Gβγ-sensitive adenylyl cyclases such as types I, V, and VI which are highly expressed in CA2 (254) and have been shown to be inhibited by Gβγ binding (19,255).

However, my data presented in Chapter 5 are inconsistent with this idea. RGS14 does not function by releasing free Gβγ as I did not observe disruption of Gαβγ heterotrimers when RGS14 is co-expressed. These results suggest RGS14 would not promote Gβγ signaling to GIRK channels or adenylyl cyclase in CA2 neurons. However, RGS14 may not receive the same post-translational modifications in HEK 293 cells that would occur in a native CA2 neuron. Moreover, previous biochemical studies in the Hepler laboratory showed RGS14 is phosphorylated by PKA at Thr494, an amino acid immediately preceding the GPR motif. Phosphomimetic mutation (T494D or T494E) of this site potentiated binding of Gαi proteins to the GPR motif (178). As PKA is integral to the initiation and maintenance of LTP, PKA phosphorylation may represent a feedback regulation on RGS14. Phosphorylation at this site may alter the way in which RGS14 regulates Gαβγ heterotrimers.

Role of RGS14 in Ras/Rap Signaling – Alternatively, binding of Gαi through the GPR motif may position RGS14 to engage Ras/Rap signaling pathways (Figure 6.2). While I have largely focused on the role of RGS14 in heterotrimeric G protein signaling, RGS14 also engages small GTPases through its first Ras binding domain (RBD1). The consequences of this interaction are still in the early stages of exploration. Previous studies have suggested RGS14 binding of activated H-Ras limits ERK activation in response to PDGF stimulation in HeLa cells (166). Co-expression of Gαi1 released RGS14-mediated ERK suppression suggesting RGS14 coordinates Gα signaling to regulate Ras/Raf/MEK/ERK signaling pathways (166). Additional studies indicate RGS14 can form a trimeric complex with inactive Gαi1 and activated H-Ras further highlighting the role of RGS14 as an integrator of GTPase signaling pathways (167).

Structurally, it remains unclear how RGS14 binds both Gαi1 and H-Ras. Moreover, it remains unclear the functional consequences of this trimeric complex in native CA2 neurons. It is possible that RGS14 coordinates heterotrimeric G protein and small G protein signaling. As our HDX data suggests RBD1 is stabilized upon binding of a G protein at the GPR motif, we expect that G protein binding may regulate RBD1 and potentially promote the formation of a trimeric complex. Alternatively, RGS14 could switch between regulation of heterotrimeric G proteins and small G proteins. This switch could be regulated by another protein binding partner or by post-translational modifications.

H-Ras signaling is important for initiation and maintenance of LTP. H-Ras signaling through the canonical Ras/Raf/MEK/ERK signaling cascade leads to phosphorylation of AMPA receptors resulting in AMPA receptor delivery to the PSD as well as translation of proteins needed to sustain LTP (256-258). As both Raf and RGS14 belong to the same family of RBD proteins and bind H-Ras through similar domains (168), it is likely that Raf

and RGS14 binding are mutually exclusive. One potential way in which RGS14 could limit LTP is by acting as a sink for activated H-Ras proteins. Another RBD containing protein, Rin1, has been shown to limit LTP at excitatory synapses in the amygdala by binding activated H-Ras and preventing interactions with Raf (259,260). Additionally, Rin1 is an H-Ras effector and upon binding H-Ras, Rin1 stimulates Rab5-mediated AMPA receptor removal from the postsynaptic density (261). It remains unclear whether RGS14 can also be considered an H-Ras effector, though H-Ras binding to RGS14 may serve to redirect H-Ras signaling away from Raf/ERK to an as yet to be identified signaling pathway.

Less well understood is the interaction between RGS14 and Rap proteins. RGS14 was originally identified as a Rap2 binding protein (140,162) and was later shown to bind activated H-Ras as well (126,165). While many RBD proteins can bind both Ras and Rap proteins, most RBDs show selectivity for either Ras or Rap (168,262). Though it has been suggested RGS14 is a selective H-Ras effector (165), selectivity may differ depending on the cellular environment and relative expression levels of H-Ras and Rap2.

Rap2 signaling has been implicated in depotentiation in dendritic spines and PSDs. Depotentiation is the reverse of LTP where molecular changes occur to remove AMPA receptors from the PSD and cAMP is effluxed to prevent further PKA activation (263). Signaling through JNK kinase and calcineurin, Rap2 activation leads to dephosphorylation of AMPA receptors with long cytoplasmic tails resulting in internalization of AMPA receptors (264). Thus, while H-Ras activation leads to increased AMPA receptor density at the PSD, Rap2 activation leads to decreased AMPA receptor density. The opposing effects of Ras and Rap proteins may be regulated by RGS14 (Figure 6.2).

RGS14 may function to facilitate depotentiation mechanisms by binding Rap2 proteins. Potentially, Rap2 binding may inhibit the action of the RGS domain to promote

Gαi/o signaling. Interestingly, adenosine signaling has been implicated in depotentiation mechanisms. Effluxed cAMP is broken down into adenosine that activates Gαi/o-coupled A1 receptors (263,265). Gαi then inhibits cAMP production through adenylyl cyclase while Gαo signaling through Gβγ enhances GIRK signaling to lower the membrane potential.

Previous *in vitro* studies with purified proteins suggest Rap2 binding does not alter the RGS or GDI activity of RGS14 (133), however, whether RGS14 retains affinity for activated Rap2 upon binding Gα has not been explored. Additionally, the effects of Rap2 binding on RGS and GPR function have not been explored in a cellular context. Future studies will assess the consequent effects of RGS14 binding of H-Ras and Rap2 proteins. Key experiments will elucidate how H-Ras/Rap2 binding impacts the capacity of RGS14 to engage G proteins at the RGS domain and GPR motif and provide insight into the manner in which RGS14 integrates heterotrimeric and small G protein signaling.

RGS14 Interactions with GPCRs – Imperative to understanding RGS14 function *in vivo* is to determine the relationship of RGS14 with GPCRs. As RGS14 localizes to dendritic spines and post-synaptic densities, we predict that RGS14 regulates GPCR function. Moreover, BRET studies in heterologous systems demonstrate that RGS14 can associate with receptors via Gα proteins and regulate downstream G protein signaling. Future studies will determine whether RGS14 regulates GPCR signaling *in vivo*. A couple of Gαi/o-linked GPCRs highly enriched within CA2 are possible candidates for RGS14 regulation including A1 adenosine receptors and GPR12, a Class A orphan GPCR (254,266,267).

A1 adenosine receptors (A1Rs) are highly expressed in CA2 and CA3 subregions of the hippocampus (267). Adenosine receptors have been implicated in depotentiation

mechanisms where activation of Gαi/o signaling inhibits adenylyl cyclase and activates GIRK channels (265,268,269). Antagonism of A1Rs in CA2 results in potentiation of synaptic transmission through enhanced cAMP production (176) highlighting the important role of adenosine signaling in CA2. Currently, it is unknown whether RGS14 regulates A1R signaling in CA2 neurons.

While little is known about GPR12, it represents an interesting point of study due to its almost identical enrichment as RGS14 in the hippocampus. Like RGS14, GPR12 is expressed highly in both area CA2 as well as the fasciola cinerea (266), an understudied area of the brain with unknown function. As an orphan GPCR, little is known about the function of GPR12. Sphingosylphosphorylcholine (SPC) has been suggested to be the endogenous ligand of GPR12 (266) though the role of SPC in synaptic plasticity is not well characterized. Some reports suggest GPR12 regulates synaptophysin and could regulate the stability of the synapse (266). GPR12 has been reported to couple to both Gαs and Gαi/o proteins (270). Studies have suggested GPR12 is constitutively active and stimulates cAMP production through Gαs (270,271). Other reports have noted GPR12 signaling is sensitive to pertussis toxin suggesting GPR12 couples to Gαi/o proteins (266). Whether RGS14 regulates the function of GPR12 remains to be tested, however, RGS14 may regulate signaling from GPR12 by negatively regulating Gαi/o signaling and promoting signaling through other Gα proteins.

6.9 Concluding Remarks

My findings presented here have made great strides in understanding the role of RGS14 in heterotrimeric G protein signaling. The data presented shows for the first time the capacity of RGS14 to bind two G proteins simultaneously. Biochemical assessment of RGS

function revealed binding of Gα through the GPR motif does not prevent RGS-mediated GAP activity. Further assessment of RGS function in live cells revealed binding of Gα through the GPR motif does not alter GAP activity of the RGS domain. These studies provide the first evidence that the actions of the RGS14 GPR motif and RGS domain independently regulate G protein signaling.

Going forward, crucial experiments will elucidate whether RGS14 regulates G protein signaling downstream of GPCRs *in vivo*. Additional experiments are required to identify the role of RGS14 regulation in H-Ras/Rap2 signaling. RGS14 may suppress LTP through inhibiting H-Ras signaling or promote depotentiation mechanisms through facilitating Rap2 signaling. Additionally, how RGS14 integrates heterotrimeric G protein signaling with small GTPase signaling is still unresolved. Crucial understanding of the mechanisms of signal integration may come from structural determination of RGS14 with its various partners. Together these studies may provide a clear picture of how RGS14 regulates heterotrimeric and small G proteins to regulate synaptic plasticity as well as learning and memory mechanisms.

References

1. Fredriksson, R., Lagerstrom, M. C., Lundin, L. G., and Schioth, H. B. (2003) The G-protein-coupled receptors in the human genome form five main families. Phylogenetic analysis, paralogon groups, and fingerprints. *Mol. Pharmacol.* **63**, 1256-1272
2. Schioth, H. B., and Fredriksson, R. (2005) The GRAFS classification system of G-protein coupled receptors in comparative perspective. *Gen. Comp. Endocrinol.* **142**, 94-101
3. Kroeze, W. K., Sheffler, D. J., and Roth, B. L. (2003) G-protein-coupled receptors at a glance. *J. Cell Sci.* **116**, 4867-4869
4. Oldham, W. M., and Hamm, H. E. (2008) Heterotrimeric G protein activation by G-protein-coupled receptors. *Nat. Rev. Mol. Cell Biol.* **9**, 60-71
5. Felder, C. B., Graul, R. C., Lee, A. Y., Merkle, H. P., and Sadee, W. (1999) The Venus flytrap of periplasmic binding proteins: an ancient protein module present in multiple drug receptors. *AAPS pharmSci* **1**, E2
6. Paavola, K. J., and Hall, R. A. (2012) Adhesion G protein-coupled receptors: signaling, pharmacology, and mechanisms of activation. *Mol. Pharmacol.* **82**, 777-783
7. Dijksterhuis, J. P., Petersen, J., and Schulte, G. (2014) WNT/Frizzled signalling: receptor-ligand selectivity with focus on FZD-G protein signalling and its physiological relevance: IUPHAR Review 3. *Br. J. Pharmacol.* **171**, 1195-1209
8. Jacoby, E., Bouhelal, R., Gerspacher, M., and Seuwen, K. (2006) The 7 TM G-protein-coupled receptor target family. *ChemMedChem* **1**, 761-782

9. Brandt, D. R., and Ross, E. M. (1985) GTPase activity of the stimulatory GTP-binding regulatory protein of adenylate cyclase, Gs. Accumulation and turnover of enzyme-nucleotide intermediates. *J. Biol. Chem.* **260**, 266-272

10. Higashijima, T., Ferguson, K. M., Sternweis, P. C., Smigel, M. D., and Gilman, A. G. (1987) Effects of Mg2+ and the beta gamma-subunit complex on the interactions of guanine nucleotides with G proteins. *J. Biol. Chem.* **262**, 762-766

11. Downes, G. B., and Gautam, N. (1999) The G protein subunit gene families. *Genomics* **62**, 544-552

12. Northup, J. K., Sternweis, P. C., Smigel, M. D., Schleifer, L. S., Ross, E. M., and Gilman, A. G. (1980) Purification of the regulatory component of adenylate cyclase. *Proceedings of the National Academy of Sciences of the United States of America* **77**, 6516-6520

13. Sternweis, P. C., Northup, J. K., Smigel, M. D., and Gilman, A. G. (1981) The regulatory component of adenylate cyclase. Purification and properties. *J. Biol. Chem.* **256**, 11517-11526

14. Bokoch, G. M., Katada, T., Northup, J. K., Ui, M., and Gilman, A. G. (1984) Purification and properties of the inhibitory guanine nucleotide-binding regulatory component of adenylate cyclase. *J. Biol. Chem.* **259**, 3560-3567

15. Katada, T., Bokoch, G. M., Northup, J. K., Ui, M., and Gilman, A. G. (1984) The inhibitory guanine nucleotide-binding regulatory component of adenylate cyclase. Properties and function of the purified protein. *J. Biol. Chem.* **259**, 3568-3577

16. Logothetis, D. E., Kurachi, Y., Galper, J., Neer, E. J., and Clapham, D. E. (1987) The beta gamma subunits of GTP-binding proteins activate the muscarinic K+ channel in heart. *Nature* **325**, 321-326

17. Logothetis, D. E., Kim, D. H., Northup, J. K., Neer, E. J., and Clapham, D. E. (1988) Specificity of action of guanine nucleotide-binding regulatory protein subunits on the cardiac muscarinic K+ channel. *Proceedings of the National Academy of Sciences of the United States of America* **85**, 5814-5818

18. Wickman, K. D., Iniguez-Lluhl, J. A., Davenport, P. A., Taussig, R., Krapivinsky, G. B., Linder, M. E., Gilman, A. G., and Clapham, D. E. (1994) Recombinant G-protein beta gamma-subunits activate the muscarinic-gated atrial potassium channel. *Nature* **368**, 255-257

19. Tang, W. J., and Gilman, A. G. (1991) Type-specific regulation of adenylyl cyclase by G protein beta gamma subunits. *Science* **254**, 1500-1503

20. Camps, M., Carozzi, A., Schnabel, P., Scheer, A., Parker, P. J., and Gierschik, P. (1992) Isozyme-selective stimulation of phospholipase C-beta 2 by G protein beta gamma-subunits. *Nature* **360**, 684-686

21. Boyer, J. L., Waldo, G. L., Evans, T., Northup, J. K., Downes, C. P., and Harden, T. K. (1989) Modification of AlF-4- and receptor-stimulated phospholipase C activity by G-protein beta gamma subunits. *J. Biol. Chem.* **264**, 13917-13922

22. Ikeda, S. R. (1996) Voltage-dependent modulation of N-type calcium channels by G-protein beta gamma subunits. *Nature* **380**, 255-258

23. Herlitze, S., Garcia, D. E., Mackie, K., Hille, B., Scheuer, T., and Catterall, W. A. (1996) Modulation of Ca2+ channels by G-protein beta gamma subunits. *Nature* **380**, 258-262

24. Smrcka, A. V. (2008) G protein betagamma subunits: central mediators of G protein-coupled receptor signaling. *Cell. Mol. Life Sci.* **65**, 2191-2214

25. Whiteway, M., Hougan, L., Dignard, D., Thomas, D. Y., Bell, L., Saari, G. C., Grant, F. J., O'Hara, P., and MacKay, V. L. (1989) The STE4 and STE18 genes of yeast encode potential beta and gamma subunits of the mating factor receptor-coupled G protein. *Cell* **56**, 467-477

26. Chen, C. A., and Manning, D. R. (2001) Regulation of G proteins by covalent modification. *Oncogene* **20**, 1643-1652

27. Wedegaertner, P. B., Wilson, P. T., and Bourne, H. R. (1995) Lipid modifications of trimeric G proteins. *J. Biol. Chem.* **270**, 503-506

28. Michaelson, D., Ahearn, I., Bergo, M., Young, S., and Philips, M. (2002) Membrane trafficking of heterotrimeric G proteins via the endoplasmic reticulum and Golgi. *Molecular biology of the cell* **13**, 3294-3302

29. Takida, S., and Wedegaertner, P. B. (2003) Heterotrimer formation, together with isoprenylation, is required for plasma membrane targeting of Gbetagamma. *J. Biol. Chem.* **278**, 17284-17290

30. Savarese, T. M., and Fraser, C. M. (1992) In vitro mutagenesis and the search for structure-function relationships among G protein-coupled receptors. *Biochem. J.* **283 (Pt 1)**, 1-19

31. Wess, J. (1997) G-protein-coupled receptors: molecular mechanisms involved in receptor activation and selectivity of G-protein recognition. *FASEB J.* **11**, 346-354

32. Slessareva, J. E., Ma, H., Depree, K. M., Flood, L. A., Bae, H., Cabrera-Vera, T. M., Hamm, H. E., and Graber, S. G. (2003) Closely related G-protein-coupled receptors use multiple and distinct domains on G-protein alpha-subunits for selective coupling. *J. Biol. Chem.* **278**, 50530-50536

33. Bae, H., Cabrera-Vera, T. M., Depree, K. M., Graber, S. G., and Hamm, H. E. (1999) Two amino acids within the alpha4 helix of Galphai1 mediate coupling with 5-hydroxytryptamine1B receptors. *J. Biol. Chem.* **274**, 14963-14971

34. Gibson, S. K., and Gilman, A. G. (2006) Gialpha and Gbeta subunits both define selectivity of G protein activation by alpha2-adrenergic receptors. *Proceedings of the National Academy of Sciences of the United States of America* **103**, 212-217

35. McIntire, W. E., MacCleery, G., and Garrison, J. C. (2001) The G protein beta subunit is a determinant in the coupling of Gs to the beta 1-adrenergic and A2a adenosine receptors. *J. Biol. Chem.* **276**, 15801-15809

36. Bokoch, G. M., Katada, T., Northup, J. K., Hewlett, E. L., and Gilman, A. G. (1983) Identification of the predominant substrate for ADP-ribosylation by islet activating protein. *J. Biol. Chem.* **258**, 2072-2075

37. Van Dop, C., Yamanaka, G., Steinberg, F., Sekura, R. D., Manclark, C. R., Stryer, L., and Bourne, H. R. (1984) ADP-ribosylation of transducin by pertussis toxin blocks the light-stimulated hydrolysis of GTP and cGMP in retinal photoreceptors. *J. Biol. Chem.* **259**, 23-26

38. Arshavsky, V. Y., and Pugh, E. N., Jr. (1998) Lifetime regulation of G protein-effector complex: emerging importance of RGS proteins. *Neuron* **20**, 11-14

39. Chan, R. K., and Otte, C. A. (1982) Isolation and genetic analysis of Saccharomyces cerevisiae mutants supersensitive to G1 arrest by a factor and alpha factor pheromones. *Mol. Cell. Biol.* **2**, 11-20

40. Chan, R. K., and Otte, C. A. (1982) Physiological characterization of Saccharomyces cerevisiae mutants supersensitive to G1 arrest by a factor and alpha factor pheromones. *Mol. Cell. Biol.* **2**, 21-29

41. Dohlman, H. G., Apaniesk, D., Chen, Y., Song, J., and Nusskern, D. (1995) Inhibition of G-protein signaling by dominant gain-of-function mutations in Sst2p, a pheromone desensitization factor in Saccharomyces cerevisiae. *Mol. Cell. Biol.* **15**, 3635-3643

42. Dohlman, H. G., Song, J., Ma, D., Courchesne, W. E., and Thorner, J. (1996) Sst2, a negative regulator of pheromone signaling in the yeast Saccharomyces cerevisiae: expression, localization, and genetic interaction and physical association with Gpa1 (the G-protein alpha subunit). *Mol. Cell. Biol.* **16**, 5194-5209

43. Koelle, M. R., and Horvitz, H. R. (1996) EGL-10 regulates G protein signaling in the C. elegans nervous system and shares a conserved domain with many mammalian proteins. *Cell* **84**, 115-125

44. Yu, J. H., Wieser, J., and Adams, T. H. (1996) The Aspergillus FlbA RGS domain protein antagonizes G protein signaling to block proliferation and allow development. *EMBO J.* **15**, 5184-5190

45. De Vries, L., Mousli, M., Wurmser, A., and Farquhar, M. G. (1995) GAIP, a protein that specifically interacts with the trimeric G protein G alpha i3, is a member of a protein family with a highly conserved core domain. *Proceedings of the National Academy of Sciences of the United States of America* **92**, 11916-11920

46. Druey, K. M., Blumer, K. J., Kang, V. H., and Kehrl, J. H. (1996) Inhibition of G-protein-mediated MAP kinase activation by a new mammalian gene family. *Nature* **379**, 742-746

47. Berman, D. M., Wilkie, T. M., and Gilman, A. G. (1996) GAIP and RGS4 are GTPase-activating proteins for the Gi subfamily of G protein alpha subunits. *Cell* **86**, 445-452

48. Watson, N., Linder, M. E., Druey, K. M., Kehrl, J. H., and Blumer, K. J. (1996) RGS family members: GTPase-activating proteins for heterotrimeric G-protein alpha-subunits. *Nature* **383**, 172-175

49. Hunt, T. W., Fields, T. A., Casey, P. J., and Peralta, E. G. (1996) RGS10 is a selective activator of G alpha i GTPase activity. *Nature* **383**, 175-177

50. He, W., Cowan, C. W., and Wensel, T. G. (1998) RGS9, a GTPase accelerator for phototransduction. *Neuron* **20**, 95-102

51. Tesmer, J. J. (2009) Structure and function of regulator of G protein signaling homology domains. *Progress in molecular biology and translational science* **86**, 75-113

52. Carman, C. V., Parent, J. L., Day, P. W., Pronin, A. N., Sternweis, P. M., Wedegaertner, P. B., Gilman, A. G., Benovic, J. L., and Kozasa, T. (1999) Selective regulation of Galpha(q/11) by an RGS domain in the G protein-coupled receptor kinase, GRK2. *J. Biol. Chem.* **274**, 34483-34492

53. Kozasa, T., Jiang, X., Hart, M. J., Sternweis, P. M., Singer, W. D., Gilman, A. G., Bollag, G., and Sternweis, P. C. (1998) p115 RhoGEF, a GTPase activating protein for Galpha12 and Galpha13. *Science* **280**, 2109-2111

54. Mao, J., Yuan, H., Xie, W., and Wu, D. (1998) Guanine nucleotide exchange factor GEF115 specifically mediates activation of Rho and serum response factor by the G protein alpha subunit Galpha13. *Proceedings of the National Academy of Sciences of the United States of America* **95**, 12973-12976

55. Hart, M. J., Jiang, X., Kozasa, T., Roscoe, W., Singer, W. D., Gilman, A. G., Sternweis, P. C., and Bollag, G. (1998) Direct stimulation of the guanine nucleotide exchange activity of p115 RhoGEF by Galpha13. *Science* **280**, 2112-2114

56. Chen, Z., Singer, W. D., Sternweis, P. C., and Sprang, S. R. (2005) Structure of the p115RhoGEF rgRGS domain-Galpha13/i1 chimera complex suggests convergent evolution of a GTPase activator. *Nat. Struct. Mol. Biol.* **12**, 191-197

57. Wells, C. D., Liu, M. Y., Jackson, M., Gutowski, S., Sternweis, P. M., Rothstein, J. D., Kozasa, T., and Sternweis, P. C. (2002) Mechanisms for reversible regulation between G13 and Rho exchange factors. *J. Biol. Chem.* **277**, 1174-1181

58. Castellone, M. D., Teramoto, H., Williams, B. O., Druey, K. M., and Gutkind, J. S. (2005) Prostaglandin E2 promotes colon cancer cell growth through a Gs-axin-beta-catenin signaling axis. *Science* **310**, 1504-1510

59. Zheng, B., Ma, Y. C., Ostrom, R. S., Lavoie, C., Gill, G. N., Insel, P. A., Huang, X. Y., and Farquhar, M. G. (2001) RGS-PX1, a GAP for GalphaS and sorting nexin in vesicular trafficking. *Science* **294**, 1939-1942

60. Stemmle, L. N., Fields, T. A., and Casey, P. J. (2006) The regulator of G protein signaling domain of axin selectively interacts with Galpha12 but not Galpha13. *Mol. Pharmacol.* **70**, 1461-1468

61. Wang, L., Sunahara, R. K., Krumins, A., Perkins, G., Crochiere, M. L., Mackey, M., Bell, S., Ellisman, M. H., and Taylor, S. S. (2001) Cloning and mitochondrial localization of full-length D-AKAP2, a protein kinase A anchoring protein. *Proceedings of the National Academy of Sciences of the United States of America* **98**, 3220-3225

62. Hu, Y., Xing, J., Chen, L., Guo, X., Du, Y., Zhao, C., Zhu, Y., Lin, M., Zhou, Z., and Sha, J. (2008) RGS22, a novel testis-specific regulator of G-protein signaling involved in human and mouse spermiogenesis along with GNA12/13 subunits. *Biol. Reprod.* **79**, 1021-1029

63. Hu, Y., Xing, J., Chen, L., Zheng, Y., and Zhou, Z. (2015) RGS22 inhibits pancreatic adenocarcinoma cell migration through the G12/13 alpha subunit/F-actin pathway. *Oncol. Rep.* **34**, 2507-2514

64. Woodard, G. E., Jardin, I., Berna-Erro, A., Salido, G. M., and Rosado, J. A. (2015) Regulators of G-protein-signaling proteins: negative modulators of G-protein-coupled receptor signaling. *International review of cell and molecular biology* **317**, 97-183

65. Wang, J., Ducret, A., Tu, Y., Kozasa, T., Aebersold, R., and Ross, E. M. (1998) RGSZ1, a Gz-selective RGS protein in brain. Structure, membrane association, regulation by Galphaz phosphorylation, and relationship to a Gz gtpase-activating protein subfamily. *J. Biol. Chem.* **273**, 26014-26025

66. Mao, H., Zhao, Q., Daigle, M., Ghahremani, M. H., Chidiac, P., and Albert, P. R. (2004) RGS17/RGSZ2, a novel regulator of Gi/o, Gz, and Gq signaling. *J. Biol. Chem.* **279**, 26314-26322

67. Soundararajan, M., Willard, F. S., Kimple, A. J., Turnbull, A. P., Ball, L. J., Schoch, G. A., Gileadi, C., Fedorov, O. Y., Dowler, E. F., Higman, V. A., Hutsell, S. Q., Sundstrom, M., Doyle, D. A., and Siderovski, D. P. (2008) Structural diversity in the RGS domain and its interaction with heterotrimeric G protein alpha-subunits. *Proceedings of the National Academy of Sciences of the United States of America* **105**, 6457-6462

68. Stewart, A., and Fisher, R. A. (2015) Introduction: G Protein-coupled Receptors and RGS Proteins. *Progress in molecular biology and translational science* **133**, 1-11

69. Kach, J., Sethakorn, N., and Dulin, N. O. (2012) A finer tuning of G-protein signaling through regulated control of RGS proteins. *Am. J. Physiol. Heart Circ. Physiol.* **303**, H19-35

70. Heximer, S. P., Watson, N., Linder, M. E., Blumer, K. J., and Hepler, J. R. (1997) RGS2/G0S8 is a selective inhibitor of Gqalpha function. *Proceedings of the National Academy of Sciences of the United States of America* **94**, 14389-14393

71. Heximer, S. P., Srinivasa, S. P., Bernstein, L. S., Bernard, J. L., Linder, M. E., Hepler, J. R., and Blumer, K. J. (1999) G protein selectivity is a determinant of RGS2 function. *J. Biol. Chem.* **274**, 34253-34259

72. Sondek, J., and Siderovski, D. P. (2001) Ggamma-like (GGL) domains: new frontiers in G-protein signaling and beta-propeller scaffolding. *Biochem. Pharmacol.* **61**, 1329-1337

73. Martemyanov, K. A., Lishko, P. V., Calero, N., Keresztes, G., Sokolov, M., Strissel, K. J., Leskov, I. B., Hopp, J. A., Kolesnikov, A. V., Chen, C. K., Lem, J., Heller, S., Burns, M. E., and Arshavsky, V. Y. (2003) The DEP domain determines subcellular targeting of the GTPase activating protein RGS9 in vivo. *J. Neurosci.* **23**, 10175-10181

74. Martemyanov, K. A., Yoo, P. J., Skiba, N. P., and Arshavsky, V. Y. (2005) R7BP, a novel neuronal protein interacting with RGS proteins of the R7 family. *J. Biol. Chem.* **280**, 5133-5136

75. Cho, H., Kozasa, T., Takekoshi, K., De Gunzburg, J., and Kehrl, J. H. (2000) RGS14, a GTPase-activating protein for Gialpha, attenuates Gialpha- and G13alpha-mediated signaling pathways. *Mol. Pharmacol.* **58**, 569-576

76. Snow, B. E., Hall, R. A., Krumins, A. M., Brothers, G. M., Bouchard, D., Brothers, C. A., Chung, S., Mangion, J., Gilman, A. G., Lefkowitz, R. J., and Siderovski, D. P. (1998) GTPase activating specificity of RGS12 and binding specificity of an alternatively spliced PDZ (PSD-95/Dlg/ZO-1) domain. *J. Biol. Chem.* **273**, 17749-17755

77. Tesmer, J. J., Berman, D. M., Gilman, A. G., and Sprang, S. R. (1997) Structure of RGS4 bound to AlF4--activated G(i alpha1): stabilization of the transition state for GTP hydrolysis. *Cell* **89**, 251-261

78. Berman, D. M., Kozasa, T., and Gilman, A. G. (1996) The GTPase-activating protein RGS4 stabilizes the transition state for nucleotide hydrolysis. *J. Biol. Chem.* **271**, 27209-27212

79. Chen, C. K., Burns, M. E., He, W., Wensel, T. G., Baylor, D. A., and Simon, M. I. (2000) Slowed recovery of rod photoresponse in mice lacking the GTPase accelerating protein RGS9-1. *Nature* **403**, 557-560

80. Osei-Owusu, P., Sun, X., Drenan, R. M., Steinberg, T. H., and Blumer, K. J. (2007) Regulation of RGS2 and second messenger signaling in vascular smooth muscle cells by cGMP-dependent protein kinase. *J. Biol. Chem.* **282**, 31656-31665

81. Heximer, S. P., Knutsen, R. H., Sun, X., Kaltenbronn, K. M., Rhee, M. H., Peng, N., Oliveira-dos-Santos, A., Penninger, J. M., Muslin, A. J., Steinberg, T. H., Wyss, J. M., Mecham, R. P., and Blumer, K. J. (2003) Hypertension and prolonged vasoconstrictor signaling in RGS2-deficient mice. *J. Clin. Invest.* **111**, 445-452

82. Tamirisa, P., Blumer, K. J., and Muslin, A. J. (1999) RGS4 inhibits G-protein signaling in cardiomyocytes. *Circulation* **99**, 441-447

83. Rogers, J. H., Tsirka, A., Kovacs, A., Blumer, K. J., Dorn, G. W., 2nd, and Muslin, A. J. (2001) RGS4 reduces contractile dysfunction and hypertrophic gene induction in Galpha q overexpressing mice. *Journal of molecular and cellular cardiology* **33**, 209-218

84. Doupnik, C. A., Davidson, N., Lester, H. A., and Kofuji, P. (1997) RGS proteins reconstitute the rapid gating kinetics of gbetagamma-activated inwardly rectifying

K+ channels. *Proceedings of the National Academy of Sciences of the United States of America* **94**, 10461-10466

85. Posokhova, E., Wydeven, N., Allen, K. L., Wickman, K., and Martemyanov, K. A. (2010) RGS6/Gbeta5 complex accelerates IKACh gating kinetics in atrial myocytes and modulates parasympathetic regulation of heart rate. *Circ Res* **107**, 1350-1354

86. Cifelli, C., Rose, R. A., Zhang, H., Voigtlaender-Bolz, J., Bolz, S. S., Backx, P. H., and Heximer, S. P. (2008) RGS4 regulates parasympathetic signaling and heart rate control in the sinoatrial node. *Circ Res* **103**, 527-535

87. Yang, J., Huang, J., Maity, B., Gao, Z., Lorca, R. A., Gudmundsson, H., Li, J., Stewart, A., Swaminathan, P. D., Ibeawuchi, S. R., Shepherd, A., Chen, C. K., Kutschke, W., Mohler, P. J., Mohapatra, D. P., Anderson, M. E., and Fisher, R. A. (2010) RGS6, a modulator of parasympathetic activation in heart. *Circ Res* **107**, 1345-1349

88. Labouebe, G., Lomazzi, M., Cruz, H. G., Creton, C., Lujan, R., Li, M., Yanagawa, Y., Obata, K., Watanabe, M., Wickman, K., Boyer, S. B., Slesinger, P. A., and Luscher, C. (2007) RGS2 modulates coupling between GABAB receptors and GIRK channels in dopamine neurons of the ventral tegmental area. *Nat. Neurosci.* **10**, 1559-1568

89. Maity, B., Stewart, A., Yang, J., Loo, L., Sheff, D., Shepherd, A. J., Mohapatra, D. P., and Fisher, R. A. (2012) Regulator of G protein signaling 6 (RGS6) protein ensures coordination of motor movement by modulating GABAB receptor signaling. *J. Biol. Chem.* **287**, 4972-4981

90. Fajardo-Serrano, A., Wydeven, N., Young, D., Watanabe, M., Shigemoto, R., Martemyanov, K. A., Wickman, K., and Lujan, R. (2013) Association of

Rgs7/Gbeta5 complexes with Girk channels and GABAB receptors in hippocampal CA1 pyramidal neurons. *Hippocampus* **23**, 1231-1245

91. Ostrovskaya, O., Xie, K., Masuho, I., Fajardo-Serrano, A., Lujan, R., Wickman, K., and Martemyanov, K. A. (2014) RGS7/Gbeta5/R7BP complex regulates synaptic plasticity and memory by modulating hippocampal GABABR-GIRK signaling. *eLife* **3**, e02053

92. Saitoh, O., Kubo, Y., Miyatani, Y., Asano, T., and Nakata, H. (1997) RGS8 accelerates G-protein-mediated modulation of K+ currents. *Nature* **390**, 525-529

93. Lambert, N. A., Johnston, C. A., Cappell, S. D., Kuravi, S., Kimple, A. J., Willard, F. S., and Siderovski, D. P. (2010) Regulators of G-protein signaling accelerate GPCR signaling kinetics and govern sensitivity solely by accelerating GTPase activity. *Proceedings of the National Academy of Sciences of the United States of America* **107**, 7066-7071

94. Hepler, J. R., Berman, D. M., Gilman, A. G., and Kozasa, T. (1997) RGS4 and GAIP are GTPase-activating proteins for Gq alpha and block activation of phospholipase C beta by gamma-thio-GTP-Gq alpha. *Proceedings of the National Academy of Sciences of the United States of America* **94**, 428-432

95. Yan, Y., Chi, P. P., and Bourne, H. R. (1997) RGS4 inhibits Gq-mediated activation of mitogen-activated protein kinase and phosphoinositide synthesis. *J. Biol. Chem.* **272**, 11924-11927

96. Hewavitharana, T., and Wedegaertner, P. B. (2012) Non-canonical signaling and localizations of heterotrimeric G proteins. *Cell. Signal.* **24**, 25-34

97. Hampoelz, B., and Knoblich, J. A. (2004) Heterotrimeric G proteins: new tricks for an old dog. *Cell* **119**, 453-456

98. Cismowski, M. J., Takesono, A., Ma, C., Lizano, J. S., Xie, X., Fuernkranz, H., Lanier, S. M., and Duzic, E. (1999) Genetic screens in yeast to identify mammalian nonreceptor modulators of G-protein signaling. *Nat. Biotechnol.* **17**, 878-883

99. Takesono, A., Cismowski, M. J., Ribas, C., Bernard, M., Chung, P., Hazard, S., 3rd, Duzic, E., and Lanier, S. M. (1999) Receptor-independent activators of heterotrimeric G-protein signaling pathways. *J. Biol. Chem.* **274**, 33202-33205

100. Afshar, K., Willard, F. S., Colombo, K., Johnston, C. A., McCudden, C. R., Siderovski, D. P., and Gonczy, P. (2004) RIC-8 is required for GPR-1/2-dependent Galpha function during asymmetric division of C. elegans embryos. *Cell* **119**, 219-230

101. Cismowski, M. J., Ma, C., Ribas, C., Xie, X., Spruyt, M., Lizano, J. S., Lanier, S. M., and Duzic, E. (2000) Activation of heterotrimeric G-protein signaling by a ras-related protein. Implications for signal integration. *J. Biol. Chem.* **275**, 23421-23424

102. Garcia-Marcos, M., Ghosh, P., and Farquhar, M. G. (2009) GIV is a nonreceptor GEF for G alpha i with a unique motif that regulates Akt signaling. *Proceedings of the National Academy of Sciences of the United States of America* **106**, 3178-3183

103. Miller, K. G., Emerson, M. D., McManus, J. R., and Rand, J. B. (2000) RIC-8 (Synembryn): a novel conserved protein that is required for G(q)alpha signaling in the C. elegans nervous system. *Neuron* **27**, 289-299

104. Fang, M., Jaffrey, S. R., Sawa, A., Ye, K., Luo, X., and Snyder, S. H. (2000) Dexras1: a G protein specifically coupled to neuronal nitric oxide synthase via CAPON. *Neuron* **28**, 183-193

105. Lo, I. C., Gupta, V., Midde, K. K., Taupin, V., Lopez-Sanchez, I., Kufareva, I., Abagyan, R., Randazzo, P. A., Farquhar, M. G., and Ghosh, P. (2015) Activation of

Galphai at the Golgi by GIV/Girdin imposes finiteness in Arf1 signaling. *Dev. Cell* **33**, 189-203

106. Graham, T. E., Key, T. A., Kilpatrick, K., and Dorin, R. I. (2001) Dexras1/AGS-1, a steroid hormone-induced guanosine triphosphate-binding protein, inhibits 3',5'-cyclic adenosine monophosphate-stimulated secretion in AtT-20 corticotroph cells. *Endocrinology* **142**, 2631-2640

107. Kemppainen, R. J., and Behrend, E. N. (1998) Dexamethasone rapidly induces a novel ras superfamily member-related gene in AtT-20 cells. *J. Biol. Chem.* **273**, 3129-3131

108. Takesono, A., Nowak, M. W., Cismowski, M., Duzic, E., and Lanier, S. M. (2002) Activator of G-protein signaling 1 blocks GIRK channel activation by a G-protein-coupled receptor: apparent disruption of receptor signaling complexes. *J. Biol. Chem.* **277**, 13827-13830

109. Anai, M., Shojima, N., Katagiri, H., Ogihara, T., Sakoda, H., Onishi, Y., Ono, H., Fujishiro, M., Fukushima, Y., Horike, N., Viana, A., Kikuchi, M., Noguchi, N., Takahashi, S., Takata, K., Oka, Y., Uchijima, Y., Kurihara, H., and Asano, T. (2005) A novel protein kinase B (PKB)/AKT-binding protein enhances PKB kinase activity and regulates DNA synthesis. *J. Biol. Chem.* **280**, 18525-18535

110. Lopez-Sanchez, I., Dunkel, Y., Roh, Y. S., Mittal, Y., De Minicis, S., Muranyi, A., Singh, S., Shanmugam, K., Aroonsakool, N., Murray, F., Ho, S. B., Seki, E., Brenner, D. A., and Ghosh, P. (2014) GIV/Girdin is a central hub for profibrogenic signalling networks during liver fibrosis. *Nature communications* **5**, 4451

111. Wang, H., Misaki, T., Taupin, V., Eguchi, A., Ghosh, P., and Farquhar, M. G. (2015) GIV/girdin links vascular endothelial growth factor signaling to Akt survival

signaling in podocytes independent of nephrin. *Journal of the American Society of Nephrology : JASN* **26**, 314-327

112. Garcia-Marcos, M., Ghosh, P., and Farquhar, M. G. (2015) GIV/Girdin transmits signals from multiple receptors by triggering trimeric G protein activation. *J. Biol. Chem.* **290**, 6697-6704

113. Tall, G. G., and Gilman, A. G. (2004) Purification and functional analysis of Ric-8A: a guanine nucleotide exchange factor for G-protein alpha subunits. *Methods Enzymol.* **390**, 377-388

114. Tall, G. G., and Gilman, A. G. (2005) Resistance to inhibitors of cholinesterase 8A catalyzes release of Galphai-GTP and nuclear mitotic apparatus protein (NuMA) from NuMA/LGN/Galphai-GDP complexes. *Proceedings of the National Academy of Sciences of the United States of America* **102**, 16584-16589

115. Nishimura, A., Okamoto, M., Sugawara, Y., Mizuno, N., Yamauchi, J., and Itoh, H. (2006) Ric-8A potentiates Gq-mediated signal transduction by acting downstream of G protein-coupled receptor in intact cells. *Genes Cells* **11**, 487-498

116. Chan, P., Gabay, M., Wright, F. A., and Tall, G. G. (2011) Ric-8B is a GTP-dependent G protein alphas guanine nucleotide exchange factor. *J. Biol. Chem.* **286**, 19932-19942

117. Von Dannecker, L. E., Mercadante, A. F., and Malnic, B. (2005) Ric-8B, an olfactory putative GTP exchange factor, amplifies signal transduction through the olfactory-specific G-protein Galphaolf. *J. Neurosci.* **25**, 3793-3800

118. Gabay, M., Pinter, M. E., Wright, F. A., Chan, P., Murphy, A. J., Valenzuela, D. M., Yancopoulos, G. D., and Tall, G. G. (2011) Ric-8 proteins are molecular chaperones

that direct nascent G protein alpha subunit membrane association. *Science signaling* **4**, ra79

119. Chan, P., Thomas, C. J., Sprang, S. R., and Tall, G. G. (2013) Molecular chaperoning function of Ric-8 is to fold nascent heterotrimeric G protein alpha subunits. *Proceedings of the National Academy of Sciences of the United States of America* **110**, 3794-3799

120. Papasergi, M. M., Patel, B. R., and Tall, G. G. (2015) The G protein alpha chaperone Ric-8 as a potential therapeutic target. *Mol. Pharmacol.* **87**, 52-63

121. Sato, M., Cismowski, M. J., Toyota, E., Smrcka, A. V., Lucchesi, P. A., Chilian, W. M., and Lanier, S. M. (2006) Identification of a receptor-independent activator of G protein signaling (AGS8) in ischemic heart and its interaction with Gbetagamma. *Proceedings of the National Academy of Sciences of the United States of America* **103**, 797-802

122. King, S. M., Dillman, J. F., 3rd, Benashski, S. E., Lye, R. J., Patel-King, R. S., and Pfister, K. K. (1996) The mouse t-complex-encoded protein Tctex-1 is a light chain of brain cytoplasmic dynein. *J. Biol. Chem.* **271**, 32281-32287

123. Sachdev, P., Menon, S., Kastner, D. B., Chuang, J. Z., Yeh, T. Y., Conde, C., Caceres, A., Sung, C. H., and Sakmar, T. P. (2007) G protein beta gamma subunit interaction with the dynein light-chain component Tctex-1 regulates neurite outgrowth. *EMBO J.* **26**, 2621-2632

124. Granderath, S., Stollewerk, A., Greig, S., Goodman, C. S., O'Kane, C. J., and Klambt, C. (1999) loco encodes an RGS protein required for Drosophila glial differentiation. *Development* **126**, 1781-1791

125. Siderovski, D. P., Diverse-Pierluissi, M., and De Vries, L. (1999) The GoLoco motif: a Galphai/o binding motif and potential guanine-nucleotide exchange factor. *Trends Biochem. Sci.* **24**, 340-341

126. Ponting, C. P. (1999) Raf-like Ras/Rap-binding domains in RGS12- and still-life-like signalling proteins. *Journal of molecular medicine* **77**, 695-698

127. Cao, X., Cismowski, M. J., Sato, M., Blumer, J. B., and Lanier, S. M. (2004) Identification and characterization of AGS4: a protein containing three G-protein regulatory motifs that regulate the activation state of Gialpha. *J. Biol. Chem.* **279**, 27567-27574

128. De Vries, L., Fischer, T., Tronchere, H., Brothers, G. M., Strockbine, B., Siderovski, D. P., and Farquhar, M. G. (2000) Activator of G protein signaling 3 is a guanine dissociation inhibitor for Galpha i subunits. *Proceedings of the National Academy of Sciences of the United States of America* **97**, 14364-14369

129. Peterson, Y. K., Bernard, M. L., Ma, H., Hazard, S., 3rd, Graber, S. G., and Lanier, S. M. (2000) Stabilization of the GDP-bound conformation of Gialpha by a peptide derived from the G-protein regulatory motif of AGS3. *J. Biol. Chem.* **275**, 33193-33196

130. Kimple, R. J., De Vries, L., Tronchere, H., Behe, C. I., Morris, R. A., Gist Farquhar, M., and Siderovski, D. P. (2001) RGS12 and RGS14 GoLoco motifs are G alpha(i) interaction sites with guanine nucleotide dissociation inhibitor Activity. *J. Biol. Chem.* **276**, 29275-29281

131. Natochin, M., Gasimov, K. G., and Artemyev, N. O. (2001) Inhibition of GDP/GTP exchange on G alpha subunits by proteins containing G-protein regulatory motifs. *Biochemistry* **40**, 5322-5328

132. Kimple, R. J., Kimple, M. E., Betts, L., Sondek, J., and Siderovski, D. P. (2002) Structural determinants for GoLoco-induced inhibition of nucleotide release by Galpha subunits. *Nature* **416**, 878-881

133. Mittal, V., and Linder, M. E. (2006) Biochemical characterization of RGS14: RGS14 activity towards G-protein alpha subunits is independent of its binding to Rap2A. *Biochem. J.* **394**, 309-315

134. Bernard, M. L., Peterson, Y. K., Chung, P., Jourdan, J., and Lanier, S. M. (2001) Selective interaction of AGS3 with G-proteins and the influence of AGS3 on the activation state of G-proteins. *J. Biol. Chem.* **276**, 1585-1593

135. Ghosh, M., Peterson, Y. K., Lanier, S. M., and Smrcka, A. V. (2003) Receptor- and nucleotide exchange-independent mechanisms for promoting G protein subunit dissociation. *J. Biol. Chem.* **278**, 34747-34750

136. Webb, C. K., McCudden, C. R., Willard, F. S., Kimple, R. J., Siderovski, D. P., and Oxford, G. S. (2005) D2 dopamine receptor activation of potassium channels is selectively decoupled by Galpha-specific GoLoco motif peptides. *J. Neurochem.* **92**, 1408-1418

137. Kwon, M., Pavlov, T. S., Nozu, K., Rasmussen, S. A., Ilatovskaya, D. V., Lerch-Gaggl, A., North, L. M., Kim, H., Qian, F., Sweeney, W. E., Jr., Avner, E. D., Blumer, J. B., Staruschenko, A., and Park, F. (2012) G-protein signaling modulator 1 deficiency accelerates cystic disease in an orthologous mouse model of autosomal dominant polycystic kidney disease. *Proceedings of the National Academy of Sciences of the United States of America* **109**, 21462-21467

138. Parmentier, M. L., Woods, D., Greig, S., Phan, P. G., Radovic, A., Bryant, P., and O'Kane, C. J. (2000) Rapsynoid/partner of inscuteable controls asymmetric division of larval neuroblasts in Drosophila. *J. Neurosci.* **20**, RC84

139. Pizzinat, N., Takesono, A., and Lanier, S. M. (2001) Identification of a truncated form of the G-protein regulator AGS3 in heart that lacks the tetratricopeptide repeat domains. *J. Biol. Chem.* **276**, 16601-16610

140. Snow, B. E., Antonio, L., Suggs, S., Gutstein, H. B., and Siderovski, D. P. (1997) Molecular cloning and expression analysis of rat Rgs12 and Rgs14. *Biochem. Biophys. Res. Commun.* **233**, 770-777

141. Jordan, J. D., Carey, K. D., Stork, P. J., and Iyengar, R. (1999) Modulation of rap activity by direct interaction of Galpha(o) with Rap1 GTPase-activating protein. *J. Biol. Chem.* **274**, 21507-21510

142. Adhikari, A., and Sprang, S. R. (2003) Thermodynamic characterization of the binding of activator of G protein signaling 3 (AGS3) and peptides derived from AGS3 with G alpha i1. *J. Biol. Chem.* **278**, 51825-51832

143. Jia, M., Li, J., Zhu, J., Wen, W., Zhang, M., and Wang, W. (2012) Crystal structures of the scaffolding protein LGN reveal the general mechanism by which GoLoco binding motifs inhibit the release of GDP from Galphai. *J. Biol. Chem.* **287**, 36766-36776

144. Blumer, J. B., and Lanier, S. M. (2014) Activators of g protein signaling exhibit broad functionality and define a distinct core signaling triad. *Mol. Pharmacol.* **85**, 388-396

145. Denker, S. P., McCaffery, J. M., Palade, G. E., Insel, P. A., and Farquhar, M. G. (1996) Differential distribution of alpha subunits and beta gamma subunits of heterotrimeric G proteins on Golgi membranes of the exocrine pancreas. *J. Cell Biol.* **133**, 1027-1040

146. Schurmann, A., Rosenthal, W., Schultz, G., and Joost, H. G. (1992) Characterization of GTP-binding proteins in Golgi-associated membrane vesicles from rat adipocytes. *Biochem. J.* **283 (Pt 3)**, 795-801

147. Oner, S. S., Vural, A., and Lanier, S. M. (2013) Translocation of activator of G-protein signaling 3 to the Golgi apparatus in response to receptor activation and its effect on the trans-Golgi network. *J. Biol. Chem.* **288**, 24091-24103

148. Giguere, P. M., Laroche, G., Oestreich, E. A., and Siderovski, D. P. (2012) G-protein signaling modulator-3 regulates heterotrimeric G-protein dynamics through dual association with Gbeta and Galphai protein subunits. *J. Biol. Chem.* **287**, 4863-4874

149. Schaefer, M., Shevchenko, A., Shevchenko, A., and Knoblich, J. A. (2000) A protein complex containing Inscuteable and the Galpha-binding protein Pins orients asymmetric cell divisions in Drosophila. *Curr. Biol.* **10**, 353-362

150. Yu, F., Morin, X., Cai, Y., Yang, X., and Chia, W. (2000) Analysis of partner of inscuteable, a novel player of Drosophila asymmetric divisions, reveals two distinct steps in inscuteable apical localization. *Cell* **100**, 399-409

151. Schaefer, M., Petronczki, M., Dorner, D., Forte, M., and Knoblich, J. A. (2001) Heterotrimeric G proteins direct two modes of asymmetric cell division in the Drosophila nervous system. *Cell* **107**, 183-194

152. Yu, F., Ong, C. T., Chia, W., and Yang, X. (2002) Membrane targeting and asymmetric localization of Drosophila partner of inscuteable are discrete steps controlled by distinct regions of the protein. *Mol. Cell. Biol.* **22**, 4230-4240

153. Bowman, S. K., Neumuller, R. A., Novatchkova, M., Du, Q., and Knoblich, J. A. (2006) The Drosophila NuMA Homolog Mud regulates spindle orientation in asymmetric cell division. *Dev. Cell* **10**, 731-742

154. Du, Q., and Macara, I. G. (2004) Mammalian Pins is a conformational switch that links NuMA to heterotrimeric G proteins. *Cell* **119**, 503-516

155. Du, Q., Stukenberg, P. T., and Macara, I. G. (2001) A mammalian Partner of inscuteable binds NuMA and regulates mitotic spindle organization. *Nat. Cell Biol.* **3**, 1069-1075

156. Siller, K. H., Cabernard, C., and Doe, C. Q. (2006) The NuMA-related Mud protein binds Pins and regulates spindle orientation in Drosophila neuroblasts. *Nat. Cell Biol.* **8**, 594-600

157. Blumer, J. B., Chandler, L. J., and Lanier, S. M. (2002) Expression analysis and subcellular distribution of the two G-protein regulators AGS3 and LGN indicate distinct functionality. Localization of LGN to the midbody during cytokinesis. *J. Biol. Chem.* **277**, 15897-15903

158. Fuja, T. J., Schwartz, P. H., Darcy, D., and Bryant, P. J. (2004) Asymmetric localization of LGN but not AGS3, two homologs of Drosophila pins, in dividing human neural progenitor cells. *J. Neurosci. Res.* **75**, 782-793

159. Chatterjee, T. K., and Fisher, R. A. (2000) Novel alternative splicing and nuclear localization of human RGS12 gene products. *J. Biol. Chem.* **275**, 29660-29671

160. Martin-McCaffrey, L., Willard, F. S., Oliveira-dos-Santos, A. J., Natale, D. R., Snow, B. E., Kimple, R. J., Pajak, A., Watson, A. J., Dagnino, L., Penninger, J. M., Siderovski, D. P., and D'Souza, S. J. (2004) RGS14 is a mitotic spindle protein essential from the first division of the mammalian zygote. *Dev. Cell* **7**, 763-769

161. Woodard, G. E., Huang, N. N., Cho, H., Miki, T., Tall, G. G., and Kehrl, J. H. (2010) Ric-8A and Gi alpha recruit LGN, NuMA, and dynein to the cell cortex to help orient the mitotic spindle. *Mol. Cell. Biol.* **30**, 3519-3530

162. Traver, S., Bidot, C., Spassky, N., Baltauss, T., De Tand, M. F., Thomas, J. L., Zalc, B., Janoueix-Lerosey, I., and Gunzburg, J. D. (2000) RGS14 is a novel Rap effector that preferentially regulates the GTPase activity of galphao. *Biochem. J.* **350 Pt 1**, 19-29

163. Hollinger, S., Taylor, J. B., Goldman, E. H., and Hepler, J. R. (2001) RGS14 is a bifunctional regulator of Galphai/o activity that exists in multiple populations in brain. *J. Neurochem.* **79**, 941-949

164. Mittal, V., and Linder, M. E. (2004) The RGS14 GoLoco domain discriminates among Galphai isoforms. *J. Biol. Chem.* **279**, 46772-46778

165. Willard, F. S., Willard, M. D., Kimple, A. J., Soundararajan, M., Oestreich, E. A., Li, X., Sowa, N. A., Kimple, R. J., Doyle, D. A., Der, C. J., Zylka, M. J., Snider, W. D., and Siderovski, D. P. (2009) Regulator of G-protein signaling 14 (RGS14) is a selective H-Ras effector. *PLoS One* **4**, e4884

166. Shu, F. J., Ramineni, S., and Hepler, J. R. (2010) RGS14 is a multifunctional scaffold that integrates G protein and Ras/Raf MAPkinase signalling pathways. *Cell. Signal.* **22**, 366-376

167. Vellano, C. P., Brown, N. E., Blumer, J. B., and Hepler, J. R. (2013) Assembly and Function of the Regulator of G protein Signaling 14 (RGS14):H-Ras Signaling Complex in Live Cells are Regulated by Galphai1 and Galphai-linked GPCRs. *J. Biol. Chem.* **288**, 3620-3631

168. Kiel, C., Wohlgemuth, S., Rousseau, F., Schymkowitz, J., Ferkinghoff-Borg, J., Wittinghofer, F., and Serrano, L. (2005) Recognizing and defining true Ras binding domains II: in silico prediction based on homology modelling and energy calculations. *J. Mol. Biol.* **348**, 759-775

169. Lee, S. E., Simons, S. B., Heldt, S. A., Zhao, M., Schroeder, J. P., Vellano, C. P., Cowan, D. P., Ramineni, S., Yates, C. K., Feng, Y., Smith, Y., Sweatt, J. D., Weinshenker, D., Ressler, K. J., Dudek, S. M., and Hepler, J. R. (2010) RGS14 is a natural suppressor of both synaptic plasticity in CA2 neurons and hippocampal-based learning and memory. *Proceedings of the National Academy of Sciences of the United States of America* **107**, 16994-16998

170. Evans, P. R., Lee, S. E., Smith, Y., and Hepler, J. R. (2014) Postnatal developmental expression of regulator of G protein signaling 14 (RGS14) in the mouse brain. *J. Comp. Neurol.* **522**, 186-203

171. Zhao, M., Choi, Y. S., Obrietan, K., and Dudek, S. M. (2007) Synaptic plasticity (and the lack thereof) in hippocampal CA2 neurons. *J. Neurosci.* **27**, 12025-12032

172. Shu, F. J., Ramineni, S., Amyot, W., and Hepler, J. R. (2007) Selective interactions between Gi alpha1 and Gi alpha3 and the GoLoco/GPR domain of RGS14 influence its dynamic subcellular localization. *Cell. Signal.* **19**, 163-176

173. Vellano, C. P., Maher, E. M., Hepler, J. R., and Blumer, J. B. (2011) G protein-coupled receptors and resistance to inhibitors of cholinesterase-8A (Ric-8A) both regulate the regulator of g protein signaling 14 RGS14.Galphai1 complex in live cells. *J. Biol. Chem.* **286**, 38659-38669

174. Robichaux, W. G., 3rd, Oner, S. S., Lanier, S. M., and Blumer, J. B. (2015) Direct Coupling of a Seven-Transmembrane-Span Receptor to a Galphai G-Protein Regulatory Motif Complex. *Mol. Pharmacol.* **88**, 231-237

175. Oner, S. S., Maher, E. M., Breton, B., Bouvier, M., and Blumer, J. B. (2010) Receptor-regulated interaction of activator of G-protein signaling-4 and Galphai. *J. Biol. Chem.* **285**, 20588-20594

176. Simons, S. B., Caruana, D. A., Zhao, M., and Dudek, S. M. (2012) Caffeine-induced synaptic potentiation in hippocampal CA2 neurons. *Nat. Neurosci.* **15**, 23-25

177. Brown, N. E., Goswami, D., Branch, M. R., Ramineni, S., Ortlund, E. A., Griffin, P. R., and Hepler, J. R. (2015) Integration of G protein alpha (Galpha) signaling by the regulator of G protein signaling 14 (RGS14). *J. Biol. Chem.* **290**, 9037-9049

178. Hollinger, S., Ramineni, S., and Hepler, J. R. (2003) Phosphorylation of RGS14 by protein kinase A potentiates its activity toward G alpha i. *Biochemistry* **42**, 811-819

179. Matte, A., Kozlov, G., Trempe, J. F., Currie, M. A., Burk, D., Jia, Z., Gehring, K., Ekiel, I., Berghuis, A. M., and Cygler, M. (2009) Preparation and characterization of bacterial protein complexes for structural analysis. *Advances in protein chemistry and structural biology* **76**, 1-42

180. Nettleship, J. E., Assenberg, R., Diprose, J. M., Rahman-Huq, N., and Owens, R. J. (2010) Recent advances in the production of proteins in insect and mammalian cells for structural biology. *Journal of structural biology* **172**, 55-65

181. Makrides, S. C. (1996) Strategies for achieving high-level expression of genes in Escherichia coli. *Microbiological reviews* **60**, 512-538

182. Sahdev, S., Khattar, S. K., and Saini, K. S. (2008) Production of active eukaryotic proteins through bacterial expression systems: a review of the existing biotechnology strategies. *Mol. Cell. Biochem.* **307**, 249-264

183. Kuo, W. H., and Chase, H. A. (2011) Exploiting the interactions between poly-histidine fusion tags and immobilized metal ions. *Biotechnol. Lett.* **33**, 1075-1084

184. Terpe, K. (2003) Overview of tag protein fusions: from molecular and biochemical fundamentals to commercial systems. *Appl. Microbiol. Biotechnol.* **60**, 523-533

185. Sun, P., Tropea, J. E., and Waugh, D. S. (2011) Enhancing the solubility of recombinant proteins in Escherichia coli by using hexahistidine-tagged maltose-binding protein as a fusion partner. *Methods in molecular biology* **705**, 259-274

186. Dyson, M. R., Shadbolt, S. P., Vincent, K. J., Perera, R. L., and McCafferty, J. (2004) Production of soluble mammalian proteins in Escherichia coli: identification of protein features that correlate with successful expression. *BMC Biotechnol.* **4**, 32

187. Scopes, R. K. (1994) *Protein Purification: Principles and Practice*, Third ed., Springer New York

188. Fonda, I., Kenig, M., Gaberc-Porekar, V., Pristovaek, P., and Menart, V. (2002) Attachment of histidine tags to recombinant tumor necrosis factor-alpha drastically changes its properties. *TheScientificWorldJournal* **2**, 1312-1325

189. Parks, T. D., Leuther, K. K., Howard, E. D., Johnston, S. A., and Dougherty, W. G. (1994) Release of proteins and peptides from fusion proteins using a recombinant plant virus proteinase. *Anal. Biochem.* **216**, 413-417

190. Lee, E., Linder, M. E., and Gilman, A. G. (1994) Expression of G-protein alpha subunits in Escherichia coli. *Methods Enzymol.* **237**, 146-164

191. Studier, F. W., and Moffatt, B. A. (1986) Use of bacteriophage T7 RNA polymerase to direct selective high-level expression of cloned genes. *J. Mol. Biol.* **189**, 113-130

192. Pan, S. H., and Malcolm, B. A. (2000) Reduced background expression and improved plasmid stability with pET vectors in BL21 (DE3). *BioTechniques* **29**, 1234-1238

193. Dumon-Seignovert, L., Cariot, G., and Vuillard, L. (2004) The toxicity of recombinant proteins in Escherichia coli: a comparison of overexpression in BL21(DE3), C41(DE3), and C43(DE3). *Protein Expr Purif* **37**, 203-206

194. Cull, M., and McHenry, C. S. (1990) Preparation of extracts from prokaryotes. *Methods Enzymol.* **182**, 147-153

195. Baneyx, F., and Mujacic, M. (2004) Recombinant protein folding and misfolding in Escherichia coli. *Nat. Biotechnol.* **22**, 1399-1408

196. Xu, Y., Piston, D. W., and Johnson, C. H. (1999) A bioluminescence resonance energy transfer (BRET) system: application to interacting circadian clock proteins. *Proceedings of the National Academy of Sciences of the United States of America* **96**, 151-156

197. Wu, P., and Brand, L. (1994) Resonance energy transfer: methods and applications. *Anal. Biochem.* **218**, 1-13

198. Xu, Y., Kanauchi, A., von Arnim, A. G., Piston, D. W., and Johnson, C. H. (2003) Bioluminescence resonance energy transfer: monitoring protein-protein interactions in living cells. *Methods Enzymol.* **360**, 289-301

199. Lohse, M. J., Nuber, S., and Hoffmann, C. (2012) Fluorescence/bioluminescence resonance energy transfer techniques to study G-protein-coupled receptor activation and signaling. *Pharmacol. Rev.* **64**, 299-336

200. Nagai, T., Ibata, K., Park, E. S., Kubota, M., Mikoshiba, K., and Miyawaki, A. (2002) A variant of yellow fluorescent protein with fast and efficient maturation for cell-biological applications. *Nat. Biotechnol.* **20**, 87-90

201. Romero-Fernandez, W., Borroto-Escuela, D. O., Tarakanov, A. O., Mudo, G., Narvaez, M., Perez-Alea, M., Agnati, L. F., Ciruela, F., Belluardo, N., and Fuxe, K. (2011) Agonist-induced formation of FGFR1 homodimers and signaling differ among members of the FGF family. *Biochem. Biophys. Res. Commun.* **409**, 764-768

202. Gales, C., Rebois, R. V., Hogue, M., Trieu, P., Breit, A., Hebert, T. E., and Bouvier, M. (2005) Real-time monitoring of receptor and G-protein interactions in living cells. *Nat. Methods* **2**, 177-184

203. Angers, S., Salahpour, A., Joly, E., Hilairet, S., Chelsky, D., Dennis, M., and Bouvier, M. (2000) Detection of beta 2-adrenergic receptor dimerization in living cells using bioluminescence resonance energy transfer (BRET). *Proceedings of the National Academy of Sciences of the United States of America* **97**, 3684-3689

204. Hamdan, F. F., Audet, M., Garneau, P., Pelletier, J., and Bouvier, M. (2005) High-throughput screening of G protein-coupled receptor antagonists using a bioluminescence resonance energy transfer 1-based beta-arrestin2 recruitment assay. *J. Biomol. Screen.* **10**, 463-475

205. Oner, S. S., An, N., Vural, A., Breton, B., Bouvier, M., Blumer, J. B., and Lanier, S. M. (2010) Regulation of the AGS3.G{alpha}i signaling complex by a seven-transmembrane span receptor. *J. Biol. Chem.* **285**, 33949-33958

206. Jiang, L. I., Collins, J., Davis, R., Lin, K. M., DeCamp, D., Roach, T., Hsueh, R., Rebres, R. A., Ross, E. M., Taussig, R., Fraser, I., and Sternweis, P. C. (2007) Use of a cAMP BRET sensor to characterize a novel regulation of cAMP by the sphingosine 1-phosphate/G13 pathway. *J. Biol. Chem.* **282**, 10576-10584

207. Lan, T. H., Liu, Q., Li, C., Wu, G., and Lambert, N. A. (2012) Sensitive and high resolution localization and tracking of membrane proteins in live cells with BRET. *Traffic* **13**, 1450-1456

208. Couturier, C., and Deprez, B. (2012) Setting Up a Bioluminescence Resonance Energy Transfer High throughput Screening Assay to Search for Protein/Protein Interaction Inhibitors in Mammalian Cells. *Front Endocrinol (Lausanne)* **3**, 100

209. Bacart, J., Corbel, C., Jockers, R., Bach, S., and Couturier, C. (2008) The BRET technology and its application to screening assays. *Biotechnol J* **3**, 311-324

210. Gilman, A. G. (1987) G proteins: transducers of receptor-generated signals. *Annu. Rev. Biochem.* **56**, 615-649

211. Hepler, J. R., and Gilman, A. G. (1992) G proteins. *Trends Biochem* **17**, 383-387

212. Hamm, H. E. (1998) The many faces of G protein signaling. *J. Biol. Chem.* **273**, 669-672

213. Hollinger, S., and Hepler, J. R. (2002) Cellular regulation of RGS proteins: modulators and integrators of G protein signaling. *Pharmacol. Rev.* **54**, 527-559

214. Ross, E. M., and Wilkie, T. M. (2000) GTPase-activating proteins for heterotrimeric G proteins: regulators of G protein signaling (RGS) and RGS-like proteins. *Annu. Rev. Biochem.* **69**, 795-827

215. De Vries, L., Zheng, B., Fischer, T., Elenko, E., and Farquhar, M. G. (2000) The regulator of G protein signaling family. *Annu. Rev. Pharmacol. Toxicol.* **40**, 235-271

216. Vellano, C. P., Lee, S. E., Dudek, S. M., and Hepler, J. R. (2011) RGS14 at the interface of hippocampal signaling and synaptic plasticity. *Trends Pharmacol. Sci.* **32**, 666-674

217. Abramow-Newerly, M., Roy, A. A., Nunn, C., and Chidiac, P. (2006) RGS proteins have a signalling complex: interactions between RGS proteins and GPCRs, effectors, and auxiliary proteins. *Cell. Signal.* **18**, 579-591

218. Vellano, C. P., Shu, F. J., Ramineni, S., Yates, C. K., Tall, G. G., and Hepler, J. R. (2011) Activation of the regulator of G protein signaling 14-Galphai1-GDP signaling complex is regulated by resistance to inhibitors of cholinesterase-8A. *Biochemistry* **50**, 752-762

219. Goswami, D., Devarakonda, S., Chalmers, M. J., Pascal, B. D., Spiegelman, B. M., and Griffin, P. R. (2013) Time window expansion for HDX analysis of an intrinsically disordered protein. *J. Am. Soc. Mass Spectrom.* **24**, 1584-1592

220. Pascal, B. D., Willis, S., Lauer, J. L., Landgraf, R. R., West, G. M., Marciano, D., Novick, S., Goswami, D., Chalmers, M. J., and Griffin, P. R. (2012) HDX workbench: software for the analysis of H/D exchange MS data. *J. Am. Soc. Mass Spectrom.* **23**, 1512-1521

221. Pettersen, E. F., Goddard, T. D., Huang, C. C., Couch, G. S., Greenblatt, D. M., Meng, E. C., and Ferrin, T. E. (2004) UCSF Chimera--a visualization system for exploratory research and analysis. *J Comput Chem* **25**, 1605-1612

222. Sievers, F., Wilm, A., Dineen, D., Gibson, T. J., Karplus, K., Li, W., Lopez, R., McWilliam, H., Remmert, M., Soding, J., Thompson, J. D., and Higgins, D. G. (2011) Fast, scalable generation of high-quality protein multiple sequence alignments using Clustal Omega. *Mol. Syst. Biol.* **7**, 539

223. Goujon, M., McWilliam, H., Li, W., Valentin, F., Squizzato, S., Paern, J., and Lopez, R. (2010) A new bioinformatics analysis tools framework at EMBL-EBI. *Nucleic Acids Res.* **38**, W695-699

224. Chen, C. K., Wieland, T., and Simon, M. I. (1996) RGS-r, a retinal specific RGS protein, binds an intermediate conformation of transducin and enhances recycling. *Proceedings of the National Academy of Sciences of the United States of America* **93**, 12885-12889

225. Goswami, D., Callaway, C., Pascal, B. D., Kumar, R., Edwards, D. P., and Griffin, P. R. (2014) Influence of domain interactions on conformational mobility of the

progesterone receptor detected by hydrogen/deuterium exchange mass spectrometry. *Structure* **22**, 961-973

226. Landgraf, R. R., Goswami, D., Rajamohan, F., Harris, M. S., Calabrese, M. F., Hoth, L. R., Magyar, R., Pascal, B. D., Chalmers, M. J., Busby, S. A., Kurumbail, R. G., and Griffin, P. R. (2013) Activation of AMP-activated protein kinase revealed by hydrogen/deuterium exchange mass spectrometry. *Structure* **21**, 1942-1953

227. Marciano, D. P., Dharmarajan, V., and Griffin, P. R. (2014) HDX-MS guided drug discovery: small molecules and biopharmaceuticals. *Curr. Opin. Struct. Biol.* **28C**, 105-111

228. Mixon, M. B., Lee, E., Coleman, D. E., Berghuis, A. M., Gilman, A. G., and Sprang, S. R. (1995) Tertiary and quaternary structural changes in Gi alpha 1 induced by GTP hydrolysis. *Science* **270**, 954-960

229. Chung, K. Y., Rasmussen, S. G., Liu, T., Li, S., DeVree, B. T., Chae, P. S., Calinski, D., Kobilka, B. K., Woods, V. L., Jr., and Sunahara, R. K. (2011) Conformational changes in the G protein Gs induced by the beta2 adrenergic receptor. *Nature* **477**, 611-615

230. Bosch, D. E., Willard, F. S., Ramanujam, R., Kimple, A. J., Willard, M. D., Naqvi, N. I., and Siderovski, D. P. (2012) A P-loop mutation in Galpha subunits prevents transition to the active state: implications for G-protein signaling in fungal pathogenesis. *PLoS Pathog* **8**, e1002553

231. Bosch, D. E., Kimple, A. J., Sammond, D. W., Muller, R. E., Miley, M. J., Machius, M., Kuhlman, B., Willard, F. S., and Siderovski, D. P. (2011) Structural determinants of affinity enhancement between GoLoco motifs and G-protein alpha subunit mutants. *J. Biol. Chem.* **286**, 3351-3358

232. Tu, Y., Popov, S., Slaughter, C., and Ross, E. M. (1999) Palmitoylation of a conserved cysteine in the regulator of G protein signaling (RGS) domain modulates the GTPase-activating activity of RGS4 and RGS10. *J. Biol. Chem.* **274**, 38260-38267

233. Ishii, M., Fujita, S., Yamada, M., Hosaka, Y., and Kurachi, Y. (2005) Phosphatidylinositol 3,4,5-trisphosphate and Ca2+/calmodulin competitively bind to the regulators of G-protein-signalling (RGS) domain of RGS4 and reciprocally regulate its action. *Biochem. J.* **385**, 65-73

234. Popov, S. G., Krishna, U. M., Falck, J. R., and Wilkie, T. M. (2000) Ca2+/Calmodulin reverses phosphatidylinositol 3,4, 5-trisphosphate-dependent inhibition of regulators of G protein-signaling GTPase-activating protein activity. *J. Biol. Chem.* **275**, 18962-18968

235. Evans, P. R., and Hepler, J. R. (2012) Regulator of G protein Signaling 14 (RGS14) interacts with calmodulin (CaM) in a calcium-dependent manner. in *Society for Neuroscience*, New Orleans, LA

236. Panja, D., and Bramham, C. R. (2014) BDNF mechanisms in late LTP formation: A synthesis and breakdown. *Neuropharmacology* **76 Pt C**, 664-676

237. Kennedy, M. B., Beale, H. C., Carlisle, H. J., and Washburn, L. R. (2005) Integration of biochemical signalling in spines. *Nat. Rev. Neurosci.* **6**, 423-434

238. Hollinger, S., and Hepler, J. R. (2004) Methods for measuring RGS protein phosphorylation by G protein-regulated kinases. *Methods in molecular biology* **237**, 205-219

239. Bourne, H. R. (1997) How receptors talk to trimeric G proteins. *Curr. Opin. Cell Biol.* **9**, 134-142

240. Brown, N. E., Blumer, J. B., and Hepler, J. R. (2015) Bioluminescence resonance energy transfer to detect protein-protein interactions in live cells. *Methods in molecular biology* **1278**, 457-465

241. Bernstein, L. S., Ramineni, S., Hague, C., Cladman, W., Chidiac, P., Levey, A. I., and Hepler, J. R. (2004) RGS2 binds directly and selectively to the M1 muscarinic acetylcholine receptor third intracellular loop to modulate Gq/11alpha signaling. *J. Biol. Chem.* **279**, 21248-21256

242. Hollins, B., Kuravi, S., Digby, G. J., and Lambert, N. A. (2009) The c-terminus of GRK3 indicates rapid dissociation of G protein heterotrimers. *Cell. Signal.* **21**, 1015-1021

243. Hynes, T. R., Yost, E. A., Yost, S. M., and Berlot, C. H. (2011) Multicolor BiFC analysis of G protein betagamma complex formation and localization. *Methods in molecular biology* **756**, 229-243

244. Masuho, I., Martemyanov, K. A., and Lambert, N. A. (2015) Monitoring G Protein Activation in Cells with BRET. *Methods in molecular biology* **1335**, 107-113

245. Masuho, I., Ostrovskaya, O., Kramer, G. M., Jones, C. D., Xie, K., and Martemyanov, K. A. (2015) Distinct profiles of functional discrimination among G proteins determine the actions of G protein-coupled receptors. *Science signaling* **8**, ra123

246. Digby, G. J., Sethi, P. R., and Lambert, N. A. (2008) Differential dissociation of G protein heterotrimers. *The Journal of physiology* **586**, 3325-3335

247. Neitzel, K. L., and Hepler, J. R. (2006) Cellular mechanisms that determine selective RGS protein regulation of G protein-coupled receptor signaling. *Semin. Cell Dev. Biol.* **17**, 383-389

248. Sarvazyan, N. A., Lim, W. K., and Neubig, R. R. (2002) Fluorescence analysis of receptor-G protein interactions in cell membranes. *Biochemistry* **41**, 12858-12867

249. Muntean, B. S., and Martemyanov, K. A. (2016) Association with the Plasma Membrane is Sufficient for Potentiating Catalytic Activity of Regulators of G protein Signaling (RGS) Proteins of the R7 subfamily. *J. Biol. Chem.*

250. Otmakhova, N. A., Otmakhov, N., Mortenson, L. H., and Lisman, J. E. (2000) Inhibition of the cAMP pathway decreases early long-term potentiation at CA1 hippocampal synapses. *J. Neurosci.* **20**, 4446-4451

251. Malinow, R. (2003) AMPA receptor trafficking and long-term potentiation. *Philosophical transactions of the Royal Society of London. Series B, Biological sciences* **358**, 707-714

252. Chavez-Noriega, L. E., and Stevens, C. F. (1992) Modulation of synaptic efficacy in field CA1 of the rat hippocampus by forskolin. *Brain Res.* **574**, 85-92

253. Luscher, C., and Slesinger, P. A. (2010) Emerging roles for G protein-gated inwardly rectifying potassium (GIRK) channels in health and disease. *Nat. Rev. Neurosci.* **11**, 301-315

254. Dudek, S. M., Alexander, G. M., and Farris, S. (2016) Rediscovering area CA2: unique properties and functions. *Nat. Rev. Neurosci.* **17**, 89-102

255. Bayewitch, M. L., Avidor-Reiss, T., Levy, R., Pfeuffer, T., Nevo, I., Simonds, W. F., and Vogel, Z. (1998) Inhibition of adenylyl cyclase isoforms V and VI by various Gbetagamma subunits. *FASEB J.* **12**, 1019-1025

256. Thomas, G. M., and Huganir, R. L. (2004) MAPK cascade signalling and synaptic plasticity. *Nat. Rev. Neurosci.* **5**, 173-183

257. Sweatt, J. D. (2001) The neuronal MAP kinase cascade: a biochemical signal integration system subserving synaptic plasticity and memory. *J. Neurochem.* **76**, 1-10

258. Mazzucchelli, C., and Brambilla, R. (2000) Ras-related and MAPK signalling in neuronal plasticity and memory formation. *Cell. Mol. Life Sci.* **57**, 604-611

259. Wang, Y., Waldron, R. T., Dhaka, A., Patel, A., Riley, M. M., Rozengurt, E., and Colicelli, J. (2002) The RAS effector RIN1 directly competes with RAF and is regulated by 14-3-3 proteins. *Mol. Cell. Biol.* **22**, 916-926

260. Dhaka, A., Costa, R. M., Hu, H., Irvin, D. K., Patel, A., Kornblum, H. I., Silva, A. J., O'Dell, T. J., and Colicelli, J. (2003) The RAS effector RIN1 modulates the formation of aversive memories. *J. Neurosci.* **23**, 748-757

261. Bliss, J. M., Gray, E. E., Dhaka, A., O'Dell, T. J., and Colicelli, J. (2010) Fear learning and extinction are linked to neuronal plasticity through Rin1 signaling. *J. Neurosci. Res.* **88**, 917-926

262. Wohlgemuth, S., Kiel, C., Kramer, A., Serrano, L., Wittinghofer, F., and Herrmann, C. (2005) Recognizing and defining true Ras binding domains I: biochemical analysis. *J. Mol. Biol.* **348**, 741-758

263. Sanderson, T. M. (2012) Molecular mechanisms involved in depotentiation and their relevance to schizophrenia. *Chonnam medical journal* **48**, 1-6

264. Stornetta, R. L., and Zhu, J. J. (2011) Ras and Rap signaling in synaptic plasticity and mental disorders. *Neuroscientist* **17**, 54-78

265. Huang, C. C., Liang, Y. C., and Hsu, K. S. (1999) A role for extracellular adenosine in time-dependent reversal of long-term potentiation by low-frequency stimulation at hippocampal CA1 synapses. *J. Neurosci.* **19**, 9728-9738

266. Ignatov, A., Lintzel, J., Hermans-Borgmeyer, I., Kreienkamp, H. J., Joost, P., Thomsen, S., Methner, A., and Schaller, H. C. (2003) Role of the G-protein-coupled receptor GPR12 as high-affinity receptor for sphingosylphosphorylcholine and its expression and function in brain development. *J. Neurosci.* **23**, 907-914

267. Ochiishi, T., Saitoh, Y., Yukawa, A., Saji, M., Ren, Y., Shirao, T., Miyamoto, H., Nakata, H., and Sekino, Y. (1999) High level of adenosine A1 receptor-like immunoreactivity in the CA2/CA3a region of the adult rat hippocampus. *Neuroscience* **93**, 955-967

268. Arai, A., Kessler, M., and Lynch, G. (1990) The effects of adenosine on the development of long-term potentiation. *Neurosci. Lett.* **119**, 41-44

269. Chung, H. J., Ge, W. P., Qian, X., Wiser, O., Jan, Y. N., and Jan, L. Y. (2009) G protein-activated inwardly rectifying potassium channels mediate depotentiation of long-term potentiation. *Proceedings of the National Academy of Sciences of the United States of America* **106**, 635-640

270. Uhlenbrock, K., Gassenhuber, H., and Kostenis, E. (2002) Sphingosine 1-phosphate is a ligand of the human gpr3, gpr6 and gpr12 family of constitutively active G protein-coupled receptors. *Cell. Signal.* **14**, 941-953

271. Tanaka, S., Ishii, K., Kasai, K., Yoon, S. O., and Saeki, Y. (2007) Neural expression of G protein-coupled receptors GPR3, GPR6, and GPR12 up-regulates cyclic AMP levels and promotes neurite outgrowth. *J. Biol. Chem.* **282**, 10506-10515